CHARACTERIZING MOLECULAR MODULATORS AT THE INTERSECTION OF METABOLISM AND IMMUNITY

by

Roxana Filip

A thesis submitted to the Department of Chemistry and Biomolecular Sciences

In conformity with the requirements for

the degree of Doctorate in Philosophy Chemistry

University of Ottawa

Ottawa, Ontario, Canada

November 2022

Abstract

Cellular metabolic and immune pathways can be acted upon by diverse molecular factors. Some examples include small molecules, regulatory proteins or RNAs, intermediary metabolites and hormones. These factors can also be introduced or induced by pathogens during infections. Indeed, it is known that complex interplay exists between metabolism and immunity. However, the ways in which these interactions occur, and the nature of the players are active subjects of research. Herein, three different studies are presented which investigate the roles of three distinct modulators of metabolism and/or immunity. Firstly, a natural product produced by a pathogenic fungus is shown to activate the aryl hydrocarbon receptor and induce the expression of xenobiotic metabolizing enzymes. Secondly, the modulation of lipid metabolism by an immunometabolic antiviral microRNA, microRNA-185, is deconvoluted using activity-based protein profiling (ABPP), transcriptomic and lipidomic analysis. This study also identifies a novel enzymatic target of microRNA-185 which can be targeted pharmacologically to reduce hepatitis C virus infectivity. Finally, a third study investigates the link between a poorly characterized enzyme, lysophospholipase-like 1 (LYPLAL1), and hepatic glucose metabolism using a specific activity-based probe. Overall, the work presented in this thesis makes use of various molecular and chemical biology methods to probe pathways which are acted upon by structurally diverse factors to improve our understanding of host-pathogen interactions and metabolism.

Acknowledgements

I would like start by thanking Dr. John Pezacki for his support during the many years I have spent in his lab. John took a chance on me and helped me realize my potential while coaching me to become a more confident scientist. I would also like to thank the many people in the Pezacki lab who have encouraged and mentored me. Firstly, Dana Foss gave me the best start a student could ask for; her energy, passion and work ethic are second to none. Thank you to former members Yanouchka Rouleau, Jenny Cheng, Mirka Strmiskova and Dave Prescott for always being there to answer all my questions. Thank you to Ragunath Singaravelu, Allison Sherratt, Megan Powdrill, Christopher Ablenas and Dennis Özcelik for being scientific role models and teaching by example.

The last few years went by in a blur thanks to the amazing company of my lab-mates and friends Nadine Ahmed, Noreen Ahmed, Rhea Alonzi, Geneviève Desrochers, Tyler Shaw, Didier Bilodeau, Mariam Serhan, Kaitlyn Margison, David Lefebvre and Shadi Masoud. I would also like to thank my undergraduate trainees Lisa Chen and Étienne Bélanger for allowing me to share my enthusiasm for science.

A huge thank you goes to my thesis advising committee, Dr. Katey Rayner and Dr. Jeff Keillor, for their invaluable input throughout the milestones of my degree. I would also like to thank the generous financial support of the Natural Sciences and Engineering Research Council (NSERC), the government of Ontario and the University of Ottawa.

Thank you to my close friends and family for always believing in me. Thank you to my mom, dad, and sister for putting up with my nerdy antics since day one. Thanks to my beloved cats Lychee and Coco for their comforting presence, may you rest in peace. Finally, a special thank you to my most caring and supportive partner, Jim Concepcion for always being there when I needed it the most.

Table of Contents

List of Figures

List of Tables

List of Abbreviations

2-AG	2-arachidonylglycerol
AADAC	arylacetamide deacetylase
ABHD6	alpha/beta-hydrolase domain containing protein 6
ABPM	allergic bronchopulmonary mycosis
ABPP	activity-based protein profiling
ACAT	acyl-CoA:cholesterol acyltransferase
ACC	acetyl-CoA carboxylase
ACOT1	acyl-CoA thioesterase 1
ACP	acyl carrier protein
AGPAT	acylglycerol-3-phosphate acyltransferase
AhR	aryl hydrocarbon receptor
AHRE	AhR responsive element
AIP	AH receptor-interacting protein
ALDH3A1	Aldehyde Dehydrogenase 3 Family Member A1
AMP	adenosine 5'-monophosphate
AMPK	5'-adenosine monophosphate-activated protein kinase
apoB	apolipoprotein B
Arnt	AhR nuclear translocator
ATGL	adipose triglyceride lipase
ATP	adenosine 5'-triphosphate
cAMP	cyclic AMP
CB1	cannabinoid receptor type 1
CBP	CREB-binding protein
CDP-DG	cytidine diphosphate-diacylglycerol
CE	cholesteryl esters
CERT	ceramide transfer protein
CES1	carboxylesterase 1
ChREBP	carbohydrate response element binding protein
CLDN1	claudin-1
CLIP	cross-linking and immunoprecipitation
CoA	Coenzyme A
CPT	carnitine-palmitoyl-transferase
CREB	cyclic AMP response element-binding protein
CRISPR	clustered regularly interspaced short palindromic repeats
CYP540	Cytochrome p450
DAG	diacylglyceride
DGAT	diacylglycerol acyltransferase
DMEM	Dulbecco's Modified Eagle Medium
DMSO	Dimethyl sulfoxide
DNV	Dengue virus
DUB	deubiquitylating enzyme
E	envelope
EGFR	epidermal growth factor receptor
ELOVL	elongation of very long chain fatty acids
ER	endoplasmic reticulum
Erk2	extracellular signal-regulated kinase 2

HCov-229E	human coronavirus 229E
HMG	3-hydroxy-3-methyl-glutaryl
HMGCR	HMG-CoA reductase
HPLC	high-performance liquid chromatography
HSL	hormone sensitive lipase
HSP90	heat shock 90 proteins
HSV-1	Herpesvirus-1
ICZ	indolo[3,2-b]carbazole
INSR	insulin receptor
IRS	insulin receptor substrate
KO	knock-out
KSHV	Kaposi's sarcoma associated herpesvirus
LAP	LC3-associated phagocytosis
LCAT	Lecithin-Cholesterol Acyltransferase
LC-MS/MS	Liquid chromatography-tandem mass spectrometry
LD	Lipid droplets
LDLR	low-density lipoprotein receptor
LIPC	lipase C
LPL	lipoprotein lipase
LVP	lipoviroparticles
LXR	liver X receptor
LYPLA	lysophospholipase
LYPLAL1	lysophospholipase-like 1
lysoPA	lysophosphatidic acid
MAG	monoacylglyceride
MAPK	mitogen-activated protein kinase
MGLL/MAGL	Monoglyceride lipase
miRNA	microRNA
MOI	multiplicity of infection
MRM	multiple reaction monitoring
MTP	mitochondrial trifunctional protein
MTTP	microsomal triacylglycerol transfer protein
NADP	Nicotinamide adenine dinucleotide phosphate
NEAA	non-essential amino acids
NF-κB	Nuclear factor kappa B
NQO1	NAD(P)H Quinone Dehydrogenase 1
NS	non-structural
OCLN	occludin
OSBP	oxysterol binding protein
PA	phosphatidic acid
pAMPK	phosphorylated AMPK
PAP	phosphatidate phosphatase
PBMC	peripheral blood mononuclear cell
PC	phosphatidylcholine
PCK1	Phosphoenolpyruvate carboxykinase (mouse)
PDK1	3-phosphatidylinositol-dependent kinase-1

PE	phosphatidylethanolamine
PEPCK	phosphoenolpyruvate carboxykinase
PG	phosphatidylglycerol
PGA_1	prostaglandin A_1
PGC-1α	proliferator-activated receptor-gamma coactivator-1 alpha
PI	phosphatidylinositol
PI3K	phosphatidylinositol 3-kinase
PI4KIIIα	phosphatidylinositol-4-kinase IIIα
PI4P	phosphatidylinositol-4-phosphate
PK	pyruvate kinase
PKA	protein kinase A
PKB/Akt	protein kinase B
PLA2G4A	phospholipase A2 Group IVA
PMH	primary mouse hepatocytes
PNPLA2	patatin-like phospholipase domain 2
PPAR	Peroxisome Proliferator Activated Receptor
PPRE	PPAR response element
PS	Phosphatidylserine
PTP1D (SHP2)	Protein Tyrosine Phosphatase, Non-Receptor Type 11
PVDF	polyvinylidene fluoride
RXR	retinoid X receptor
SCAP	sterol regulatory element-binding protein cleavage-activating protein
SCD	stearoyl-CoA desaturase
SD	standard deviation
SDS-PAGE	sodium dodecyl sulfate polyacrylamide gel electrophoresis
SARS-CoV-2	severe acute respiratory syndrome coronavirus 2
SM	sphingomyelin
SR-BI	scavenger receptor BI
SREBP	sterol regulatory element-binding protein
STAT	signal transducer and activator of transcription
TAGs	triacylglycerols
TAMRA	tetramethylrhodamine
TBTA	Tris((1-benzyl-4-triazolyl)methyl)amine
TCA	tricarboxylic acid
TCDD	2,3,7,8-tetrachlorodibenzo-p-dioxin
TCEP	tris(2-carboxyethyl)phosphine
TGH	triacylglycerol hydrolase
UGT1A1	UDP Glucuronosyltransferase Family 1 Member A1
UGT1A6	UDP Glucuronosyltransferase Family 1 Member A6
VLDL	very low density lipoprotein particles
XAP2	HBV X-associated protein 2
XRE	xenobiotic-responsive element

Chapter 1: Introduction

1.1 Preface

Understanding the relationship between metabolism and host-pathogen interactions is of importance for the development of therapeutic strategies. Indeed, as exemplified in the following chapters, pathogens such as fungi and viruses interact with and significantly modulate host metabolic pathways. Identifying host targets such as enzymes, signalling molecules, and intermediate metabolites at the centre of pathways which are acted upon during infection allows for the specific targeting of these factors as antipathogenic approaches. An advantage of investigating host interactions is the ability to develop potentially broad therapeutics with effects on multiple pathogens which affect the same pathways. For example, such strategies are currently being investigated for the treatment of multiple flavivirus infections such as Zika virus, West Nile virus and Dengue virus, all of which interact with lipid metabolic pathways[1]. Alternatively, single host targets may be identified which are central to a pathogen's replication, propagation, or over-activation of the immune system, and targeting of that host factor can illicit a potent therapeutic effect. For these reasons, characterising molecular modulators at the intersection of metabolism and immunity is the focus of this thesis.

The following introduction serves as a broad overview of metabolic pathways, host-pathogen interactions, immunometabolism and activity-based protein profiling (ABPP) as a tool to study these processes. More specifically, the topics of xenobiotic, lipid and glucose metabolism are first introduced, followed by an overview of host-pathogen interactions of fungi and viruses with focus on two pathogens: *Schizophyllum commune* and the hepatitis C virus. Finally, a technical explanation of ABPP is presented. These topics are relevant for contextualizing the work presented in the following chapters which cover different aspects of cellular metabolism and investigate distinct molecular modulators of cellular pathways using chemical biology approaches. The

research presented in the three research chapters following the introduction will be investigating the effects of a small molecule (schizocommunin), a microRNA (microRNA-185) and an enzyme (Lysophospholipase-like 1), each with roles in metabolism and/or immunity, with the aim of delineating some of the complex interplay between metabolic and immune actors in the cell and gaining a better understanding of host-pathogen interactions.

1.2 Overview of relevant metabolic pathways and their physiological roles

1.2.1 Cytochrome metabolism and the aryl hydrocarbon receptor pathway

The Cytochrome p450 (CYP540) enzyme superfamily is a large group of monooxygenase enzymes with a spectrum of roles in the metabolism of steroids, fatty acids, vitamins and xenobiotics. The broad CYP designation is further divided into families denoted by Arabic numerals and then in subfamilies indicated with a capital letter based on sequence homology and gene organization[2]. There are currently 57 known human cytochrome enzymes of which at least 42 have well defined roles[3]. Some examples include CYP7A1 which catalyzes the rate limiting step in the conversion of cholesterol to bile acids[4], the CYP26 retinoic acid hydrolases which are responsible for the metabolism and homeostasis of vitamin A derivatives[5], and CYP17A1 which performs essential transformations in steroid metabolism for the synthesis of androgens[6]. At the centre of all cytochrome P450 enzymes is an iron (III) protoporphyrin-IX group which facilitates the necessary electron transfer for the oxidation of structurally varied substrates. For the reaction to occur, two electrons are provided by NAD(P)H via the action of an associated reductase protein while molecular oxygen (O_2) becomes reduced to a water molecule[7]. The general equation for this reaction is shown below (Figure 1-1).

The first cytochrome enzyme to be named according to modern nomenclature[2] and certainly one of the most infamous cytochromes is CYP1A1. This enzyme's main function is the metabolism of

lipophilic xenobiotics such as environmental toxins, pollutants, and drugs to their more soluble oxidized forms for elimination. Although this function seems to be an adaptive detoxification response, many metabolites resulting from these transformations are known to be cytotoxic and/or carcinogenic[8]. Substrates of the CYP1 family are mainly planar molecules such as polycyclic aromatic hydrocarbons. In particular, CYP1A1 is known to hydrolyze hydrophobic aromatic compounds such as benzo[a]pyrene and polychlorinated biphenyls, the latter being well known environmental pollutants[9].

$$R + O_2 + 2e^- + 2H^+ \xrightarrow{\text{CYP450}} R\text{-}O + H_2O$$

Figure 1-1. Equation for the oxidation of a substrate (R) by a cytochrome P450 enzyme. The reaction requires the input of two electrons, two protons and molecular oxygen. Adapted from Meunier *et al.*[7]

Classical aryl hydrocarbon receptor signalling

Induction of CYP1A1 expression is tightly linked to the activation of the aryl hydrocarbon receptor (AhR), also known as the dioxin receptor[10]. Early understanding of AhR signalling was based on its activation by 2,3,7,8-tetrachlorodibenzo-p-dioxin (TCDD), a potent dioxin produced as a by-product of herbicide synthesis. Exposure to TCDD leads to chloracne, liver toxicity, altered lipid metabolism, immune function decline and disorders of the endocrine and nervous systems[11]. In light of these effects, large efforts to understand AhR signalling were undertaken. The aryl hydrocarbon receptor is a ligand-activated transcription factor which resides in the cytosol complexed to four proteins: two heat shock 90 proteins (HSP90), the AH receptor-interacting protein (AIP), also known as HBV X-associated protein 2 (XAP2), and the p23 co-chaperone. Ligand binding leads to nuclear translocation and dissociation of the complex followed by AhR association with the AhR nuclear translocator (Arnt). This complex can then bind to xenobiotic-

responsive elements (XREs), also known as AhR responsive elements (AHRE), in the enhancer regions of AhR-regulated genes to recruit RNA polymerase II and transcriptional co-activators[10]. CYP1A1 is the most ubiquitous AhR-responsive gene but other metabolic genes in the canonical AhR battery include CYP1A2, CYP1B1, UDP Glucuronosyltransferase Family 1 Member A1 (UGT1A1), UDP Glucuronosyltransferase Family 1 Member A6 (UGT1A6), Glutathione S-Transferase Alpha 2 (GSTA2), NAD(P)H Quinone Dehydrogenase 1 (NQO1) and Aldehyde Dehydrogenase 3 Family Member A1 (ALDH3A1)[12]. The UDP glucuronosyltransferases catalyze the addition of a glucuronic acid to lipophilic substrates to enhance their solubility and renal elimination[13]. Glutathione-S-transferases are responsible for the addition of glutathione to electrophilic substrates for detoxification[14]. NQO1 mediates the two-electron reduction of quinones to hydroquinones to facilitate excretion[15] and ALDH3A1 catalyzes the oxidation of environmental aldehydes to their corresponding acids to support resistance to cellular oxidative stress[16]. The functions of these enzymes seem to support a protective role for the aryl hydrocarbon receptor pathway, so why is it that potent activation of the receptor by TCDD elicits several toxic biological consequences? The answer, although yet to be fully understood, lies in the large set of non-canonical AhR targets and in the complex crosstalk between AhR signalling and cell proliferation, differentiation, and immune pathways.

Cellular roles of AhR

AhR has been shown to directly induce the expression of the cyclin-dependent kinase inhibitors $p21^{CIP1}$ and $p27^{KIP1}$ as well as that of the protooncogenes c-jun and junD[12]. Additionally, TCDD was shown to indirectly activate c-jun via the p38-mitogen-activated protein kinase (MAPK) pathway[17] and to increase levels of epidermal growth factor receptor (EGFR)-associated tyrosine kinases in rodents[18]. Furthermore, a significant increase in H-Ras protein levels and extracellular signal-regulated kinase 2 (Erk2), also known as MAPK1, activity was observed in cells from TCDD-treated primates[19]. Taken together, these interactions with factors involved in cell

proliferation, differentiation and cell cycle regulation are likely the cause of the carcinogenic effects observed with potent AhR activation. There is also evidence for interaction and mutual functional repression between AhR and Nuclear factor kappa B (NF-κB)[20], a central transcription factor with roles in immunity and inflammation[21]. Other links between AhR and immunity have been established. For instance, the receptor has been shown to interact with and regulate the signal transducer and activator of transcription 1 (STAT1) in macrophages and T_H17 helper T cells[22,23]. Interestingly, there is evidence for ligand-specific modulation of T cell differentiation by AhR. Indeed, TCDD activation of AhR promotes T_{reg} cell differentiation and immunosuppression while activation of the pathway by the agonist 6- formylindolo[3,2-b]carbazole (FICZ) represses T_{reg} differentiation and increases the levels of pro-inflammatory T_H17 cells[24]. The AhR pathway has also been shown to influence neutrophils, dendritic cells, macrophages and B lymphocytes[25] and to participate in the allergic response through mast cell activation[26]. Overall, it is clear that activation of AhR is a complex process with ramification far beyond that of a simple xenobiotic detoxification mechanism. Therefore, identifying activators of the pathway and understanding their effects on physiology is imperative for delineating the role of AhR in disease.

In light of AhR's crosstalk with immune pathways, it is not surprising that the receptor has been associated with the response to numerous pathogenic infections. For instance, activation of AhR by TCDD has been reported to increase morbidity and mortality in mice infected with the Influenza virus[27]. The receptor was also found to be activated by the Zika virus via elevated levels of the kynurenine tryptophan metabolite in infected cells. In the same study, inhibition of AhR decreased both Zika virus and Dengue virus replication[28]. Most recently, it was reported that AhR is activated by infection with multiple coronaviruses, including human coronavirus 229E (HCov-229E) and severe acute respiratory syndrome coronavirus 2 (SARS-CoV-2), the root cause of the ongoing global Covid-19 pandemic. Interestingly, pharmacological inhibition of the receptor decreases

replication of both these viruses *in vitro*[29]. From a different perspective, activation of AhR by commensal gut microbes has been associated with amelioration of inflammation in inflammatory bowel diseases such as Crohn's disease and andulcerative colitis. Indeed, AhR metabolites produced by pro-biotic microorganisms, including *Lactobacillus reuteri* and *Lactobacillus bulgaricus*, have been shown to restore intestinal barrier function[30,31]. Interactions between AhR and pathogenic fungi have also been reported. This will be the focus of chapter 2 of this thesis and will be explored in detail in section 5.1 of the discussion.

1.2.2 Liver lipid metabolism and regulation

The transformation of lipid species through catabolic and anabolic pathways is central to cell structural integrity, energetics, signalling, and immunity. For that purpose, a large array of enzymes have evolved specific roles in lipid metabolism. Understanding of the functions of these enzymes and their regulators is essential to unraveling the complex metabolic interplays which occur during disease and host-pathogen interactions. An abridged schematic of liver lipid metabolic pathways and their main actors is shown in figure 1-2 and an overview of the relevant transformations is given in the text. Some examples of how these pathways are pertinent to host-pathogen interactions are also provided.

Fatty acid synthesis

De novo fatty acid synthesis occurs in the cytosol of hepatocytes and is catalyzed by fatty acid synthase (FASN), a large homodimeric megasynthase enzyme. Each polypeptide of the enzyme is comprised of seven functionally specific domains, each catalyzing a subsequent step of the synthesis process[32]. The starting substrates for FASN are acetyl-coenzyme A (CoA) and malonyl-CoA. Acetyl-CoA is a central metabolite in lipid transformation as it is found at the intersection of catabolism and anabolism[33]. It is generated in the mitochondria by the oxidative decarboxylation of pyruvate, the final product of glycolysis, but must be first transformed into citrate to be exported

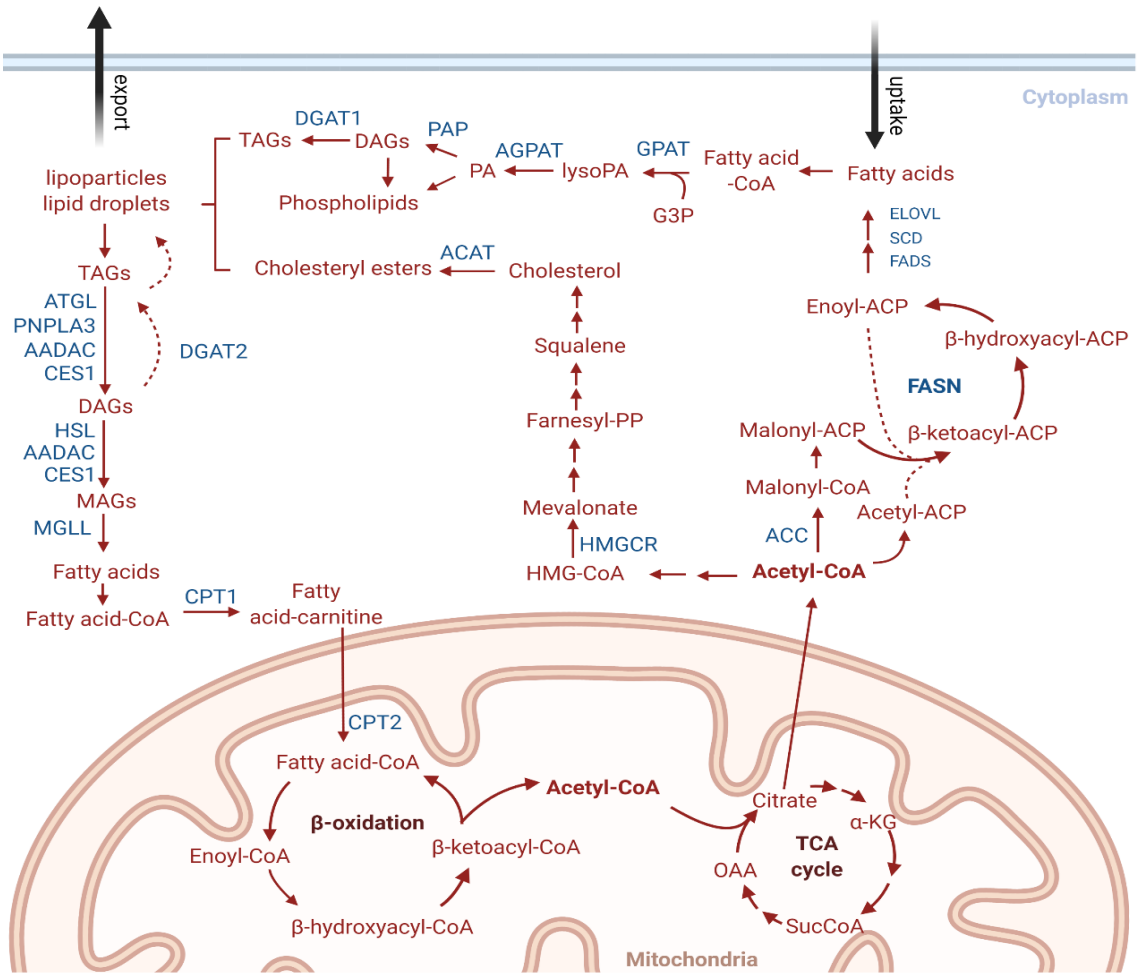

Figure 1-2. Overview of liver lipid metabolic pathways. Acetyl-CoA is found at the intersection of beta-oxidation, the tricarboxylic acid (TCA) or Krebs cycle, fatty acid synthesis and cholesterol synthesis. Fatty acids generated through the action of fatty acid synthases (FASN) or uptaken from the circulation are esterified to triacylglycerols (TAGs) or phospholipids. TAGs, phospholipids, and cholesteryl esters can be packaged into lipoparticles for export or lipid droplets for storage within hepatocytes. Lipolysis of TAGs to fatty acids is modulated by the activity of multiple enzymes. See text for details and regulation of these pathways. Enzymes involved in the biotransformation of critical metabolites are shown in blue. Dotted lines arrows represent alternative pathways. Scheme generated with BioRender.com.

into the cytoplasm though the tricarboxylate transporter. After transport, it is reverted to acetyl-CoA and can be used for both fatty acid and sterol synthesis[34]. Malonyl-CoA is generated from acetyl-CoA by acetyl-CoA carboxylase (ACC), a heavily regulated enzyme which acts as the main rate-limiting steps in fatty acid synthesis. ACC is activated by dephosphorylation and allosterically regulated by citrate binding which leads to its polymerization into filaments[35]. Feedback inhibition of ACC is mediated by palmitoyl-CoA generated by FASN. Additionally, expression of ACC is controlled by sterol regulatory element-binding protein (SREBP)[36]. Acetyl-CoA and malonyl-CoA enter the FASN complex by sequentially binding the acyl carrier protein (ACP) domain of the enzyme. The malonyl-CoA serves as a chain extender, adding on to the acetyl-CoA in a condensation reaction coupled to an energetically favourable decarboxylation. The resulting β-ketoacyl-ACP molecule (acetoacyl-ACP in the first round) is reduced to a β-hydroxyacyl-ACP which subsequently loses water to form an enoyl-ACP[32]. After one final reduction of the resulting double bond, the molecule is shuttled back to the transferase domain to receive another malonyl-CoA. This process is repeated for 7 cycles after which the resulting palmitoyl-ACP (16 carbons) is released from FASN through the action of the thiosesterase domain to form palmitic acid[37]. Further processing of palmitate into various fatty acid species occurs most commonly in the endoplasmic reticulum (ER) through the action of "elongation of very long chain fatty acids" (ELOVL) proteins, stearoyl-CoA desaturases (SCD) and fatty acid desaturases (FADS). These enzymes are transcriptionally regulated by SREBPs, liver X receptors (LXRs) and Peroxisome Proliferator Activated Receptors (PPARs)[38]. The liver is also able to import non-esterified fatty acids from the blood via transporters (fatty acid transport proteins), diffusion or through lipid rafts[39].

Due to the versatile nature of fatty acids as both energy sources and signalling molecules, fatty acid synthesis is a process which is often taken advantage of by pathogens. For instance, *M. tuberculosis* has been shown to scavenge host fatty acids to fuel its metabolism and as starting materials for its

own biosynthetic pathways[40]. Such utilisation of host fatty acids also occurs in multiple other bacterial infection such as ones with *Mycoplasma pneumoniae*, *Streptococcus agalactiae* and *Staphylococcus aureus*[41]. From a viral perspective, direct inhibition of mammalian fatty acid synthase has been reported to inhibit respiratory syncytial virus (RSV), human parainfluenza 3 (PIV3), and human rhinovirus 16[42]. More recently, Chu *et al.* demonstrated that pharmacological inhibition of FASN with the anti-obesity drug Orlistat is antiviral against SARS-CoV-2[43]. Finally, the dependence of hepatitis C virus on fatty acid synthesis will be discussed in more detail in section 1.3.2., but inhibition and downregulation of FASN have been shown to decrease HCV viral infectivity[44].

Triglyceride and phospholipid synthesis

The fatty acids produced through the processes described above can subsequently be used in triglyceride and phospholipid synthesis. Under normal conditions, the liver does not store considerable amount of triacylglycerides (TAGs); instead liver-synthesized TAGs are exported as part of very low density lipoprotein particles (VLDLs) for distribution to extrahepatic tissues[45]. TAG synthesis occurs on the ER membrane. The first and rate-limiting step is the esterification of long-chain fatty-acyl-CoAs to glycerol-3-phosphate (G3P) to form lysophosphatidic acid (lysoPA). This step is catalyzed by G3P acyltransferase (GPAT) which is transcriptionally upregulated by insulin and SREBP-1. GPAT activity is inhibited by 5'-adenosine monophosphate-activated protein kinase (AMPK), a sensor of low intracellular adenosine 5'-triphosphate (ATP) levels, to divert cell processes away from storage and towards energy production[46]. Subsequent acylation of lysoPA to phosphatidic acid (PA) is mediated through the action of acylglycerol-3-phosphate acyltransferases (AGPAT)[47]. PA can be further transformed to cytidine diphosphate-diacylglycerol (CDP-DG), the precursor to phosphatidylinositol (PI) and phosphatidylglycerol (PG) phospholipids[48]. The formation of diacylglycerides (DAGs) from PA by dephosphorylation is facilitated by phosphatidate phosphatase (PAP) enzymes, also known as Lipins. In hepatocytes, PAP1

translocates from the cytosol to the ER membrane to become activated[49]. Lipins have been shown to play roles not only in the synthesis of diacylglycerides, but also in lipid gene regulation by acting as transcriptional co-activators to PPARα and peroxisome proliferator-activated receptor-gamma coactivator-1 alpha (PGC-1α)[50]. Increasing the expression of lipin-1 (PAP1) in hepatocytes upregulates the expression of genes involved in fatty acid oxidation and suppresses expression of genes involved in de novo lipogenesis such as SREBP-1, FASN, and SCD[51]. Lipin-1 expression is increased by glucocorticoids such as glucagon and by elevated cyclic AMP (cAMP) levels.[52] This regulation is an example of the complex feedback loops governing the homeostatic response to energy needs in the cell. The DAGs formed through this pathway can be used to synthesize TAGs or several phospholipid species. For instance, the most common and second most common phospholipids, phosphatidylcholine (PC) and phosphatidylethanolamine (PE) respectively, are synthesized by the addition of CDP-choline or CDP-ethanolamine to diacylglycerol. Phosphatidylserine (PS) is synthesized by a base-exchange reaction from either PC or PE[48]. Finally, the addition of one more acyl chain to DAGs to form TAGs is the only committed step in biosynthesis of TGs and is catalyzed by diacylglycerol acyltransferase (DGAT) enzymes[53]. Under healthy conditions, the liver stores a small amount of triglycerides as lipid droplets (LD). These are transient and dynamic structures composed of a TAG and sterol ester core and surrounded by phospholipids and proteins such as DGAT2 and members of the perilipin family[54].

Extensive host-pathogen interactions occur in cellular lipid droplets. The most well-known example is that of the hepatitis C virus which hijacks lipid droplets for its replication[55]. However, this is not the only instance. For example, it is known that the *Chlamydia trachomatis* bacterium causes the accumulation of LDs rich in cholesterol esters at the cytosolic side of bacterial inclusions. This process allows for the association of bacterial proteins with the droplets, utilisation of host lipids, and eventually mediation of the pathogen's cytotoxic effect[56]. Other examples of

pathogens which target TAG synthesis and lipid droplet metabolism include the hepatitis B virus, the *Mycobacterium tuberculosis* bacterium, the *Mycobacterium leprae* bacterium, and the *Plasmodium falciparum* protist parasite[57].

Cholesterol synthesis

Cholesterol synthesis starts either in the cytoplasm or peroxisome with the condensation of two molecules of acetyl-CoA to form acetoacetyl-CoA, followed by a third condensation catalyzed by 3-hydroxy-3-methyl-glutaryl-CoA (HMG-CoA) synthase to form HMG-CoA[58]. The subsequent transformation of HMG-CoA to mevalonate is the rate-limiting and most regulated step in cholesterol synthesis. It is mediated by the action of the membrane-bound enzyme HMG-CoA reductase (HMGCR) which is regulated at the transcriptional and post-translational level[59]. Transcriptional regulation of the HMGCR gene occurs through the SREBP2 transcription factor[60]. Briefly, under low cholesterol conditions, SREBP2 is found on the ER membrane in complex with the sterol regulatory element-binding protein cleavage-activating protein (SCAP) which in turn binds with high affinity to the insulin-induced protein Insig. Low levels of cholesterol lead to degradation of Insig and transport of the SCAP:SREBP2 complex to the Golgi where the site proteases SP1 and SP2 cleave SREBP2 to allow the bHLH N-terminal domain to translocate to the nucleus and bind sterol-regulatory elements upstream of the HMGCR gene to induce its expression[61]. Post-translationally, Insig causes HMGCR degradation by recruiting ubiquitination enzymes to the N-terminal of the protein under high sterol conditions[62]. Additionally, under low ATP conditions, AMPK phosphorylates HMGCR to inhibit its activity allosterically[59]. HMGCR is also the pharmacological target for the highly prescribed cholesterol-lowering statin family of drugs[63]. Mevalonate produced in the cytosol is imported into the peroxisome where it is transformed into two isoprenoid intermediates through a series of phosphorylations and a decarboxylation. The intermediates, isopentenyl-PP and dimethylallyl-PP, combine to form farsenyl-PP which is converted to squalene and brought back to the ER. Cyclization of squalene

leads to the formation of lanosterol through several intramolecular rearrangements and is followed by a series of demethylation steps to form cholesterol[58]. The esterification of cholesterol is catalyzed by acyl-CoA:cholesterol acyltransferases (ACAT1 and ACAT2) using long chain fatty acyl-CoAs. Both isoforms are expressed in hepatocytes and their activities has been shown to be allosterically activated by cholesterol and other sterols[64,65].

Cholesterol is an important component of cellular membranes, which makes it an attractive host factor for invading pathogens. For instance, the human immunodeficiency virus Gag protein associates with cholesterol-enriched rafts on the plasma membrane, and cholesterol depletion of infected cells reduces viral particle formation[66]. Similarly, the influenza virus hemagglutinin glycoprotein interacts with lipid rafts rich in cholesterol and sphingomyelin[67]. Another example is that of the non-enveloped positive-stranded RNA enteroviruses which hijack clathrin-mediated endocytosis to traffic cholesterol from the plasma membrane to replication organelles, where the sterol can regulate viral polyprotein processing and enable genome synthesis[68].

VLDL synthesis and secretion

In the liver, cholesterol esters and triacylglycerols are packaged into very low-density lipoprotein (VLDL) particles for export. The structural backbone of VLDL particles is the apolipoprotein B (apoB). TAG association with ApoB is thought to occur via two steps. The first step consists of the formation of a small dense precursor particle in the ER membrane containing a phospholipid shell, apoB and a small number of TAGs[69]. This step is dependent on the activity of the microsomal triacylglycerol transfer protein (MTTP)[70]. The subsequent step consists of the fusion of the precursor with a large TAG droplet in the ER lumen. Interestingly, sufficient evidence exists that newly synthesized TAGs do not get directly packaged into VLDL particles, but instead, cytosolic TAGs undergo lipolysis and are re-esterified by DGAT2. This turnover lytic process is believed to be mostly catalyzed by the serine hydrolases arylacetamide deacetylase (AADAC) and

triacylglycerol hydrolase, also known as carboxylesterase 1 (CES1)[71]. Insulin is an inhibitor of VLDL secretion[72,73] and was shown to decrease ApoB levels by promoting its degradation in hepatocytes[74].After their formation in the ER, VLDL particles are transported to the Golgi via VLDL transport vesicles for final processing and maturation before being excreted into the bloodstream[75]. Processing of VLDL particles in the circulation is catalyzed by lipoprotein lipase (LPL)[76] while hepatic lipase (HL), also known as lipase C (LIPC), is thought to bridge high-density lipoprotein (HDL) lipid metabolism to cellular lipid metabolism in the liver through its ability to metabolize phospholipids and triglycerides[77]. VLDL metabolism is an essential part of the hepatitis C virus life cycle, an aspect which is explored in chapter 3 of this thesis.

Lipolysis

Lipid pools within hepatocytes are dynamic and frequent turnover of lipid species requires the breakdown of triglyacylcerides, diglyacylcerides and monoacylglycerides (MAGs) to release fatty acids and glycerol. Unlike in lipid synthetic pathways, the nature of the specific enzymes responsible for each step of this process has yet to be fully determined. The canonical enzyme for TAG hydrolysis is adipose triglyceride lipase (ATGL), also known as patatin-like phospholipase domain 2 (PNPLA2)[78]. However, ATGL expression in the liver is low and recent evidence has uncovered the contribution of other lipases such as the previously mentioned AADAC and CES1 to TAG breakdown[79]. Another enzyme believed to contribute is PNPLA3, a close relative to PNPLA2, with high expression in hepatocytes. PNPLA3 localises to lipid droplets and is transcriptionally regulated by the carbohydrate response element binding protein (ChREBP) and by SREBP1c[80]. While hydrolysis of DAGs to MAGs is catalysed by hormone sensitive lipase (HSL) in adipocytes, its contribution to hepatic catabolism in human liver is controversial. However, AADAC and CES1 are also believed to contribute to DAG hydrolysis in hepatocytes[78]. Monoglyceride lipase (MGLL or MAGL) is the main enzyme responsible for the conversion of MAGs to free fatty acids and glycerol which is considered the rate limiting step for the full

breakdown of TAGs[81]. MGLL-deficient fasted mice have impaired lipolysis and reduced plasma and liver TAG levels[82]. Its activity regulates the production of a large number of signalling lipids, the most studied being 2-arachidonylglycerol (2-AG). This abundant MAG is a potent endogenous activator of endocannabinoid signalling acting on the cannabinoid receptor type 1 (CB1) receptor[83]. Additionally, 2-AG's fatty acid metabolite, arachidonic acid, is a precursor for prostaglandin synthesis and plays roles in inflammation and immunity[84]. The last few years have seen a tremendous increase in the development of MGLL inhibitors, with over 20 patents filed between 2018 and 2021 alone[85]. This interest is fueled by the enzyme's apparent roles in pain, inflammatory disorders, depression, metabolic disorder, cardiovascular disease and cancer[86]. MGLL regulation is not fully understood, but the gene is believed to be under PPARα transcriptional control[87].

PPAR alpha

Free fatty acids, both saturated and unsaturated, activate the PPARα ligand-activated nuclear receptor[88]. This regulator of transcription controls the expression of genes involved in fatty acid oxidation, fatty acid elongation and desaturation, triglycerides synthesis and breakdown, lipoprotein and lipid droplets metabolism, gluconeogenesis and bile acid metabolism[89]. PPARα binds specific PPAR response elements (PPREs) upstream of target genes as a heterodimer with retinoid X receptor (RXR) to promote association with transcriptional complexes[90]. As part of its effect on lipid metabolism, it enhances cellular uptake of fatty acids by increasing the expression of the fatty acid transport protein (FATP) and fatty acid translocase (FAT) and increases the expression of genes in beta-oxidation[91]. Synthetic ligands of PPARα are currently under clinical use for the reduction of plasma triglycerides and regulation of VLDL levels[89].

Beta oxidation

The catabolism of fatty acids occurs via the process of beta oxidation in the mitochondrial matrix. However, cytosolic free fatty acids are not able to directly cross the mitochondria membrane and must first be primed for transport through the carnitine shuttle. Acyl-CoA synthetase catalyzes the

addition of coenzyme A to free fatty acids[92]. Subsequently, carnitine-palmitoyl-transferase 1 (CPT1) replaces CoA with carnitine to form acyl-carnitine and allow its passage through the carnitine-acylcarnitine translocase carrier in the mitochondrial membrane. Once in the mitochondrial matrix, carnitine-palmitoyl-transferase 2 (CPT2) transfers CoA back to fatty acyls to form acyl-CoAs ready for beta-oxidation[93]. The process of fatty acid oxidation roughly follows the same steps as fatty acid synthesis, but in reverse. Fatty-acid CoA is first dehydrogenated to an enoyl-CoA to which water is added to form a β-hydroxyacyl-CoA. A subsequent dehydrogenation forms a β-ketoacyl-CoA and lastly, the release of acetyl-CoA allows the cycle to restart[94]. In order to avoid the formation of a futile cycle, malonyl-CoA regulates beta oxidation by inhibiting CPT1[95].

Several viruses have been shown to impair beta-oxidation. This is again a well-known effect of the hepatitis C virus which has been shown to downregulate the mitochondrial trifunctional protein (MTP) responsible for catalysing three out of the four steps in beta oxidation[96]. Similarly, the Japanese encephalitis virus nonstructural protein 5 associates with MTP to block fatty acid degradation[97]. It has also been shown that mice with dysregulated beta oxidation are more susceptible to Influenza A infection[98].

1.2.3 Liver glucose metabolism and regulation

Liver lipid and glucose metabolism are intrinsically linked by the flow of metabolites and the energy demands of the body. The liver has the unique ability to store and release glucose in response to various metabolic signals. The predominant glucose transporter in hepatocytes is the passive bidirectional glucose transporter-2 (GLUT2)[99]. Following cellular entry, glucose is phosphorylated to glucose 6-phosphate (G6P) by hexokinase enzymes[100]. The main liver hexokinase, hexokinase IV or glucokinase, is upregulated in expression by insulin and downregulated by glucagon[101]. This is the first step of glycolysis, but it is also a crucial step for the formation multiple other metabolic

intermediates. Indeed, G6P can be used in glycogen synthesis, in the hexosamine pathway, as well as in the pentose phosphate pathway[102]. The formation of pyruvate from glycolysis leads to the generation of acetyl-CoA via the action of pyruvate dehydrogenase and links the breakdown of glucose to lipid anabolism and to ATP production via the Krebs cycle. Gluconeogenesis is in principle the reverse of glycolysis, producing glucose from pyruvate and Krebs cycle intermediates for export into the circulation during periods of starvation[103]. The two pathways share seven enzymes which catalyse reversible steps. However, the process of gluconeogenesis also involves four unique enzymes not implicated in glycolysis. Regulation of these two pathways occurs at their respective unique enzymatic transformations. An overview of the steps of glycolysis and gluconeogenesis are presented in figure 1-3. The dephosphorylation of G6P in gluconeogenesis is the last step to release glucose and is catalysed by glucose-6-phosphatase (G6Pase). This enzyme is under the opposite hormonal regulation of glucokinase, as its expression is downregulated by insulin and upregulated by glucagon[104]. Phosphoglucose isomerase, catalyses the transformation of G6P to fructose-6-phosphate (F6P) and vice-versa[105]. The next step in glycolysis is the phosphorylation of F6P to fructose-1,6-bisphosphate. This is the first committed and rate-determining step of glycolysis and it is catalysed by phosphofructokinase-1. The activity of this enzyme is upregulated by AMP, ADP, fructose 2,6-bisphosphate and downregulated by ATP, citrate and acyl-CoAs[106]. The inverse reaction in gluconeogenesis is catalysed by fructose bisphosphatase and is inhibited by fructose 2,6- bisphosphate and AMP[107]. The following six reversible reactions are catalyzed by a series of enzymes common to glycolysis and gluconeogenesis. Briefly, in glycolysis, fructose-1,6-bisphosphate is converted to two molecules of glyceraldehyde 3-phosphate which are sequentially transformed to two molecules of phosphoenolpyruvate. Gluconeogenesis follows the same steps in reverse[108]. The conversion of phosphoenolpyruvate to pyruvate in glycolysis is catalysed by one enzyme, pyruvate kinase (PK), who's activity is highly regulated. The affinity of the enzyme for its substrate is increased

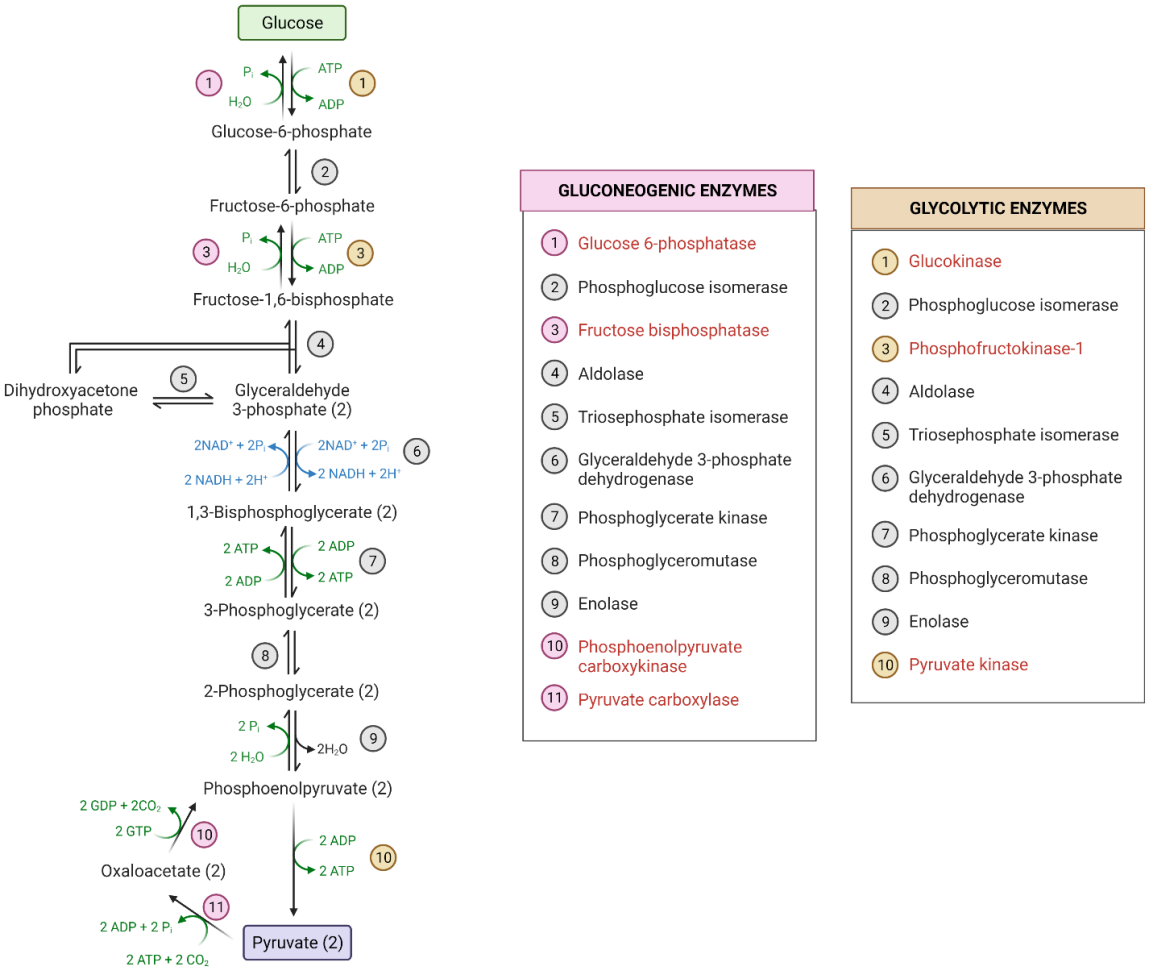

Figure 1-3. Overview of the main enzymatic steps of glycolysis and gluconeogenesis. Enzymes unique to gluconeogenesis are numbered with a pink circle while enzymes unique to glycolysis are numbered with a yellow circle. These respective enzymes (red font in the legend) are the main sites of regulation of these pathways, see text for details. Scheme made in BioRender.com.

allosterically by fructose-1,6-bisphosphate[109]. Inhibition of PK is mediated by several metabolites, including phenylalanine, alanine and thyroid hormone triiodo-l-thyronine. The activity of this enzyme is also modulated by phosphorylation and acetylation[110]. The opposite transformation of pyruvate to phosphoenolpyruvate in gluconeogenesis occurs through two steps. Firstly, pyruvate carboxykinase transforms pyruvate into oxaloacetate. This biotin-dependent enzyme is allosterically activated by acetyl-CoA and inhibited by aspartate[111]. In the second step, phosphoenolpyruvate carboxykinase (PEPCK) catalyzes the conversion of oxaloacetate to phosphoenolpyruvate. Two forms of PEPCK exist, one mitochondrial form (PEPCK-M) and one cytosolic form (PEPCK-C)[112]. The latter is most studied in the context of gluconeogenesis and its expression is known to be reduced by insulin and increased by glucagon[113].

Insulin and glucagon are hormones central to the regulation of glucose metabolism as exemplified by their regulation of multiple enzymes in these pathways. Insulin signalling starts by binding of the hormone to the insulin receptor (INSR) which acts as a tyrosine protein kinase and phosphorylates insulin receptor substrate (IRS) proteins[114]. Evidence suggests that regulation of gluconeogenic genes by insulin is mediated through the phosphatidylinositol 3-kinase (PI3K) pathway[115]. Activation of PI3K by IRS proteins promotes the phosphorylation of the secondary messenger PI-(4,5)-bisphosphate which in turn increase the activity of 3-phosphatidylinositol-dependent kinase-1 (PDK1). PDK-1 phosphorylates and activates protein kinase B (PKB, also termed Akt)[116]. It has been shown that overexpression and activation of PKB in hepatocytes decreases PEPCK and G6Pase gene transcription[117]. Part of this effect is thought to be mediated by the phosphorylation of the Forkhead Box O1 (FoxO1) transcription factor, a key regulator of PEPCK and G6Pase expression, leading its translocation outside of the nucleus[118,119]. Glucagon signalling is initiated at its seven transmembrane G-protein-coupled receptor. Binding of the hormone leads to a conformational change which activates G_s alpha subunit ($G_{\alpha s}$)-coupled proteins,

leading to activation of adenylate cyclase and an increase in cyclic AMP (cAMP) levels[120]. Increased intracellular cAMP activates protein kinase A (PKA) which phosphorylates the cyclic AMP response element (CRE)-binding protein (CREB) at serine residue 133. This allows CREB to promote recruitment of the transcriptional co-activator CREB-binding protein (CBP) upstream of target genes such as G6Pase and PEPCK to induce their expression[121]. Additionally, PKA phosphorylates the phosphofructokinase and fructose 2,6-bisphosphatase enzymes, activating the former and inhibiting the latter, thereby promoting gluconeogenesis. Finally, this kinase also inhibits the activity of pyruvate kinase, decreasing the overall rate of glycolysis[122].

From a whole-body perspective, starvation is known to activate liver gluconeogenesis and inhibit glycolysis. This is because the brain is an obligatory glucose user and therefore, the liver must maintain sufficient blood glucose levels to offset utilization in the brain. Once glycogen stores are depleted, glucose is produced from substrates such as lactate, amino acids and glycerol through gluconeogenesis[123]. This increase in liver gluconeogenesis is in major part mediated by higher production of glucagon and decreased insulin secretion from the pancreas[124]. However, recent evidence suggests that glucose starvation also modifies histone acetylation patterns in metabolic genes[125,126]. Additionally, there is considerable support for a perturbed response to starvation in cancer cells with the activity of gluconeogenic enzymes being repurposed to promote proliferation[127,128]. This is in addition to the classical hijacking of glycolytic and lactate producing pathways by cancer cells which makes the study of glucose metabolism challenging in these models[129].

1.3 Immunometabolism and host-pathogen interactions

Immunometabolism is defined as the interplay between immunological and metabolic processes[130]. This broad term can refer to metabolic pathway stimulation within immune cells[131], to activation of the immune system by metabolic disorders[132] or to modulation of metabolism during the immune

response to external pathogens[133]. Herein, we will be focussing on the latter, aiming to understand the role of metabolism in host-pathogen interactions at the cellular level. Obligate pathogens depend on host processes to replicate and spread. This reliance gives rise to complex interactions between host factors and components of the invading organism. Metabolic pathways are central to energy production, immune support, signalling and for generating the building blocks necessary for cellular remodeling. Therefore, pathogenic infections often lead to perturbations of metabolism, either as a host response to infection or as an effect mediated by the invading pathogen. Some examples of this phenomenon were presented in the previous section. The following segments provide an overview of known immune and metabolic host-pathogen interactions in fungal infections and in viral infections with focus on the *Schizophyllum commune* fungus and the hepatitis C virus (HCV) respectively.

1.3.1 Host-pathogen interactions in fungal infections with focus on *Schizophyllum commune*

Fungal infections in humans are often overlooked in the study of host-pathogen interactions. However, they can be of significant burden to health-care systems and have a broad range of disease outcomes from mild discomfort to high mortality rates[134]. Immunometabolic changes are known to frequently occur in fungal infections[135]. For example, *Candida albicans* infection perturbs glucose homeostasis in the host, leading to significant macrophage cell death[136]. This fungus was also shown to downregulate host IL-17 secretion in peripheral blood mononuclear cells (PBMCs) by releasing soluble factors which modulate host tryptophan metabolism[137]. The *Cryptococcus gattii* fungus is able to modulate metabolic gene expression in lung cells to generate a Warburg-like phenotype. Indeed, proteomic analysis of infected rats demonstrated changes in aerobic glycolysis, the TCA cycle, and pyrimidine and purine metabolism[138]. Finally, the *Aspergillus fumigatus* fungus produces a melanin molecule which inhibits LC3-associated phagocytosis (LAP), an anti-fungal phagocytotic mechanism in macrophages. This inhibition is achieved by selectively excluding the p22phox subunit of the membrane-associated enzyme phagocyte NADPH-oxidase from the

phagosome membrane[139]. Overall, these examples demonstrate how fungi are capable of modulating pathways to promote their pathogenesis.

The *Schizophyllum commune* fungus is a common environmental mould of the Basidiomycetes phylum[140]. In the literature, it is often described as an "uncommon" human pathogen, however, over 15 clinical cases have been reported of invasive infections with this fungus, the majority of them occurring in immunocompromised individuals[141]. Allergic sinusitis as well as pneumonia are major manifestations of infection with his pathogen[142–144], but infections of the brain have also been reported[145,146]. However, the molecular mechanisms through which this specific fungus activates the immune system have not been studied. Chapter 2 of this thesis investigates the transcriptomic changes which occur in liver and lung cells when exposed to a natural alkaloid compound produced by *Schizophyllum commune.*

1.3.2 Host-pathogen interactions in viral infections with focus on the hepatitis C virus

Viruses do not possess the molecular tools to self-replicate and must therefore hijack host pathways to generate the macromolecules necessary to produce new viral particles. Currently, there is a large pool of evidence that many viruses illicit significant cellular metabolic changes[147,148]. Commonly dysregulated pathways in viral infections include nucleotide biosynthesis, glycolysis, lactate generation, the Krebs cycle, fatty acid synthesis and oxidation, cholesterol metabolism and glutamine processing[149]. Modulation of glycolysis is a metabolic perturbation common to multiple viruses, including human cytomegalovirus (HCMV)[150], Herpesvirus-1 (HSV-1)[151], Dengue virus (DNV)[152] and hepatitis C virus[153]. Similarly, perturbations of lipid turnover occur in hepatitis B virus[154], hepatitis C virus[155], Dengue virus[156] and Kaposi's sarcoma associated herpesvirus (KSHV)[157] infections. Due to its ability to hijack, modulate and influence multiple metabolic processes, HCV has particularly been the subject of extensive immunometabolic investigation. The

hepatitis C virus is an enveloped *Flaviviridae* family positive-stranded RNA virus with a global infectious prevalence of over 2% (2005 WHO estimate). It is the foremost cause of liver transplantation in the developed world and currently, no vaccine exists for this virus[158]. HCV is known to extensively interact with the cellular machinery following infection. Amongst others, the virus modulates lipid metabolism[155,159], glucose processing[160,161] and microRNA (miRNA) expression[162,163].

It has long been established that HCV requires high lipid content in the liver for its pathogenesis. Even before the nature of virus was fully understood, the disease was characterized by an accumulation of neutral lipids observed in biopsies of livers from infected patients[164]. Additionally, chronic HCV infection is known to lead to steatosis, cirrhosis and hepatocellular carcinoma[165]. Each step of the viruses' life cycle is intrinsically linked to lipid metabolism. Attachment to hepatocytes involves the low-density lipoprotein receptor (LDLR) and the scavenger receptor BI (SR-BI), in addition to interactions with glycosaminoglycans (GAGs) and the CD81 cell surface protein. Lipoprotein lipase (LPL) has been shown to play a role in HCV entry by mediating binding and internalization of lipoviral particles[166]. Viral entry occurs by endocytosis and is partly mediated by epidermal growth factor receptor (EGFR) signalling and interactions with claudin-1 (CLDN1) and occludin (OCLN)[167]. Following entry, the particle undergoes uncoating to release the viral positive-strand viral RNA which is translated in the ER to produce a single polypeptide precursor. This precursor is then cleaved by host and viral proteases to produce the non-structural (NS) proteins NS3, NS4A, NS4B, NS5A and NS5B as well as the structural proteins core, envelope 1 (E1), envelope 2 (E2) and p7[168]. The RNA-dependent RNA polymerase NS5B performs RNA replication in a cholesterol and sphingolipids-rich vesicular membranous web. This web is thought to be derived from the ER and to be formed in large part by the NS4B protein[169]. The virus' NS5A protein has been shown to modulate membrane composition by controlling the subcellular

localization and activity of the lipid kinase phosphatidylinositol-4-kinase IIIα (PI4KIIIα)[170]. This leads to an increase in phosphatidylinositol-4-phosphate (PI4P) product and recruitment of PI4P effector proteins such as ceramide transfer protein (CERT) and oxysterol binding protein (OSBP), proteins involved in ceramide and cholesterol transport respectively[171]. HCV has also been shown to induce de novo lipid and membrane biosynthesis by modulating the expression of sterol regulatory element-binding protein 1c (SREBP-1c), thereby increasing the expression of fatty acid synthase[172,173]. Lipid droplets (LDs) form the assembly platforms for new viral particles. The core viral protein localize to LDs and plays key roles in the viral assembly process by recruiting nonstructural proteins and replication complexes to LD-associated membranes[55]. Diacylglycerol acyltransferase-1 (DGAT1) was shown to interact with core and facilitate its trafficking to lipid droplets[174]. HCV infection also induces upregulation of ACAT genes and increases the levels of cholesteryl esters (CE)[175], major components of LDs and lipoparticles. In line with this, pharmacological inhibition of TAG and CE synthesis significantly impairs assembly of infectious viral particles in infected cells[176]. Assembly of the replication complexes within LDs is dependent on the hyperphosphorylation of the NS5A viral protein[177] and the production of infectious particles requires the activity of the host phospholipase A2 Group IVA (PLA2G4A)[178]. Maturation and release of the HCV lipoviroparticle is thought to be mediated by interaction with lipoproteins and in tight connection with the VLDL assembly pathway. Indeed, HCV viral particles are of low density and are often referred to as lipoviroparticles (LVPs) due to their association with apolipoproteins such as apoB, apoE, apoC1[179]. Additionally, inhibition of the microsomal triglyceride transfer protein (MTTP) as well as siRNA-mediated knock-down of apoB decrease HCV particle production[180]. Secretion of the particles requires host-factors involved in ER to Golgi trafficking, lipid and protein kinases that regulate budding from the trans-Golgi network and the recycling endosome[181].

In addition to its interactions with lipid metabolic pathways, HCV is well known to influence glucose metabolism. Infection with the virus is significantly associated with glucose abnormalities such as diabetes mellitus and insulin resistance[182,183]. In cell culture, the virus was shown to decrease GLUT2 expression and to promote hepatic gluconeogenesis by upregulating the gluconeogenic enzymes G6Pase and PEPCK via decreased phosphorylation of FOXO1[161,184]. These effects were also observed in cells overexpression the HCV core protein[185]. Additionally, HCV infected or NS5A transfected cells showed an increased phosphorylation of IRS-1 and Akt[186]. Transgenic mice expressing the full HCV open reading frame had reduced glucose uptake and higher hepatic glucose production[160]. Taken together, this evidence draws a clear link between deregulated glucose metabolism and HCV infection.

To enact its effect on metabolism, HCV has been shown to interact with various molecular intermediates in the cell. Recently, the interplay between the virus and host RNA silencing pathway has gained interest. More specifically, the virus has been shown to modulate, hijack and interact with host microRNAs, small non-coding RNAs which modulate gene expression. microRNAs are known to act as important endogenous regulators of cellular pathways, including metabolism[187] and immunity[188]. They are transcribed in the nucleus by RNA polymerase II into primary transcripts which are then processed by the Drosha enzyme complex, cleaved by the Dicer enzyme to generate a 20-26 nucleotide long microRNA duplexes, and incorporated into the RISC complex as single strands to bind complementary gene sequences in target mRNAs[189]. microRNAs can either interact directly with the viral genome or can influence cellular pathways which are essential to viral replication[190]. The best-known example of the former is the interaction between microRNA-122 (miR-122) and the HCV genome. This liver-abundant microRNA was shown to promote HCV replication by binding at two target sites in the 5' UTR of the viral genome and stabilizing the viral RNA against degradation[191,192]. This interaction was also shown to derepress host miR-122 target

genes, demonstrating that the HCV genome can acts as a "sponge" for the microRNA and can influences gene regulation in the cell[193]. Over the years, profiling studies have identified many other microRNAs either up or downregulated during HCV infection with roles in signalling, hepatocyte growth, lipid metabolism, fibrosis and cancer[194]. Of note, activation of innate immune pathways by viral infection has been shown to change cellular microRNA profiles[195]. In the case of HCV, interferon beta signalling triggers the expression of several antiviral microRNAs with direct targets in the viral genome. Examples of such microRNAs are miR-196, miR-296, miR-351, miR-431 and miR-448 which were shown to significantly inhibit viral replication[196]. Other anti-viral microRNAs act by modulating lipid metabolic pathways which are essential to HCV replication. For instance, miR-27a overexpression was shown to decrease viral infectivity via repression of FASN, SREBP1-2, PPARα and several Apo lipoproteins[197]. Recently, research in our group has identified miR-185 as an immune-stimulated microRNA with antiviral effects against HCV[198]. This microRNA is upregulated in hepatocytes by 25-hydroxycholesterol, an antiviral oxysterol produced by interferon-stimulated macrophages and dendritic cells. miR-185 was previously known to regulate genes in lipid metabolic pathways such as cholesterol and fatty acid synthesis[199,200]. Chapter 3 of this thesis has a closer look at direct and indirect targets of this small RNA to better elucidate its roles in metabolism and immunity against HCV.

1.4 ABPP as a chemical biology tool for studying cellular pathways and host-pathogen interactions

Proteomics is a vast field of study which aims to deepen understanding of protein expression, structure, function and interactions. Proteomics studies complement genomics work by directly investigating the downstream products of genes and allowing a thorough analysis of healthy and diseased states[201]. Early proteomics approaches focused mostly on protein separation and identification. For example, proteins in cellular extracts could be isolated by two-dimensional

electrophoresis or liquid chromatography and identified by mass-spectrometry[202–204]. However, demystifying protein function and regulation has proven more challenging. Various genetic approaches exist which make use of gene knock-down such as siRNAs-mediated silencing[205] and genome editing[206]. More recently, bioinformatics has played a central role in functional proteomics by allowing function determination based on structural information and protein-protein interactions[207,208]. Still, these techniques only provide an indirect estimate of true function and are not suitable for quantifying changes in enzymatic activities. To address those limitations, the methodology of activity-based protein profiling (ABPP) has been gaining traction. Activity-based protein profiling is a method which provides reliable reporting of enzymatic activity by direct interaction with enzymes. This technique makes use of small-molecule probes often built from known mechanism-based inhibitors of enzymatic activity such as synthetic drugs or natural products. The compounds act as "war heads" and become irreversible inhibitors for the enzymes, covalently binding the active site of the proteins. They are conjugated to reporter tags to allow purification and identification of the labeled targets[209,210]. Using ABPP over transcriptional analysis or abundance quantification allows the direct measurement of protein activity which may be affected by post-transcriptional modifications or protein-protein interactions. In addition, ABPP methodology can be specifically tailored for various types of analytical techniques, for *in vitro* or *in vivo* experiments and for labelling of different enzymes groups[211].

Traditional ABPP relies on protein separation using sodium dodecyl sulfate polyacrylamide gel electrophoresis (SDS-PAGE). Most often, probes are attached to fluorescent tags which allow for in-gel fluorescence scanning of labelled proteins. This method has advantages in terms of the small amount of proteome required, its low cost and quick experimental procedure. However, it carries many limitations such as a low resolution power, the inability to detect lowly-expressed proteins and the difficulty of identifying the labelled enzymes[212]. The nature of the probe and the molecular

weight can provide a rough estimate of which proteins are differentially active between samples, but for more accurate identification, in-gel tryptic digestion and subsequent mass spectrometry are necessary. Liquid chromatography-tandem mass spectrometry (LC-MS/MS) has gained popularity as a robust analytical method for ABPP[213]. This analytical technique works by separating proteins using high-performance liquid chromatography (HPLC), followed by mass determination through tandem mass spectrometry (MS/MS) and finally by peptide identification via specialized software linked to protein databases. LC-MS/MS can be used not only to identify proteins digested from gels, but also for complex mixture analysis[214]. In this way, gel electrophoresis is not required which simplifies the procedure and reduces contamination. In addition, this technique can be used for accurate identification of the target polypeptides or to analyze only the active-site-containing peptides attached to the probe[215]. One of the most used isolation methods is that of biotin-streptavidin "pull-down" where enzymes are first labelled with a biotinylated probe and can be separated from non-labelled proteins by streptavidin bead enrichment. For whole protein identification, the isolated proteins are digested off the beads with trypsin and then run through LC-MS/MS[210]. Alternatively, following streptavidin-enrichment, the peptides can be eluted from the beads and run on SDS-PAGE for western-blotting[216]. Anti-biotin or anti-avidin antibodies can then be used to probe the membrane. Similarly to the fluorescent gel, this method's main limitation is the identification of the proteins based solely on molecular weight. However, when the nature of the protein of interest is known, this method allows for probing with peptide-specific antibodies and can therefore provide confirmation of mass-spectrometry results. For a visual overview of the ABPP workflow, the reader is referred to chapter 3 and its corresponding appendix.

Simple LC-MS/MS allows for the identification of the labelled proteins; however, it can be inaccurate to quantify activity change in separate samples due to inter-run variability. Ideally, the samples to be compared should be combined and differentiated. This can be achieved using stable

isotope labelling. In this method, proteins are labelled with chemical groups of near identical properties but which contain stable isotopes, conferring a different mass to each label. The mass-spectrometry analysis can then be tailored to separate the peptides identified according to the label mass, and quantification can be performed across the differentially labelled groups[217]. An example of such is stable isotope dimethyl labelling where peptide terminal amines and primary amines on lysine amino acids are dimethylated with formaldehyde composed of a combination of ^{12}C or ^{13}C and hydrogen or deuterium[218]. Each group adds increasing weight to the primary amine, yielding a "light", "intermediate" and "heavy" label. The light label is generated using regular formaldehyde and cyanoborohydride creating a mass increase of 28 Da per primary amine, the intermediate label is formed using deuterated formaldehyde, generating a mass increase of 32 Da per primary amine while the heavy label can be produced by combining deuterated and ^{13}C-labelled formaldehyde with cyanoborodeuteride for a mass increase of 36 Da (Figure 1-4A)[219]. The labelling is performed by reacting the amines with formaldehyde to create an iminium ion intermediate which is subsequently reduced with cyanoborohydride. This method is fast, inexpensive and allows three groups of samples to be analysed simultaneously with LC-MS/MS. However, a limitation of this method is that differences are only measured for peptide fragments that contain lysine residues.

A large number of chemical probes have been developed over the past years to specifically label diverse groups of enzymes including serine hydrolases, cysteine proteases, metallohydrolase, kinases, glycosidases, cytochrome P450 enzymes and phosphatases[210]. Fluorophosphonate (FP) is classic covalent ABPP probe which specifically labels active serine hydrolases. The electrophilic reactive moiety of FP is small and reporter tags such as tetramethylrhodamine (TAMRA) or biotin can be easily added to this warhead via a linker region to allow for isolation of labelled proteins (Figure 1-4B). All serine hydrolases are distinguished by a serine-histidine-aspartic acid catalytic triad which allows for electron transfer and nucleophilic attack by the hydroxyl group on the

serine[220]. In the case of FP, the serine attack leads to the loss of fluoride and the formation of a covalent bond between the phosphate group of the probe and the serine at the enzyme active site (Figure 1-4C)[221]. Serine hydrolases are one of the largest enzyme groups, accounting for 1% of the human proteome. They exhibit a large diversity of functions, being able to hydrolyse amide, ester and thioester bonds of proteins and metabolites. However, only about 50% of these enzymes have been well characterized. Of the known serine hydrolases, about half are proteases such as trypsin and chymotrypsin and the other half are considered "metabolic" enzymes[222]. Some examples include fatty acid synthase[223], hepatic lipase[77], lipoprotein lipase[76], the carboxyl esterases[224], acyl-CoA thioesterases[225] and monoacylglyceride lipase[83]. Therefore, probing the activity of these serine hydrolase enzymes can report on the state of metabolic pathways under varying conditions. This approach has previously been applied to the study of host-pathogen interactions in our group which resulted in the identification of CES1 as an important host factor for HCV propagation[226]. The FP probe is similarly used in chapter 3 of this thesis to interrogate the activity of serine hydrolases modulated by an immunometabolic microRNA.

In contrast to the traditional promiscuous ABPP probes which can interrogate large groups of enzymes, probes can also be specifically engineered to target a single enzyme. This can be achieved by either modifying an existing drug to allow the addition of a reporter tag, or by sequentially optimizing a scaffold molecule for increased specificity[227]. Often times, such probes are designed to possess a "clickable handle" which allows for the addition of various linkers or reporter tags through a biorthogonal click chemistry reaction[228]. One of the most widely used biorthogonal reaction for such applications is the Copper(I)-Catalyzed Azide-Alkyne [3 + 2] Cycloaddition (Figure 1-4D) [229]. An example of this is the fatty acid synthase probe based on the FDA-approved anti-obesity drug Orlistat. This alkyne probe was used by our group to report on the increased activity of FASN during HCV infection[230]. Such probes can also be tailored to target and report on

the activity of viral proteins. For instance, the alkyne-hinged 3-fluorosialylfluoride (DFSA) probe and its ester- protected derivative (PDFSA) were designed to target sialidases and were shown to label the influenza virus neuraminidase[231].

ABPP probes can be used to investigate the function of poorly characterized enzymes by reporting on their functional states under various physiological conditions. Recently, Ahn. *et al.* developed a selective inhibitor and probe of the lysophospholipase-like 1 (LYPLAL1) serine hydrolase (Figure 1-4E)[232]. Polymorphism near or in the gene locus for LYPLAL1 has long been associated with multiple metabolic phenotypes such as obesity[233], visceral fat area[234], non-alcoholic fatty liver disease[235] and insulin resistance[236]. However, the endogenous substrates and physiological roles of this enzyme are unknown. Using their probe, Ahn *et al.* observed an increase in LYPLAL1 activity in hepatocellular carcinoma cells. They also showed that treating hepatocytes with the LYPLAL1 inhibitor increases glucose secretion in the media, pointing to a role of the enzyme in glucose metabolism[232]. To further delineate the roles of the enzyme, Kok *et al.* used a ABPP-guided medicinal chemistry method to generate a small molecule allosteric activator of LYPLAL1 and showed that activating LYPLAL1 activity in obese mice improves glucose homeostasis[237]. The alkyne-linked probe synthesised by Ahn. *et al.* is used in chapter 4 of this thesis to probe LYPLAL1 activity under conditions of metabolic stress.

1.5 Rationale and chapter objectives

The work presented in this thesis is diverse and multidisciplinary. Each chapter stands within its own subcategory under the broad umbrella of immunometabolism with the common aim of providing a better understanding of the molecular players within complex interactions in metabolic pathways. The first chapter investigates the transcriptomic changes which occur within cells following exposure to a fungal metabolite. This study ties fungal infection with activation of the

aryl hydrocarbon receptor, a metabolic xenobiotic detoxifying mechanism with roles in immunity. The second chapter of this thesis shifts the focus to host-pathogen interactions in viral infection with emphasis on the anti-HCV microRNA-185 and its modulation of lipid metabolism. This chapter introduces activity-based protein profiling (ABPP) as a useful proteomic tool for identifying direct and indirect microRNA-modulated proteins and identifying potential pharmacological targets in metabolic pathways. Finally, the third chapter of this thesis makes use of a specific ABPP probe to investigate the function of a poorly characterised enzyme, LYPLAL1. This study demonstrates changes in the enzyme's activity under conditions of metabolic starvation and sets the groundwork for further investigation of its role in primary mouse hepatocytes. The last chapter provides a generalised discussion of the implications of each chapter's findings as well as future directions for these projects.

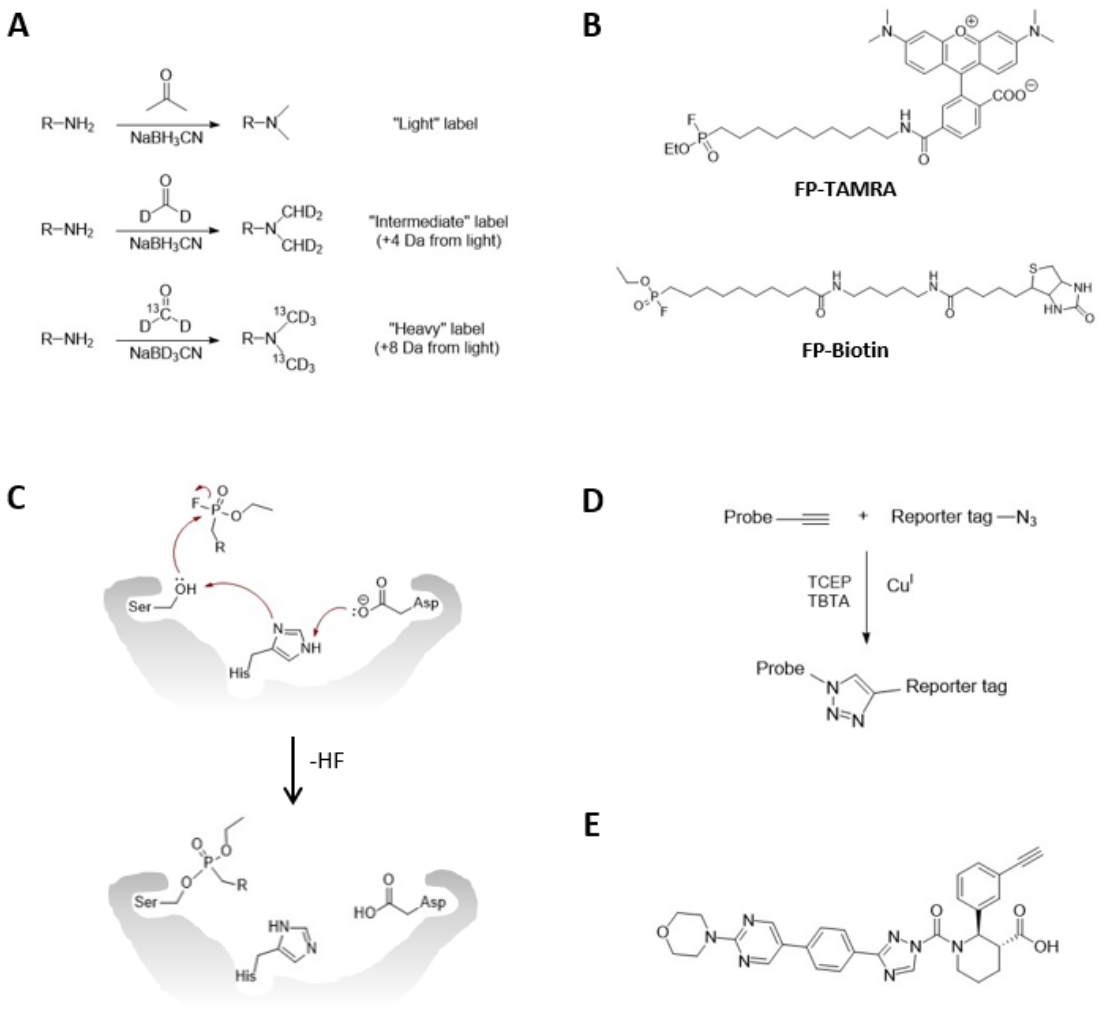

Figure 1-4. Tools for activity-based protein profiling. A. Dimethyl labelling labels used to modify lysine residues for simultaneous MS/MS analysis. The reaction of isotopically labelled formaldehyde and cyanoborohydride adds a "light", "intermediate" or "heavy" label with a mass difference of 4 Da between each. Adapted from Boersema *et al.*[219] **B**. Structures of FP-TAMRA and FP-Biotin probes. **C.** Simplified mechanism of FP-labelling at the active site of serine hydrolases. **D.** Copper-catalysed alkyne-azide click reaction used to join an alkyne probe and a reporter tag. TCEP (tris(2-carboxyethyl)phosphine) is a reducing agent and TBTA (tris((1-benzyl-4-triazolyl)methyl)amine) ligand stabilizes the copper(I)-oxidation state to promote catalysis[388]. **E.** Structure of the LYPLAL1 probe developed by Ahn. *et al.*[232].

Chapter 2: Fungal natural alkaloid schizocommunin activates the aryl hydrocarbon receptor pathway

Initially published as **Filip, R.,** Shaw, T. A., Nishida, A., & Pezacki, J. P. (2019). Fungal natural alkaloid schizocommunin activates the aryl hydrocarbon receptor pathway. MedChemComm, 10(6), 985-990.

2.1 Statement of contributions

This chapter consists of data previously published in RSC Medicinal Chemistry, previously known as MedChemComm, as a research article entitled "Fungal natural alkaloid schizocommunin activates the aryl hydrocarbon receptor pathway". It is reproduced in this thesis with permission from the publisher. This publication was authored by me (Roxana Filip), Tyler A. Shaw, Atsushi Nishida and John P. Pezacki. As first author of this publication, I made significant experimental and intellectual contributions to this article. Atsushi Nishida, John P. Pezacki and I conceived the project idea. The schizocommunin compound and its derivative were kind gifts of Atsushi Nishida. I have performed the majority of the biological experiments with the exception of the cytotoxicity curve treatments which were done by Tyler Shaw. RNA microarray profiling was performed by The Centre for Applied Genomics (TCAG), The Hospital for Sick Children, Toronto, Ontario, Canada. I performed the data analysis, interpretation and wrote the manuscript. Editing of the manuscript was performed by all authors.

2.2 Abstract

Fungi, including mushrooms and mycelia, are a rich source for natural products with medicinal properties. In some cases, they can lead to opportunistic infections in humans and other mammals. In 1994, the first case of bronchopulmonary mycosis caused by the *Schizophyllum commune* fungus was described. Culture of the isolated specimen led to the extraction of an alkaloid compound, schizocommunin, which was more recently synthesized for biological characterization. Herein we describe schizocommunin and one of its analogues as cytotoxic against human hepatoma cells at low micromolar concentrations. Schizocommunin is shown to be a potent activator of the aryl hydrocarbon receptor (AhR) gene battery, more specifically increasing expression of the CYP1A1, CYP1B1 and UGT1A genes in human liver and lung cells. A luciferase reporter assay further confirms induction of transcription by these compounds at the xenobiotic response element. This study improves our understanding of the interaction between this fungal metabolite and xenobiotic detoxifying mechanisms in the body, and points to schizocommunin as a putative mediator of the allergic response and a useful molecule for the study of the AhR pathway.

2.3 Introduction

The *Schizophyllum commune* fungus is an edible basidiomycete species found throughout the globe mostly as a saprobic tree pathogen[140]. It is one of the only species of fungi that can retract by movement. It has also attracted attention for medicinally relevant properties including immunomodulatory functions[238]. Interestingly, in 1989, a specimen was found to cause allergic bronchopulmonary mycosis (ABPM) by growing in the upper lobe bronchus of a patient at the Chiba University Hospital in Japan[142]. The first isolation of the associated natural product schizocommunin was performed from this specimen and it was characterized as a cytotoxic pigment with potential anticancer activity against murine lymphoma[239]. Recently, the structure of the molecule was revised (Figure 2-1A) and a synthetic approach was developed to produce

amounts amenable to biological characterization. It was also shown to be antiproliferative against a cervical cancer cell line[240]. However, the effects of this fungal molecule on cell biology have not yet been clearly established.

The aryl hydrocarbon receptor (AhR) is a highly conserved ligand-activated transcription factor which responds to chemical stimuli to activate adaptive responses of detoxification, homeostasis and immunity[241]. Despite recent advancements regarding the endogenous activation of AhR, its best characterized role is in the xenobiotic response. AhR was first discovered as the main target of 2,3,7,8-tetrachlorodibenzo-p-dioxin (TCDD), the most infamous of the dioxins. Normal activation of the receptor leads to the expression of oxidizing enzymes as a defensive mechanism against environmental toxins. However, over-activation was proven highly toxic, as exposure to TCDD has been shown to cause chloracne, cancer and teratogenicity[242,243]. Inactivated AhR is cytosolic and complexed with Hsp90, XAP2 and p23 (Figure 2-1C). Upon ligand penetration in the cell and binding to AhR, the receptor translocates to the nucleus where the ligand-receptor complex dissociates and subsequently binds the Arnt nuclear protein. This complex then binds AhR responsive elements (AHRE), also referred to as xenobiotic-responsive elements (XREs), upstream of target genes and induces expression of AhR battery genes[244]. The best known examples of AhR activated genes are the cytochromes CYP1A1, CYP1A2 and CYP1B1, aldehyde dehydrogenase 3 (ALDH3A1), the UDP glucuronosyltransferase UGT1A and glutathione S-transferase alpha 1 (GSTA1)[25,245].

In an effort to uncover the mechanism of action of schizocommunin and its synthetic analogue (Figure 2-1B), we have performed genomic profiling and functional assays. Herein, we report that schizocommunin is an exogenous activator of the aryl hydrocarbon receptor. Treatments with the compound as well as with a synthetic analogue showed toxicity against cultured Huh7 human

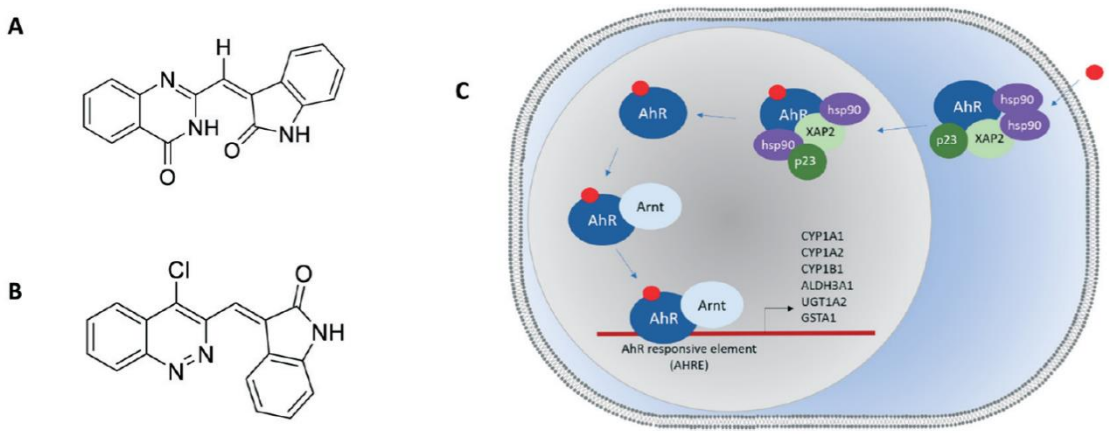

Figure 2-1. A. Structure of schizocommunin and **B.** a synthetic analogue of schizocommunin. **C.** AhR transduction pathway. Introduction of the ligand in the cell results in translocation of the receptor complex to the nucleus and activation of the AhR battery genes (see text for details).

hepatoma cells in the low micromolar range. Transcriptomic analysis showed an increase in the expression of CYP1A1, as well as other genes in the AhR pathway with sub-toxic treatments of liver and lung cells. Transcription activation through the xenobiotic response element (XRE) is confirmed using a reporter assay. Activation of the aryl hydrocarbon receptor by schizocommunin may be one of the mechanisms through which the *Schizophyllum commune* fungus was able to elicit an allergic response in the bronchopulmonary mycosis case.

2.4 Results and discussion

2.4.1 schizocommunin exhibits toxicity towards Huh7 cells

Uehata *et al.* have previously reported low-micromolar toxicity of schizocommunin and its analogue against HeLa human cervical cancer cells[240]. Similarly, we observed a dose-dependent decrease in the metabolic activity of Huh7 cells using an oxidoreductase MTT assay (Figure 2-2). Treatment with the schizocommunin analogue exhibited an EC_{50} value of 9.6 μM, indicative of increased cytotoxicity when compared with an EC_{50} of 31.1 μM for the fungal compound. Interestingly, a tautomerizing hydroxy analogue of this compound in its keto form did not exhibit cytotoxicity in the previously mentioned study on Hela cells[240].

2.4.2 schizocommunin activates the expression of genes in the AhR battery

After determining the EC_{50} of each compound, concentrations of 10 μM for schizocommunin and 0.5 μM for the analogue were chosen for further experiments to avoid cytotoxicity while generating maximal cellular effects. A microarray screen was first performed in Huh7 liver cells to assess the effects of the compounds on cellular transcriptome. This allowed the identification of genes differentially regulated at the RNA level, including messenger RNAs and small non-coding RNAs. Figure 2-3A shows a heat-map representation of the fold changes of major gene categories. Notably, schizocommunin highly upregulated the expression of cytochrome (CYP) genes.

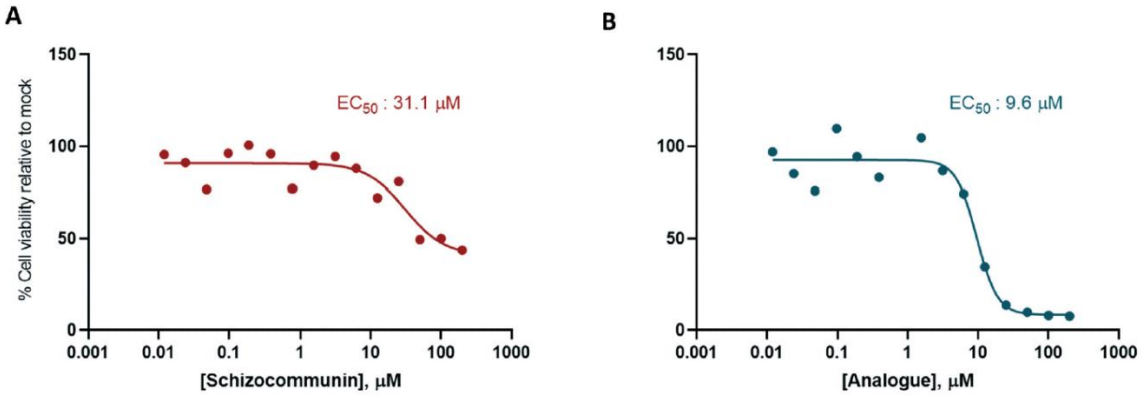

Figure 2-2. Cytotoxicity curves for A. schizocommunin and **B.** the schizocommunin analogue. Cells were treated with compound at concentrations of 0.012 μM to 200 μM for 24 hours after which the cell metabolic activity was quantified via MTT assay.

Expression of CYP1A1 and CYP1B1 enzymes was strongly upregulated (10.5 and 8.6-fold respectively) with the compound, and somewhat upregulated with analogue treatment (3.28 and 1.35-fold). As these enzymes are primarily under the control of the aryl hydrocarbon receptor, we sought to check the expression levels of other genes in the AhR battery using quantitative RT-PCR. As shown in figure 2-3B and C, the levels of CYP1A1, CYP1B1 and UGT1A were increased by treatments with both schizocommunin and its analogue in both human liver (Huh7) and lung cells (A549), although to a generally lower extent in the latter. CYP1A2 basal expression was too low to accurately quantify. Expression levels of GSTA1 were not noticeably affected in the liver cells and could not be accurately detected in the lung cells. Interestingly, while ALDH3A1 did not change in expression with analogue treatment in the liver cells, we observed a decrease in its levels with schizocommunin to 0.65-fold expression, but also noted a significant increase in the lung cells. This points to some variability in the effects of AhR activation in different tissues. The overall lower levels of gene activation by the analogue compound could be due to the lower concentration used in the treatment but could also be reflective of a reduced affinity of the analogue compound for the aryl hydrocarbon receptor. Additionally, the levels of the receptor itself (AhR) and its interacting protein (XAP2) did not change, pointing to a classic xenobiotic ligand activation of AhR. This was confirmed through a xenobiotic response element reporter assay where luciferase expression was indicative of transcriptional activation by induction of the AhR pathway (Figure 2-4). Schizocommunin and its analogue activate the receptor to a lesser degree than the potent AhR agonist 6-formylindolo[3,2-b]carbazole (FICZ); however, they show dose-dependent induction up to 17-fold with 10 μM schizocommunin. Activation of AhR by these compounds is not surprising as a diverse array of polycyclic aromatic hydrocarbon have been shown to affect the pathway[244].

This study has shed some light on the biological effects of the compounds, but it has also opened an array of further investigative avenues. Notably, activation of the AhR has been linked to

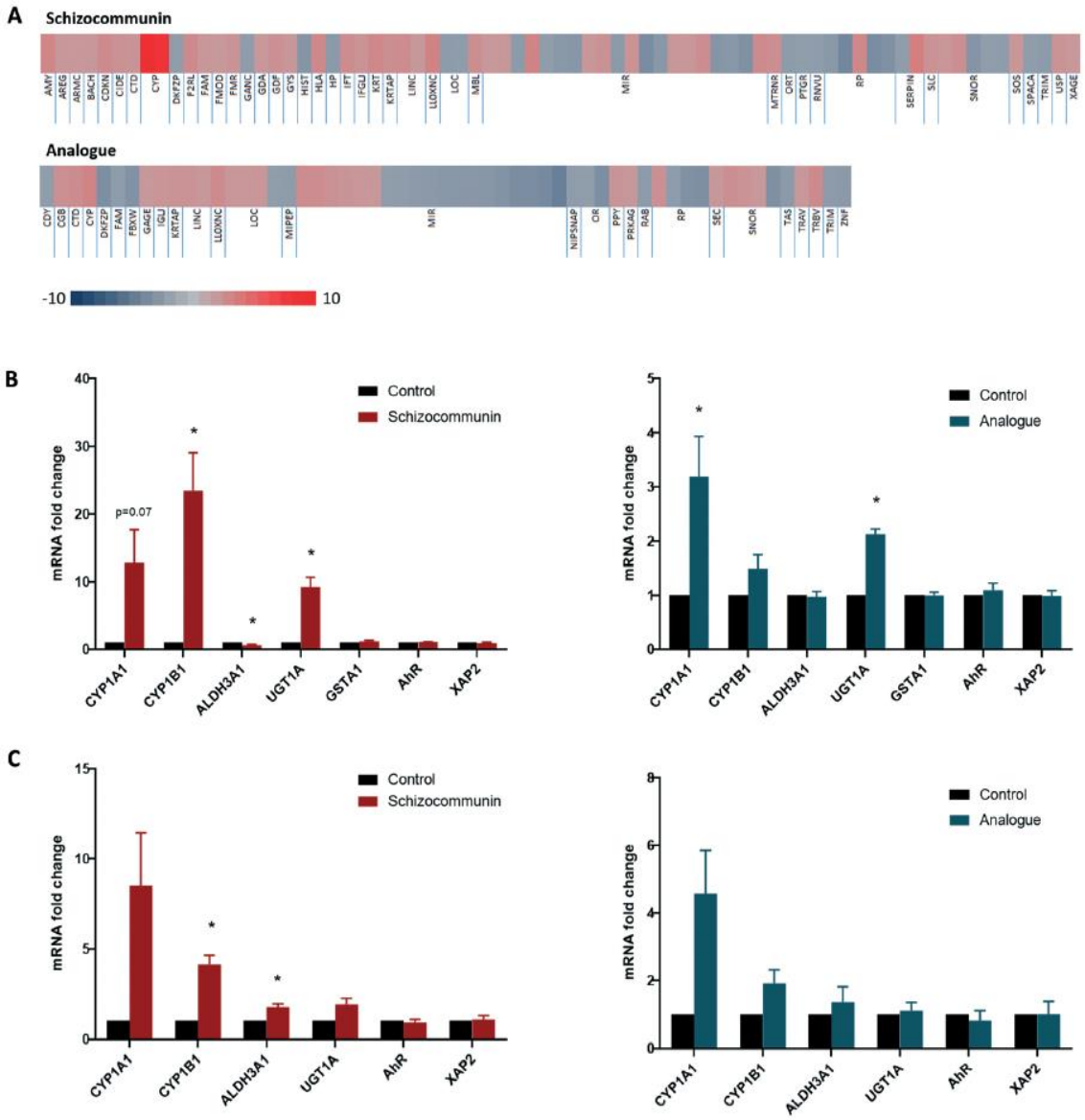

Figure 2-3. Schizocommunin increases expression of genes in the aryl hydrocarbon receptor battery. A. Heat map representing microarray mRNA profiling of gene categories with over 2-fold differential expression in Huh7 hepatoma cells treated with schizocommunin and the schizocommunin analogue. Red represents an increase and blue a decrease, up to 10-fold. **B.** and **C.** Messenger RNA fold changes relative to mock treatment for genes under the regulation of AhR, as well as AhR and XAP2; B. Huh7 cells (n = 5) and C. A549 cells (n = 3). Cells were treated for 24 hours with 10 μM schizocommunin or 0.5 μM of analogue before RNA extraction and RT-qPCR analysis; error bars represent standard error of the mean, * = $p < 0.05$.

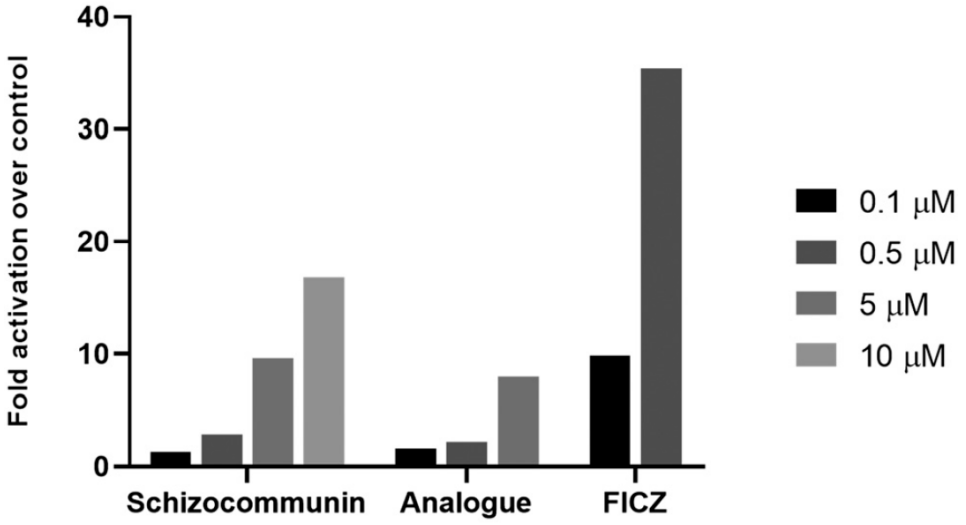

Figure 2-4. Treatments with schizocommunin and its analogue activate the XRE response element in a dose-dependent manner. Cells were transfected with a XRE-luciferase reporter plasmid and treated for 24 hours with the indicated concentrations of the compound. FICZ is a known activator of the AhR pathway. Signal was normalised over cotransfected Renilla luciferase plasmid and DMSO vehicle control.

modulation of immune and allergic responses. AhR expression is high in lungs, liver and a number of immune cells such as Th17 and Treg CD4 T cells as well as activated dendritic cells and macrophages[246]. TCDD exposure has been shown to be immunosuppressive[247]; however, the effects of AhR activation have been reported to be ligand specific. Indeed, in a mouse model of autoimmune encephalomyelitis (EAE), while activation of the receptor by TCDD reduced severity of the disease, activation by FICZ prevented Treg differentiation and worsened the disorder by modulating Th17 cells[24,248]. Additionally, induction of AhR has been linked to mast cell activation and IgE response by both endogenous and exogenous ligands[26]. For example, kynureninem, a metabolite of tryptophan was shown to enhance mast cell degranulation in a AhR-dependent manner[249] while, from a xenobiotic perspective, treatments with FICZ lead to IL-17 and IL-6 pro-inflammatory cytokine production in human and murine mast cells[250]. More recently, tryptophan metabolites have also been shown to mediate CD1d-dependent intestinal inflammation via AhR in response to oxazole exposure[251]. Furthermore, AhR has been shown to modulate the recruitment of inflammatory leukocytes in response to bacterial virulence factors[252]. Therefore, the activation of the pathway by schizocommunin may lead to various direct and indirect immunological effects which may explain the allergic symptoms experienced by the ABPM patient, such as increased serum IgE levels[142].

The AhR receptor has different established functions depending on the cellular context. While induction of AhR is a putative mechanism for the development of ABPM, activation of the pathway has also been linked to apoptosis in several cell types. AhR ligands have been shown to cause cell death in colorectal cancer[253], primary melanocytes[254] and while TCDD is known to prevent apoptosis in some instances, it was shown to activate it in a large number of lineages[255]. It is therefore possible that schizocommunin and its analogue exert some of their cytotoxic activity through AhR.

Potent AhR ligands are useful tools for investigating this detoxifying pathway, as well as signal transduction pathways involving AhR that are medicinally important. We have shown that schizocommunin provides strong upregulation of AhR battery genes, indicating its potential as an AhR modulating small molecule. Future studies should aim to investigate the relationship between these small molecules and the effects of aryl-hydrocarbon receptor induction in the contexts of immunity and cancer.

2.5 Materials and methods

Cell culture and treatments

Human hepatoma (Huh7) or human lung carcinoma (A549) cells were grown at 37°C in DMEM (Gibco, Life Technologies) with 10% FBS (Wisent) and 10 mM non-essential amino acids. One day prior to treatment, cells were seeded at $2.75x10^5$ cells per well in a 6-well plate. The following day, schizocommunin or its analogue were added to final concentrations of 10 μM or 0.5 μM respectively and 0.1% final DMSO. Mock treatment consisted of DMSO only. Cells were incubated with the compounds for 24 hours, after which they were washed with PBS and lysed for RNA isolation.

RT-qPCR

RNA isolation was performed using the RNeasy (Qiagen) isolation kit as per manufacturer's protocol. Reverse transcription was performed using the iScript cDNA Synthesis Kit (Bio-Rad) using 500 ng of RNA as per manufacturer's protocol. Quantitative PCR (qPCR) was performed using SYBR Green Supermix (Bio-Rad) as per manufacturer's protocol on the CFX Real-Time PCR Detection System (Bio-Rad) with the following primer sequences (5' – 3'): CYP1A1 fwrd TCGGCCACGGAGTTTCTTC, CYP1A1 rev GGTCAGCATGTGCCCAATCA; CYP1B1 fwrd AAGTTCTTGAGGCACTGCGAA, CYP1B1 rev GGCCGGTACGTTCTCCAAAT; ALDH3A1

fwrd TGTTCTCCAGCAACGACAAGG, ALDH3A1 rev AGGGCAGAGAGTGCAAGGT; UGT1A fwrd TTGTCTGGCTGTTCCCACTTA, UGT1A rev GGTCCGTCAGCATGACATCA; GSTA1 fwrd CTGCCCGTATGTCCACCTG, GSTA1 rev TCAAAGGCAGGGAAGTAGCG; AhR fwrd CAAATCCTTCCAAGCGGCATA, AhR rev CGCTGAGCCTAAGAACTGAAAG; XAP2 fwrd GAAGGGGAGATTGCCCAGTTC, XAP2 rev CGATGTTGCGGAGACTCTTGG. 18S rRNA was used for normalization and expression fold changes relative to mock treatments were calculated using the $2^{-\Delta\Delta Ct}$ method. Significance assessed with two-tailed, unpaired student's t-test where $p < 0.05$ was considered significant.

MTT cytotoxicity assays

Huh7 cells were cultured and treated as described. One day before treatment, cells were seeded at 10 000 cells per well in a 96 well plate. The next day, cells were treated with a serial dilution of schizocommunin or its analogue for final concentrations between 0.012 and 200 μM and 2% final DMSO. Cells were incubated with the compounds for 24 hours after which they were washed with PBS and incubated with 50 μL MTT reagent (2.5 mg/mL 3-(4,5-dimethylthiazol-2-yl)-2,5-diphenyltetrazolium (Sigma-Aldrich) in PBS) for 3 hours. Excess reagent was removed, and crystals were dissolved in 50 μL DMSO. Absorbance was read at 562 nm using a SpectraMax i3 plate reader (Molecular Devices). Raw values were normalized relative to mock treatment.

Microarray analysis

Huh7 cells were cultured and treated as described. RNA isolation was performed using the RNeasy (Qiagen) isolation kit as per manufacturer's protocol. Expression profiling was performed at the TCAG Facilities of the Centre for Applied Genomics of the Hospital for Sick Children using Affymetrix Human Gene ST.2.0 arrays. Analysis was performed using the Affymetrix Expression Console and Transcriptome Analysis Console. Data is available at NCBI Gene Expression Omnibus, accession number GSE129836.

XRE-reporter assay

Huh7 cells were cultured as described. One day before transfection, cells were seeded at 20 000 cells per well in a 24-well plate. The next day, cells were simultaneously transfected with 50ng/well pGL4-Renilla and 200ng/well pGL4.43[luc2P/XRE/Hygro] (Promega) using 1.25ul per ug of DNA lipofectamine 2000 (Invitrogen, ThermoFisher). The next day, cells were treated with schizocommunin, its analogue or FICZ to final concentrations of 0.1, 0.5, 5 or 10 μM respectively and 1% final DMSO and incubated for 24 hours. Cells were washed with PBS and lysed in passive lysis buffer (Promega). Luciferase assay was performed in technical triplicates in a 96 well-plate as previously described[256].

Chapter 3: Profiling of microRNA targets using activity-based protein profiling: linking enzyme activity to microRNA-185 function

Initially published as **Filip, R.**, Desrochers, G. F., Lefebvre, D. M., Reed, A., Singaravelu, R., Cravatt, B. F., & Pezacki, J. P. (2021). Profiling of microRNA targets using activity-based protein profiling: linking enzyme activity to microRNA-185 function. Cell Chemical Biology, 28(2), 202-212.

3.1 Statement of contributions

This chapter consists of data previously published in Cell Chemical Biology as a research article entitled "Profiling of microRNA targets using activity-based protein profiling: linking enzyme activity to microRNA-185 function". It is reproduced in this thesis with permission from the publisher. This publication was authored by me (Roxana Filip), Geneviève F. Desrochers, David M. Lefebvre, Alex Reed, Ragunath Singaravelu, Benjamin F. Cravatt, and John P. Pezacki. As first author of this publication, I made significant experimental and intellectual contributions to this article. Geneviève F. Desrochers, John P. Pezacki and I conceived the project idea. I have performed the majority of the biological experiments. David M. Lefebvre performed cell treatments with the MGLL inhibitor and western blotting of MJN110 treated samples. Alex Reed performed the targeted MAG and FFA species lipid mass-spectrometry analysis of miR-185 transfected samples at the Scripps Research Institute, La Jolla, CA, USA. RNA microarray profiling was previously performed by Ragunath Singaravelu. Proteomic mass spectrometry analysis and lipid analysis of MJN110-treated samples was performed at the John L. Holmes Mass Spectrometry Facility at the University of Ottawa by former staff Gleb G. Mirinov and current facility manager Zoran Minic respectively. Shotgun lipidomics analysis was performed by Lipotype GmbH, Tatzberg, Dresden, Germany. I performed the data analysis, interpretation and wrote the manuscript with valuable input from Geneviève F. Desrochers, Benjamin F. Cravatt, and John P. Pezacki. Editing of the manuscript was performed by all authors.

3.2 Abstract

MicroRNAs (miRNAs) act as cellular signal transducers through repression of protein translation. Elucidating targets using bioinformatics and traditional quantitation methods is often insufficient to uncover global miRNA function. Herein, alteration of protein function caused by miRNA-185 (miR-185), an immunometabolic miRNA, was determined using activity-based protein profiling, transcriptomics, and lipidomics. Fluorophosphonate-based activity-based protein profiling of miR-185-induced changes to human liver cells revealed that exclusively metabolic serine hydrolase enzymes were regulated in activity, some with roles in lipid and endocannabinoid metabolism. Lipidomic analysis linked enzymatic changes to levels of cellular lipid species, such as components of very-low-density lipoprotein particles. Additionally, inhibition of one miR-185 target, monoglyceride lipase, led to decreased hepatitis C virus levels in an infectious model. Overall, the approaches used here were able to identify key functional changes in serine hydrolases caused by miR-185 that are targetable pharmacologically, such that a small molecule inhibitor can recapitulate the miRNA phenotype.

3.3 Introduction

As an integral part of RNA interference (RNAi), microRNAs (miRNAs) act to prevent endogenous gene transcript translation and induce mRNA destabilization through RNA-RNA interactions. miRNAs influence a large number of cell processes, and have been shown to play important roles in host-pathogen interactions[257]. In the last decade, many in silico methods have been developed to predict targets of miRNAs via seed sequence alignment, including platforms such as miRanda[258] and TargetScan[259]. However, predicted seed sequence interactions in the 3'UTR do not always translate into repression of expression[260] and bioinformatics only allows prediction of direct targets of miRNAs. Techniques involving cross-linking and immunoprecipitation (CLIP) have helped to identify direct miRNA-mRNA interactions[261], yet such data still do not always accurately predict

miRNA function. Complex interactions such as those in signalling cascades lead to changes in the proteome that are difficult to predict, and post-translational modifications substantially alter the functional proteomic landscape. Consequently, the outcome of a single miRNA's expression cannot easily be foretold from its putative targets.

To deduce the functional effects of a specific miRNA, we used activity-based protein profiling (ABPP) as a screening method to determine the impact of miRNA-185 (miR-185) on a subset of the human hepatoma proteome. miRNA-185 has emerged as a modulator of immunometabolism in the liver. This miRNA was previously known to repress cholesterol uptake[200] and was recently shown to target a number of genes involved in lipid biosynthesis and metabolism regulation, leading to a lipid-depleted antiviral state during hepatitis C virus (HCV) and other viral infections[198].

In the following study, we used ABPP (Figure 7-1A) to characterize the activity of serine hydrolase enzymes during miR-185 signalling. The human proteome contains over 200 serine hydrolases, many of which have been shown to have important roles in metabolism[262,263] and infection[264]. Furthermore, these enzymes have proven to be attractive pharmacological targets owing to their crucial roles in complex biological pathways, with multiple drugs targeting these enzymes already available on the market[220]. Results from quantitative ABPP involving multiplex stable isotope dimethyl labeling allowed several miR-185-modulated serine hydrolases to be identified. Interestingly, all the hits fell within the metabolic serine hydrolase family, and amongst these, not all were predicted targets of the miRNA. Classification of these enzymes showed enrichment of pathways such as lipid metabolism and endocannabinoid hydrolysis and pointed to modulation of a peroxisome proliferator-activated receptor (PPAR) by miR-185. Lipidomic analysis showed a decrease in cholesteryl ester and triglyceride species consistent with known roles of the small RNA

and provided further insight into the structural variations within lipid classes resulting from the enzymatic changes observed with ABPP. Finally, pharmacological inhibition and siRNA-mediated knock-down of one of the targets, MGLL, significantly reduced HCV levels in an infectious cell model, further validating the role of the enzyme in miR-185's antiviral effect. Overall, our results demonstrate the applicability of ABPP as a useful tool, in conjunction with systematic –omic analysis, as illustrated in summary figure 3-1A, for the investigation of non-coding RNA function. This study further demonstrates that miR-185 has functional roles in lipid metabolism, endocannabinoid metabolism and very-low density lipoprotein (VLDL) synthesis.

3.4 Results

3.4.1 Activity-based protein profiling reports on microRNA function

Given that miR-185 has been shown to modulate metabolism in the liver to give rise to an antiviral state, we wanted to identify enzymes which contribute to this immunometabolic effect. Of the 238 currently known serine hydrolases, about half are considered metabolic enzymes, including lipases, peptidases, esterases, and amidases (Figure 3-1D)[220]. This large enzyme class can be characterized by ABPP using fluorophosphonate (FP) reactive groups coupled to reporter tags such as biotin (Figure 3-1B)[265]. In order to identify differentially regulated metabolic serine hydrolases, we transfected Huh7.5 human hepatoma cells with a miR-185 mimic and after a 72 hours incubation, lysed the cells to collect the active proteome. We incubated this lysate with a FP-biotin probe and isolated the labelled enzymes with streptavidin bead enrichment, column purification and trypsin digestion (Figure 3-1C). Mass spectrometry analysis of activity-labelled serine hydrolases in the presence or absence of miR-185 in these cells yielded a total of 17 enzymes represented in three trials with average activity fold changes under 0.8 or above 1.2 (Figure 3-1E, Table 7-1). Interestingly, only two of the hits (ACOT1 and PREPL) were strongly predicted to be direct targets

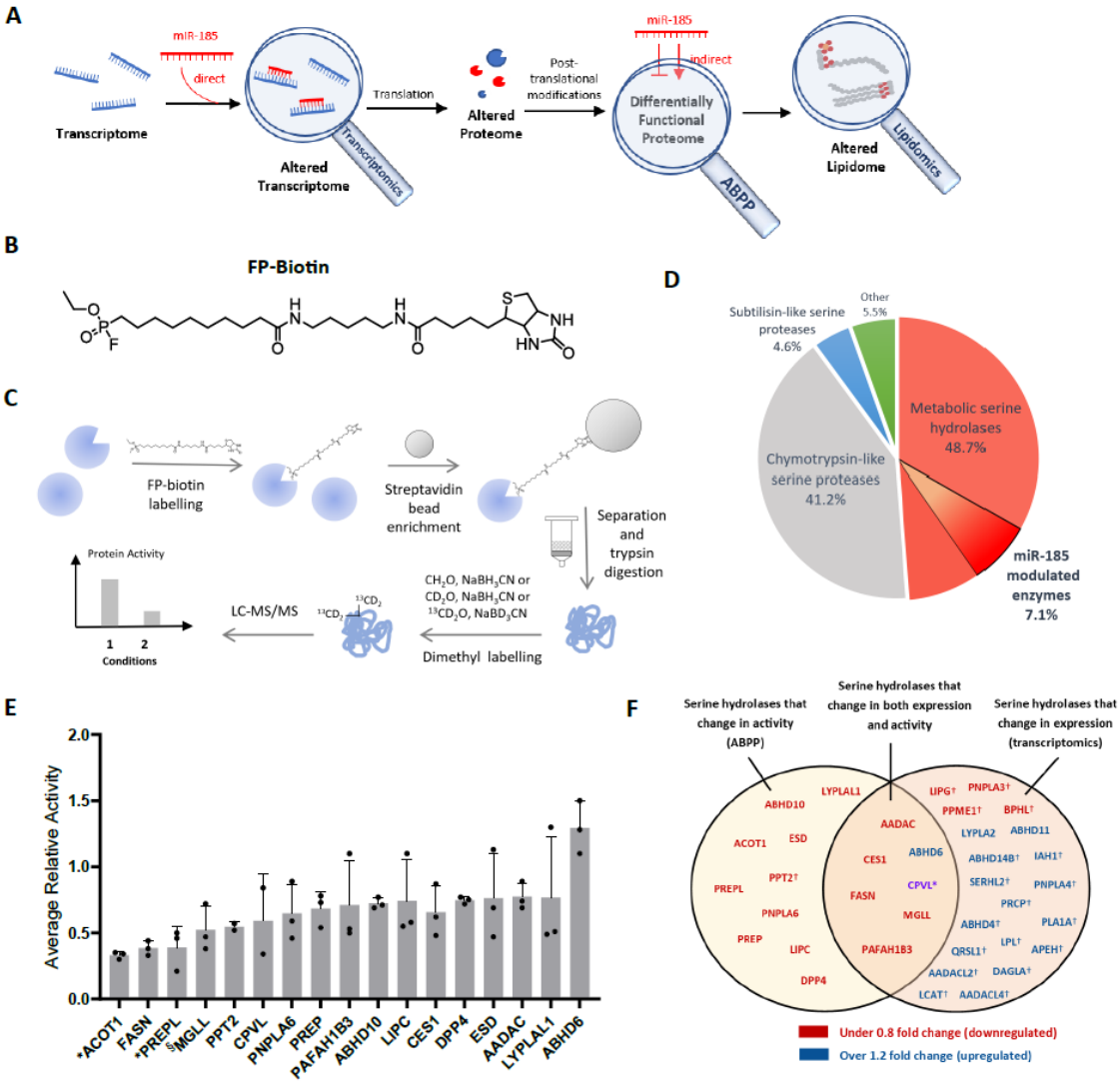

Figure 3-1. miR-185 alters protein activity and lipid metabolism. A. miR-185 exerts its effects both directly, by binding to mRNAs and modifying the proteome, or indirectly by affecting downstream post-translational modifications and interactions. A combination of transcriptomics, ABPP, and lipidomics analysis allows probing of the pathway at intermediate and end-point states. **B.** Structure of FP-biotin. **C.** Workflow of the mass spectrometry ABPP experiment. The active serine hydrolases are labelled with FP-biotin, enriched with streptavidin beads, and separated from the rest of the proteome. They are then digested with trypsin before being isotopically labelled and analyzed via liquid chromatography-tandem mass spectrometry (LC-MS/MS). **D.** Pie-chart depicting classification of the known serine hydrolases based on sequence relatedness[220]. All miR-185-regulated enzymes are metabolic. [caption continued on next page]

[Figure 3-1. caption continued]

E. Average relative activity of serine hydrolases from miR-185 transfected cells compared with a non-targeting control RNA ± SD as determined with mass spectrometry analysis. Hits with changes between 0.8 and 1.2 were excluded n = 3. *Predicted miR-185 targets; §validated miR-185 target. Data for each trial can be found in Table 7-1. **F.** Metabolic serine hydrolases with changes lower than 0.8 (red) or higher than 1.2 (blue) in activity (determined with FP-ABPP), expression (determined with microarray transcriptome analysis), or both. *One enzyme in purple, CPVL, was seen to increase in mRNA abundance and decrease in activity. Dagger (†) indicates enzymes that were not detected with the other method. Fold changes for the microarray data can be found in Table 7-2.

of the miRNA through the miRanda and TargetScan platforms. Figure 3-1F compares the direction of the activity changes of serine hydrolases determined via ABPP with their transcript abundance as determined with microarray analysis. We identified six enzymes with similar changes in activity and transcript abundance, ten enzymes that were seen to only decrease in activity, and one enzyme that had lower activity while exhibiting a slight increase in mRNA abundance. These differences illustrate the ability of ABPP to report on functional changes in enzymes which may be due to post-translational modifications or interactions with other cellular factors. To obtain a visual idea of the changes in activity, we labelled miR-185 transfected lysates with fluorophosphonate attached to a fluorescent tag, FP-TAMRA. After running these samples on an SDS-PAGE gel, a change in the activity of FASN and MGLL was observable (Figure 7-1B). However, due to the low abundance of some serine hydrolases as well as the poor sensitivity of this technique, other changes were not identified. Working with the hits list obtained via mass spectrometry, activity changes of enzymes with known metabolic functions and deemed of interest in the context of miR-185 were further validated with western-blot pull-downs and their change in expression was confirmed via RT-qPCR. They were then assigned into one of two categories based on their functions: lipid metabolism or endocannabinoid metabolism.

3.4.2 miRNA-185 downregulates the activity of serine hydrolases involved in lipid metabolism

In order to determine which of the serine hydrolases identified by ABPP might be relevant to lipid metabolism, we classified them based on their putative functions. Approximately half of the hits we found to be involved in pathways previously shown to be relevant to miRNA-185 function. Amongst the enzymes that were seen to decrease in activity, fatty acid synthase (FASN), arylacetamide deacetylase (AADAC), acyl-CoA thioesterase 1 (ACOT1) and lipase C (LIPC) are proteins well known for their roles in lipid metabolic pathways. These enzymes are involved in

fatty acid biosynthesis, triglyceride hydrolysis, fatty acid β-oxidation and lipoprotein remodelling respectively[266–269].

To validate the changes observed via mass-spectrometry, we labelled proteomes of miR-185 transfected cells with FP-biotin, performed streptavidin pull-downs and ran the labelled fractions on an SDS-PAGE gel, followed by transfer and immunodetection for these specific enzymes (Figure 3-2A). This technique provides a visual confirmation of activity changes which can be compared with abundance changes in the whole lysates. We also probed the levels of messenger RNA using RT-qPCR. We observed a reduction in both the activity and abundance of the FASN, AADAC and ACOT1 enzymes (Figure 3-1E, 3-2B, C). ACOT1 was the only one predicted to be a target of miR-185 by both the miRanda and TargetScan platforms. Interestingly, our results show a downregulation of LIPC activity by miR-185 (Figure 3-1E, 3-2B) while the abundance of the protein was not seen to vary significantly via western blotting and had a modest decrease in mRNA (Figure 3-2B, C), pointing to an enzymatic regulation mechanism which is affected by miR-185. Therefore, the reduction in the activities of these four enzymes at various steps of lipid synthesis and degradation is one of the ways in which the non-coding RNA changes the lipid profile of cells.

3.4.3 miRNA-185 regulates the activity of serine hydrolases involved in endocannabinoid lipid metabolism

To further delineate the role of miR-185, we grouped three enzymes with a common link to endocannabinoid metabolism. Functions of the endocannabinoid pathway vary based on tissue localization, but from a metabolic perspective, activation of the receptors has been linked to obesity[270], hepatic insulin signalling[271] and hepatitis C[270,272]. The system is comprised of the G-protein coupled receptors CB1 and CB2, their endogenous lipid ligands anandamide (N-

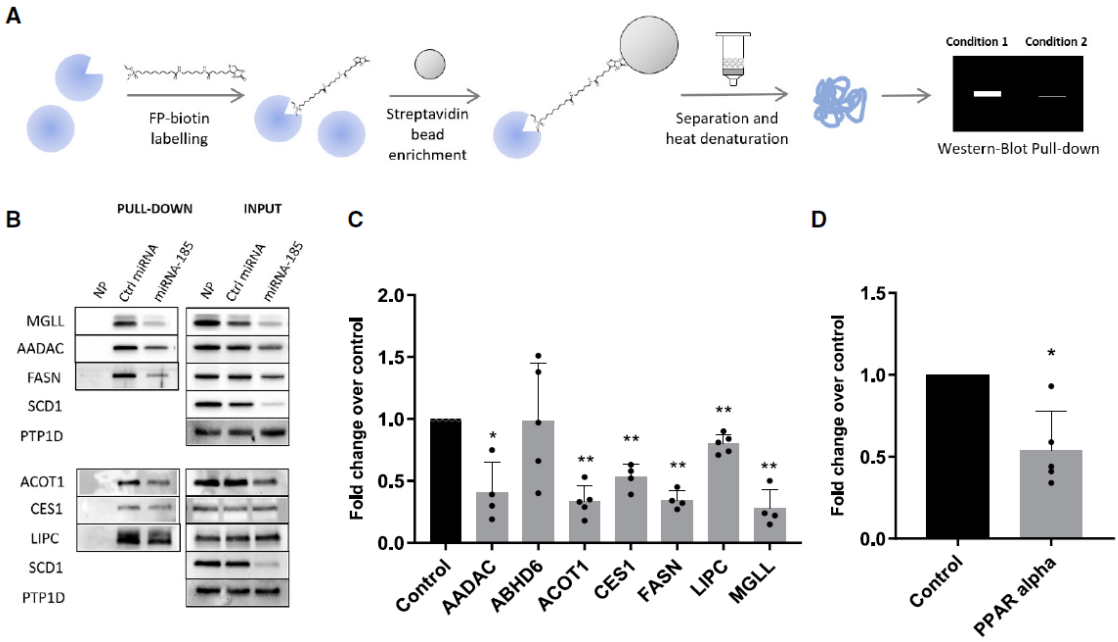

Figure 3-2. miR-185 acts on genes involved in lipid regulation and endocannabinoid metabolism. A. Workflow of the western-blot ABPP experiments. The active serine hydrolases are labelled with FP-biotin, enriched with streptavidin beads, and separated from the rest of the proteome. They are then heat denatured and run on an SDS-PAGE gel, followed by transfer and immunoblotting for the target of interest. **B.** Western-blot analysis of FP-biotin pull-down in miR-185 transfected Huh7.5 cells. The left column shows blotted enzymes that were labelled by FP-biotin and pulled down with streptavidin beads, representing their change in activity. The right column shows the abundance of the same proteins in their respective whole lysate input before streptavidin enrichment. SCD1 is a validated non-hydrolase miR-185 target. PTP1D was used as loading control in the input blots. **C.** Graph of miR-185-induced mRNA changes of hit genes ± SD as analyzed by RT-qPCR. n = 4, except for ABHD6, ACOT1, and LIPC, where n = 5. **D.** PPAR alpha mRNA fold change ± SD as determined by RT-qPCR in miR-185 transfected cells, n = 5. Significance assessed with two-tailed, unpaired Student's t test, *$p < 0.05$, **$p < 0.01$.

arachidonoylethanolamide) and 2-arachidonoylglycerol (2-AG), and the enzymes which act upon them[273]. Breakdown of 2-AG is modulated through the activity of a few serine hydrolases, amongst them monoglyceride lipase (MGLL), alpha/beta-hydrolase domain containing protein 6 (ABHD6) and carboxylesterase 1 (CES1). These enzymes all show functional changes upon miR-185 overexpression.

As previously described, activity and abundance changes were validated using western-blotting pull-downs and RT-qPCR respectively. Although not a predicted target of miR-185, MGLL demonstrated one of the most significant activity decreases out of all the proteins not predicted to be direct targets, and showed the strongest mRNA downregulation (Figure 3-1E, 3-2B, C). However, a 3'UTR luciferase reporter assay demonstrated the same decrease in luciferase signal with miR-185 as with our positive control, miR-182, a miRNA strongly predicted to bind the MGLL 3'UTR (Figure 7-1C). It is therefore possible that the interaction between miR-185 and the MGLL 3'UTR is non-canonical in nature. ABHD6 was the only enzyme that demonstrated an increase in activity in our profiling with no accompanying change in its mRNA levels (Figure 3-1E, 3-2C). Finally, our results show that miR-185 decreases CES1 activity by approximately a third (Figure 3-1E). A similar miR-185 mediated decrease in CES1 mRNA levels was observed (Figure 3-2C), indicating that CES1 activity is altered by transcriptional regulation. We have previously shown that CES1 siRNA knockdown leads to reduced HCV levels[226]. In accordance with this, pharmacological inhibition with the WWL113 inhibitor showed up to a 50% decrease in HCV infection in a luciferase subgenomic replicon model (Figure 7-1D). Therefore, the action of miR-185 on the CES1 enzyme is likely part of its anti-viral outcome. Together, the differential regulation of three different enzymes known to degrade 2-AG by miR-185 demonstrates a connection between miR-185 and the endocannabinoid pathway.

3.4.4 miRNA-185 downregulated serine hydrolases are putative PPAR-α targets

Overall, the decrease in the activities of these enzymes further confirms the role of miR-185 in modulating intracellular lipid metabolism while suggesting a common regulation mechanism. The peroxisome proliferator-activated receptors (PPARs) are nuclear transcription factors that act as central regulators of lipid metabolism in the cell and are well known to be differentially regulated during HCV infection[274]. Interestingly, five of the aforementioned genes involved in lipid and 2-AG metabolism, AADAC, ACOT1, CES1, MGLL and LIPC, are putative PPAR-α targets and have been either observed or proposed to be regulated by the transcription factor[275–277]. Since all of the putative PPAR-α target genes were seen to be significantly downregulated, we hypothesized that miR-185 acts as a co-regulator of this signal transduction pathway and may affect the levels of PPAR-α itself. RT-qPCR analysis showed that indeed, following miR-185 transfection, there was a significant decrease in the mRNA levels of the receptor (Figure 3-2D). Interestingly, PPAR-α was not reliably predicted to be a target of miR-185 with bioinformatics. Thus, its perturbed function would not be predicted, highlighting the importance of using ABPP to determine functional effects of the miRNA.

3.4.5 Lipidomic analysis of microRNA function

To further cement the role of miR-185 in lipid metabolism, we set out to understand the changes to lipid species brought about by the microRNA. We expected variations in the major lipid classes known to affect the hepatitis C virus, as well as links to previously identified direct and indirect targets of the microRNA. Shotgun lipidomic analysis was performed on Huh7.5 cells overexpressing miR-185. As shown in figure 3-3, the miRNA causes a significant decrease in cholesteryl esters (CEs) and triacylglycerides (TAGs). This is consistent with the previously observed antiviral role of miR-185 against HCV via modulation of lipid membranes and droplets[198]. Interestingly, cholesteryl esters and triacylglycerides are the main components at the

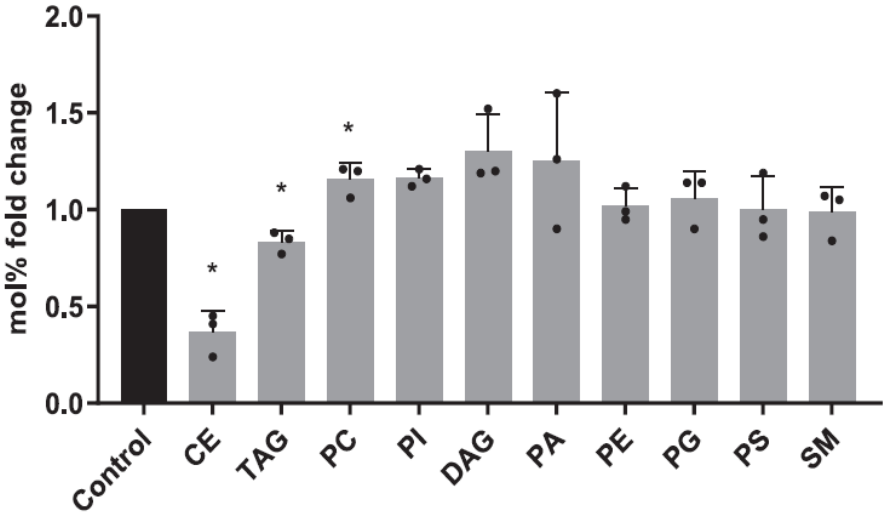

Figure 3-3. miR-185 changes the lipidomic profile of Huh7.5 cells. Cells were transfected with 100 nM miR-185 for 72 h, harvested, and sent for shotgun lipidomics at Lipotype GmbH. Ratio of lipid mol% in treated versus control cells shows a significant decrease in cholesteryl esters and triglycerides, as well as a modest but significant increase in phosphatidylinositols. Error bars represent SD, n = 3. Significance assessed with two-tailed, unpaired Student's t test, *$p < 0.05$. Fold changes for each lipid species by category can be found in Figure S2. CE: cholesteryl ester, TAG: triacylglycerol, PC: phosphatidylcholine, PI: phosphatidylinositol, DAG: diacylglycerol, PA: phosphatidate, PE: phosphatidylethanolamine, PG: phosphatidylglycerol, PS: phosphatidylserine, SM: sphingomyelin.

core of VLDL lipoprotein particles whose assembly pathway is intricately connected to the formation and release of HCV viral particles[180,278].

Unsaturation of lipids also plays an important role in both cellular membrane fluidity and maturation. We observed changes in lipid species based on the saturation of their acyl chains (Figure 7-3A). Within triglycerides and phosphatidylglycerols we detected a decrease in saturated acyl chains, while species with more double bonds were seen to increase. In contrast, phosphatidates, phosphatidylethanolamines and phosphatidylserines showed a shift towards more saturated chains. This data suggests that microRNA-185's antiviral effect is partly elicited via changes in lipid chain saturation.

To better understand how these changes to the lipid profile occur, we overlaid previous knowledge of miR-185 function with new information generated through our microarray and proteomic analysis. Figure 3-4 summarizes the enzymes involved in the synthesis of the major cellular lipid classes to visualize the changes that this small RNA induces in metabolic pathways. Fatty acid synthesis is at the basis of triacylglycerol and phospholipid synthesis and therefore, downregulation of FASN by miR-185 has a large impact on downstream products. In addition, numerous enzymes involved in lipid biosynthesis such as fatty acid elongases (ELOVL2-6) and acyl transferases (GPAT, AGPAT) were seen to decrease in transcript abundance via microarray (Table 7-3). These changes likely account for the significant reduction in TAGs, while downregulation of lipases such as MGLL and CES1 may explain the small increase in diacylglycerides (DAGs). Overall, the observed lipid phenotypes result from a complex combination of factors and changes in signalling cascades brought about by the miR-185's effect on multiple transcripts.

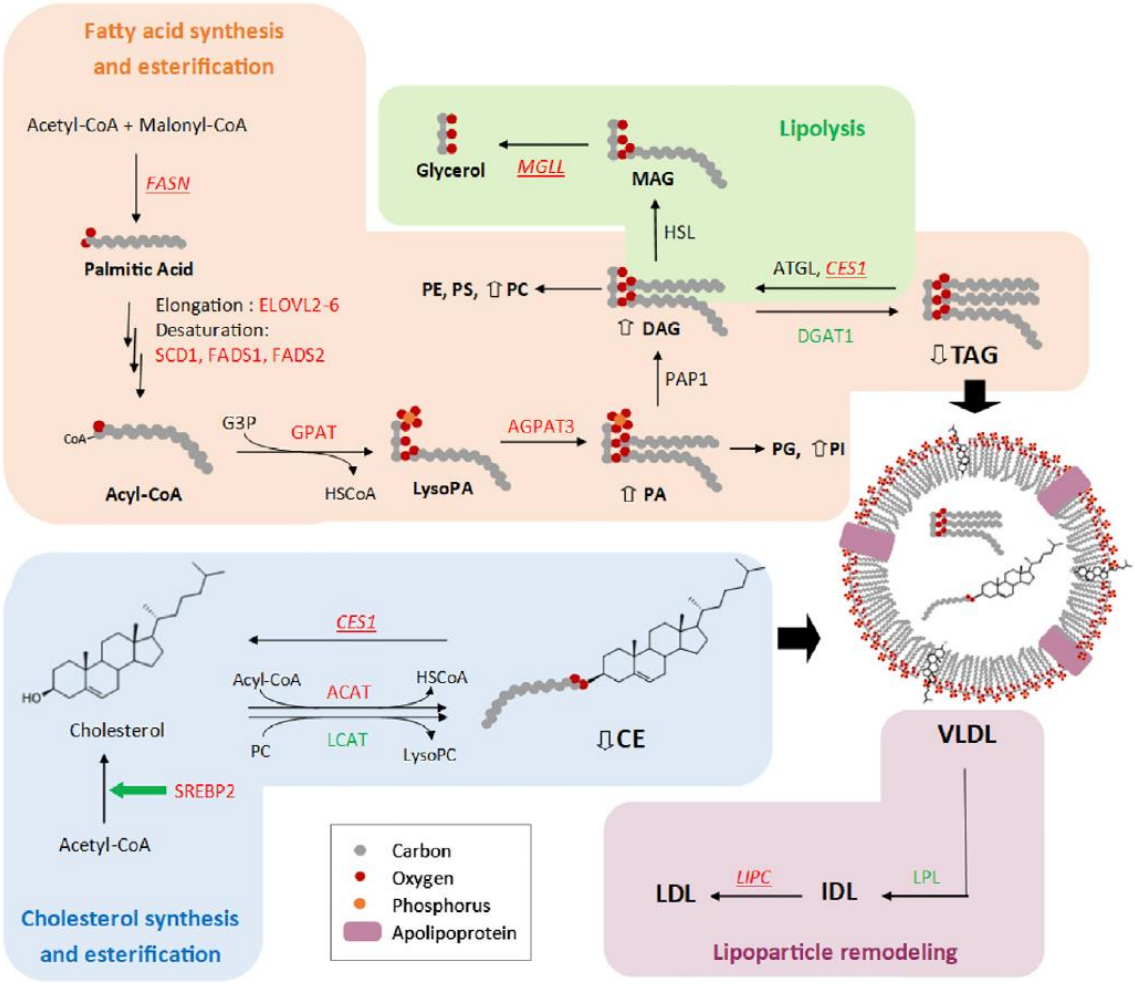

Figure 3-4. miR-185 regulates lipid metabolic pathways. miR-185-upregulated enzymes are in green while downregulated enzymes are in red. Enzymes in italics and underlined were present in the ABPP screen. Fold changes can be found in Tables 7-1–7-3. PC, phosphatidylcholine; PI, phosphatidylinositol; PA, phosphatidate; PE, phosphatidylethanolamine; PG, phosphatidylglycerol; PS, phosphatidylserine.

3.4.6 Inhibition of MGLL reduces hepatitis C virus levels

Serine hydrolases are known to be good pharmacological targets, with drugs indicated for diseases such as obesity, diabetes and Alzheimer's being prescribed everyday[220]. Therefore, we sought to determine if the antiviral effect of miR-185 could be recreated by targeting one of its principal serine hydrolase targets. Using a pharmacological inhibitor of MGLL, MJN110[279], on Huh7.5 cells infected with the JFH1 2a strain of HCV resulted in a potent antiviral effect (Figure 3-5A). However, this effect was not seen when the compound was used in cells harbouring the HCV luciferase subgenomic replicon model (data not shown). MGLL hydrolyses 2-AG into glycerol and arachidonic acid. We hypothesised that the antiviral effect may be due to an increase in 2-AG levels acting upon the CB1 pathway. Activation of the CB1 receptor by 2-AG is known to decrease cAMP production and therefore lower downstream targets such as phosphorylated AMPK (pAMPK), an inhibitor of SREBP1[280,281]. Sustained activation of CB1 has also been shown to result in receptor desensitization and functional antagonism of the pathway[282–284], ultimately resulting in a downregulation of SREBP1. However, treatment with 1 μM MJN110 did not significantly affect pAMPK nor SREBP1 levels (Figure 3-5B), suggesting a minimal effect on CB1. MGLL inhibition by MJN110 in the liver may exert its antiviral effects through reduced hydrolysis of 2-AG and other monoacylglycerols leading to broader effects on lipid homeostasis. Consistent with this hypothesis, an analysis of monoacylglycerol (MAG) and free fatty acid (FFA) species after a 72 hours treatment with the drug revealed a significant elevation in 18:1 MAG in both MJN110-treated and miR-185-treated cells, as well as a trend toward similar increases in 2-AG (C20:4 MAG) that did not achieve statistical significance (Figure 7-3B).

We tested the selectivity of MJN110 using competitive ABPP with the FP probe and confirmed that, as previously described[279], MJN110 is highly selective for MGLL with the exception of a

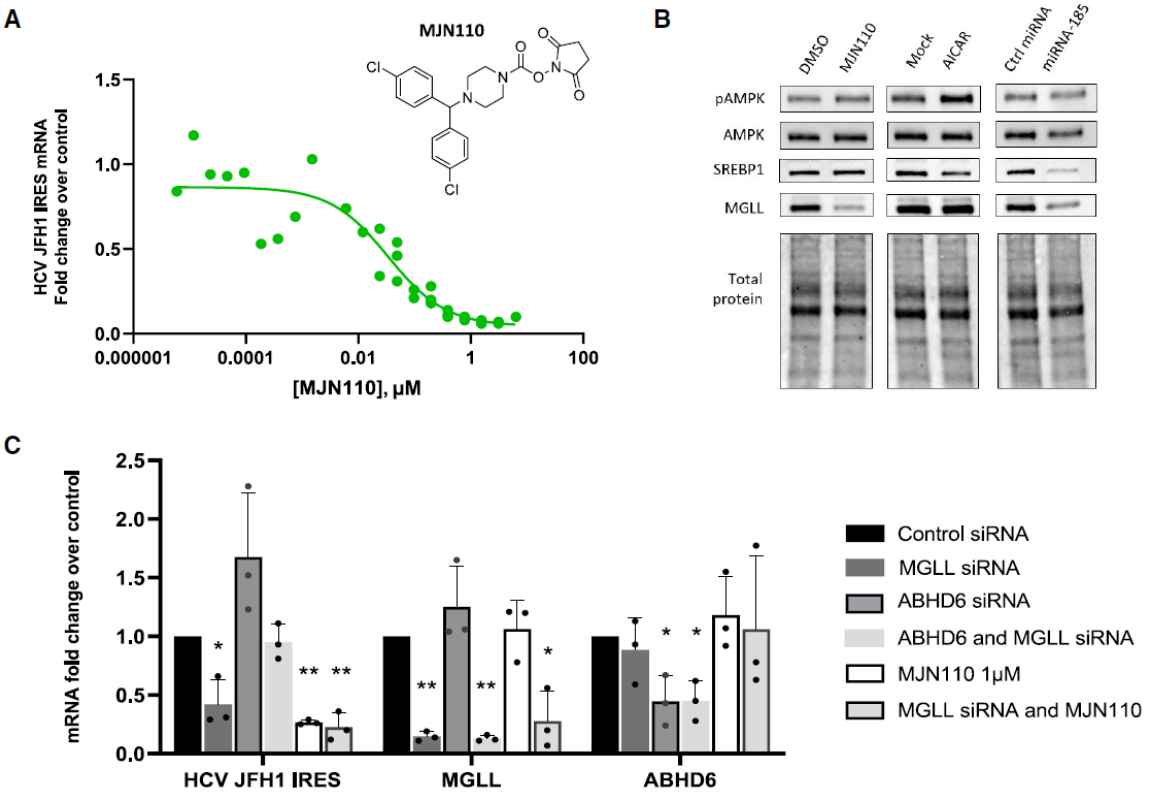

Figure 3-5. The miR-185 target MGLL is part of miR-185's antiviral effect. A. The MGLL inhibitor MJN110 inhibits HCV JFH1 infection in a dose-dependent manner with an EC50 (half-maximal effective concentration) of 34 nM, as measured by RT-qPCR of the HCV internal ribosome entry site (IRES). Cells were infected with HCV JFH1 for 5 h, after which the medium was changed for fresh medium containing MJN110, followed by a 72 h incubation. **B.** Treatment with 1 mM MJN110 does not result in a change in phospho-AMPK or SREBP1 levels. miR-185 transfection does not change phospho-AMPK levels, but does affect SREBP1 levels, as expected. 5-Aminoimidazole-4-carboxamide ribonucleotide (AICAR) is used as a positive control for AMPK phosphorylation. Both MJN110 and miR-185 lead to a decrease in MGLL levels. **C.** siRNA-mediated knockdown of MGLL, but not ABHD6, results in a significant downregulation of HCV JFH1 mRNA, comparable with the effects of MJN110. Cells were transfected with siRNA and incubated for 48 h before being infected with HCV and incubated for another 72 h. HCV JFH1 mRNA was measured by RT-qPCR, n = 3. Error bars represent SD. Significance assessed with two-tailed, unpaired Student's t test, *$p < 0.05$, **$p < 0.01$.

partial inhibition of ABHD6 (Figure 7-4). Interestingly, we observed a substantial decrease in MGLL protein abundance with the drug, with no change to ABHD6 levels (Figure 7-4B), suggesting potential degradation of the drug-enzyme complex. To our knowledge, degradation of MGLL by MJN110 has not been previously reported. We further confirmed that 2-AG levels were affected by treatment of Huh7.5 cells with MJN110. After 4 and 24 hours of treatment, levels of 2-AG increased approximately 7-fold and increased by 3-fold after 72 hours (Figure 7-3C), supporting the hypothesis that 2-AG levels are regulated significantly by MGLL activity in human hepatoma cells. Unexpectedly, arachidonic acid levels were also seen to increase, potentially as a feedback response to treatment. In order to determine if ABHD6 was contributing to MJN110's effect on HCV, we used small interfering RNAs to specifically knock-down MGLL, ABHD6 or both enzymes. Infection of MGLL siRNA-transfected cells with HCV JFH1 lead to a significant reduction in viral RNA after a 72 hours incubation, similar to that seen with MJN110 (Figure 3-5C). Knock-down of ABHD6 alone as well as simultaneous knock-down of both the enzymes did not show reduction in viral load. Interestingly, these effects were not as pronounced when the infected cells were only incubated for 48 hours (Figure 7-5A). Successful reduction in MGLL and ABHD6 protein levels were confirmed via western blotting at 48, 96 and 120 hours post-transfection (Figure 7-5B) and a time-dependent reduction in MGLL levels with MJN110 was once again observed up to 96 hours post-treatment (Figure 7-5C). Overall, downregulation of MGLL by miR-185 in the liver may be an important part of its antiviral effect.

3.5 Discussion

The interest in miR-185 stems from its well-known function in regulating metabolism[199,200,285], and its recently identified antiviral activity against hepatitis C and other viruses[198]. However, the mechanisms through which the microRNA exerts its effects are complex and not fully understood. We sought to investigate the implication of metabolic serine hydrolases in miR-185's reshaping of

the cellular lipid profile through activity-based protein profiling, supplemented with transcriptomic and lipidomic analysis. Our findings not only identified new targets of the microRNA, but also demonstrate that ABPP can report on enzyme behavior which would be otherwise missed with traditional transcriptomics analysis.

Firstly, we identified FASN, AADAC, ACOT1 and LIPC as lipid metabolic enzymes regulated by miR-185. FASN catalyzes the *de novo* synthesis of fatty acids[269] and has been shown to increase in activity during HCV infection[230]. It is clear that interference in *de novo* fatty acid synthesis via down-regulation of FASN expression represents one of the mechanisms by which miR-185 decreases lipid abundance. Overexpression of AADAC, an enzyme responsible for triglyceride hydrolysis, in hepatoma cells has been shown to reduce triacylglycerol levels and increase fatty acid oxidation[268]. The enzyme has also been shown to be involved the mobilization of triacylglycerols for the production of VLDL precursors and its knock-down impaired HCV infectivity[286]. Acyl-CoA thioesterase 1 (ACOT1) hydrolyses acyl-CoAs to free fatty acids and CoA, and is considered an auxiliary enzyme in β-oxidation[267]. Modulation of ACOT1 by miR-185 could potentially decrease lipid levels by affecting β-oxidation. LIPC, also known as hepatic lipase, is able to hydrolyze triglycerides from chylomicrons, catalyze the conversion between lipoproteins of different densities and facilitate uptake of lipoprotein remnants[266]. Hepatotropic viruses such as HCV interact significantly with lipoprotein pathways during their life cycle and some studies have shown that the activity of LIPC may have an anti-viral role by disrupting those interactions[287,288]. Interestingly, we observed a greater reduction in LIPC activity than abundance. It is known that this enzyme resides in the ER in association with calnexin and requires post-translational modifications to be secreted in its active form[289]. Our data suggests that the activity of this enzyme is decreased by miR-185, demonstrating a functional connection between enzyme activity and metabolic and immunometabolic function.

In assessing the changes in enzyme activity induced by miR-185, we discovered a possible link between miRNA signalling and the endocannabinoid pathway. Specifically, three enzymes (MGLL, ABHD6 and CES1) identified in our screen are known to hydrolyze 2-AG, one of the two main endocannabinoid lipid species. Of these enzymes, MGLL and CES1 were downregulated by miR-185 while ABHD6 showed a modest increase in activity. MGLL catalyzes the conversion of monoacylglycerides to free fatty acids and glycerol and is responsible for the majority of 2-AG degradation in the brain[290]. Interestingly, mice deficient in the enzyme have been shown to exhibit high liver triacylglycerol levels and reduced VLDL secretion[82] and expression of MGLL mRNA was shown to be decreased in liver biopsies of chronic HCV patients[272]. ABHD6 has been shown to degrade 2-AG in the brain[291]; however, the function of the enzyme in other tissues and systems is not well understood. Interestingly, Thomas, G. *et al.* have shown that ABHD6 is an important modulator of the metabolic syndrome and that knockdown of the enzyme protected mice from high-fat-diet-induced obesity and hepatic steatosis. Furthermore, ABHD6 knockdown increased expression of lipolytic genes such as hormone-sensitive lipase and MGLL[263]. It is therefore plausible that a feedback mechanism exists between ABHD6 and MGLL to maintain 2-AG levels. CES1, also known as triacylglycerol hydrolase (TGH), plays an important role in lipid metabolism[292] and a 2010 study has shown that CES1 is also capable of hydrolyzing 2-AG[293]. It is thought that although most 2-AG degradation in the brain occurs through MGLL and ABHD6, CES1 may play a role in the endocannabinoid pathway in peripheral tissues[293]. Inhibition of the enzyme decreased apoB-100 secretion in primary rat hepatocytes and altered VLDL production[294]. It is therefore not surprising that the enzyme was shown to increase in activity with HCV infection[226] and that our results show an antiviral effects with inhibition of the enzyme. Overall, since the endocannabinoid pathway has been shown to be intricately linked to lipid metabolism and signalling, miR-185 may play a more complex cellular role than previously thought.

When taken together, it is the simultaneous changes in the activities of all these serine hydrolases, as well as other non-enzymatic factors previously described[198] which most likely lead to an antiviral lipid-poor cellular environment. We further show that microRNA-185 decreases levels of the nuclear receptor PPAR-α. This is the most highly expressed PPAR in the liver[295], and it responds to intracellular levels of free fatty acids to regulate β-oxidation, triglyceride hydrolysis, lipogenesis and ketone body synthesis. We previously showed that PPAR-α antagonism has antiviral effects on the hepatitis C virus by altering lipid metabolism in the cell[296]. It is also noteworthy that ACOT1 and CES1 were shown to regulate PPAR-α activity by producing fatty acid ligands for the receptor[297,298]. Thus miR-185's immunometabolic function and ultimate antiviral effects are connected with co-regulation of PPAR signalling through functional targeting of lipid metabolism.

To gain greater insight into miR-185's effects on lipid pools, we performed shotgun lipidomic analysis and observed a decreased in cholesteryl esters and triacylglycerides. We linked these changes to the enzymes identified via ABPP as well as other miR-185 targets found in our microarray analysis and summarized them in figure 3-4. Part of the miR-185-altered phenotype is thought to be achieved through a decrease in the transcripts of regulatory genes such as SREBPs and PPARs. SREBP2, previously shown to be downregulated by miR-185[198], is the main transcription factor responsible for the regulation of cholesterol biosynthesis. Cholesterol is acylated into cholesteryl esters via two ways, the ACAT and LCAT pathways. Although microarray analysis (Table 7-2) showed an upregulation of ACAT and a downregulation of LCAT, our ABPP profiling results (Figure 3-1E) indicated a decrease in the activity of CES1, which is able to hydrolyze cholesteryl esters. Though this might be expected to increase total CE levels, the overall decrease in CE indicates that these changes may be eclipsed by the reduction in cholesterol substrate brought about by the downregulation of SREBP2.

TAGs and CEs are incorporated into the core of VLDL particles for release from hepatocytes into the circulation. HCV is well known for using the VLDL pathway for its own secretion[180]. The virus has also been shown to increase CE synthesis through modulation of ACAT genes, and inhibition of cholesterol esterification is known to be antiviral[175,299]. Therefore, by decreasing the levels of TAGs and CEs, miR-185 could be reducing the release of viral particles. VLDL particles are remodeled into intermediate density IDL particles by lipoprotein lipase and into LDL particles by LIPC. We observed a small increase in LPL abundance but a significant decrease in the activity, but not the abundance, of LIPC. This suggests that miR-185 is not only affecting the internal lipid environment but also remodeling the profile of lipoproteins secreted externally.

Interestingly, we also observed a significant increase in phosphatidylinositols, a signalling lipid species known to be enriched in arachidonic acid[300]. This may be brought about by miR-185's modulation of the enzymes MGLL, ABHD6 and CES1 involved in endocannabinoid lipid metabolism as previously described. However, miR-185's effect on this pathway remain to be investigated.

To better understand how the microRNA affects lipid-rich structures, we focused our attention on the saturation levels of each lipid species. We observed a decrease in saturated triglycerides and phosphatidylglycerols and an increase in saturated phosphatidates, phosphatidylethanolamines and phosphatidylserines. These changes may be part of the miR-185-induced remodeling of lipid membranes compositions which occurs during the immune response to HCV infection. Indeed, many RNA viruses are known to prefer unsaturated fatty acids and to form modified ER-membrane compartments where viral replication occurs. miR-185 was previously shown to downregulate stearoyl-CoA desaturase 1 (SCD-1), one of the principal enzymes in fatty acid desaturation[301]. We also observed a decrease in the fatty acid desaturases 1 and 2. Overall, these changes in the

phospholipids may affect chain flexibility and membrane fluidity as well as curvature, contributing to miR-185's antiviral effect. Taken together, there is a strong correlation between changes in enzyme activity, transcript abundance and downstream changes in lipid content mediated by miR-185.

Finally, we show that pharmacological inhibition of MGLL by the inhibitor MJN110, as well as siRNA-mediated knock-down of the enzyme, results in a potent downregulation of HCV JFH-1 infection. We confirmed that knock-down of ABHD6, a potential off target of MJN110, does not lead to a reduction in infection, validating that the drug is acting through its primary target. Although we observed an increase in MGLL's substrate, 2-AG, there was no effect on genes downstream of the CB1 receptor, suggesting that the antiviral effect may not be mediated through this pathway. Therefore, other possibilities likely contribute to the observed antiviral effect. MGLL is responsible for the hydrolysis of a large variety of monoacylglycerols which affects free fatty acid (FFA) pools. Nomura *et al.* have shown that increased MGLL activity significantly affects cellular FFA levels and promote carcinogenicity[302], and the link between endogenous fatty acids and HCV pathogenesis is well established[303,304]. Although we did not observe significant changes in palmitic, stearic and oleic acid levels, MJN110 did significantly increase the levels of the 18:1 oleic acid monoacylglycerol, a lipid previously shown to prevent LDL oxidation[305]. Interestingly, transfection with miR-185 also led to an increase in this species, as well as in 2-AG and arachidonic acid. It is therefore possible that MJN110 acts by creating an unfavourable lipid turnover environment for the virus. Additionally, arachidonic acid is at the base of prostaglandin synthesis through the action of cyclooxygenase enzymes, and prostaglandin A_1 (PGA_1) has been shown to have antiviral potential against HCV[306]. Finally, the antiviral effect of MJN110 was not observed in a subgenomic replicon model of HCV, suggesting the metabolic changes may affect cell entry or release, as opposed to replication. This is corroborated by the observation that MGLL deficient

mice have reduced VLDL secretion[82]. Future work should be directed at better understanding the link between this enzyme and HCV.

In this work, using a combination of ABPP, transcriptomics and lipidomics, we determined new functional roles for miR-185 by targeting a sub-population of the proteome. We confirmed miR-185's role in lipid metabolism via direct and indirect enzymatic modulation, as well as a more intricate involvement of this microRNA in lipid signalling pathways. Our study has shown that miR-185 affects many more targets functionally than previously thought, both directly and indirectly. Its role in lipid turnover and shuttling is furthered by its regulation of PPAR-α, thereby influencing the expression of downstream lipolytic genes. Generally, we have demonstrated that miR-185 regulates the levels of total lipid pools. All these changes taken together improve our understanding of miR-185's metabolic and anti-viral effects. Additionally, our results clearly demonstrate the utility of ABPP in uncovering new direct and indirect targets of non-coding RNAs. Here we show that a systematic analysis of the functional proteome can provide a global view of the influence of miR-185 on lipid metabolism. Furthermore, we demonstrate that it is possible to achieve pharmacological recapitulation of miRNA phenotype using inhibitors of the protein targets regulated by the microRNA. Since microRNA therapeutics are challenging to produce and deliver, our study points to a path for replicating microRNA phenotypes with small molecules.

3.6 Materials and methods

Data and code availability

Microarray data was obtained from Singaravelu *et al.*[198]. Data files are available on NCBI GEO depository (GSE73165). Mass spectrometry raw data for the activity-based protein profiling experiment is available in Mendeley data (DOI:10.17632/2h8mf2k3kt.1).

Experimental Model and Subject Details

The human hepatoma Huh7.5 cell line (sex: male) was derived from the Huh7 line for the purpose of permissive HCV infection[307]. The line was a kind gift from Dr. C.M. Rice (Rockefeller University). Huh7 cells harboring the luciferase sub genomic replicon (pFK-I389neo/luc/NS3-3′/5.1) were previously generated in our group[308]. All cells were grown at 37°C, 5% CO_2 in high glucose DMEM (Gibco, Life Technologies) with 10% FBS (Wisent) and 10 mM non-essential amino acids (ThermoFisher Scientific).

miRNA transfection and lysis for active proteome labeling

hsa-miRNA-185-5p miRNA mimic or control miRNA (miRVana, ThermoFisher Scientific) were combined with Lipofectamine RNAiMAX transfection reagent (ThermoFisher Scientific) in Optimem (Gibco, Life Technologies) medium as previously described[198]. The mixtures were added to the growth media of cells for a final concentration of 100 nM of miRNA. Cells were lysed after 72 hours. Confluent cells were washed with sodium phosphate buffer saline (PBS) and harvested with 1% Triton-X 100 in 10 mM PBS. Cells were lysed by sonication (15 one second pulses), centrifuged at 20000g, 4°C for 5 min, and the supernatant was stored at -80°C until labelling. Protein content was quantified using a DC protein assay (Bio-Rad).

Active proteome labelling with fluorophosphonate-TAMRA

Huh7.5 cells were cultured, transfected with miR-185 and lysed as described above. The lysates were diluted at 1mg/mL in 50µl of lysis buffer and labelled with FP-TAMRA (Thermo Fisher) at

1μM for 1hour at 37°C. “No probe” samples were incubated with the equivalent amount of DMSO only. Heat denatured samples were heated for 15 minutes at 95°C before labelling. The reaction was quenched by the addition of SDS gel loading buffer and the samples were run on a large 10% SDS-PAGE gel. The gel was imaged for rhodamine fluorescence using the ChemiDoc MP system (Bio-Rad) after which it was stained for whole protein with Coomasie stain, destained and re-imaged.

Active proteome labelling with fluorophosphonate-biotin

ABPP labelling of serine hydrolases with FP-biotin was performed as described by Barglow and Cravatt[309]. Protein lysates were diluted in lysis buffer to 1 mL of 1 mg/ml for western-blots pull downs and 2 mg/mL for mass-spectrometry. Fluorophosphonate-biotin probe (Santa Cruz Biotechnologies) or DMSO negative control was added to active proteome for a final concentration of 5 μM and incubated with rotation for 1 hour at 37°C. Proteins were precipitated in 5X volume of acetone for at least 15 minutes at -80°C and centrifuged 5 minutes at 6500 g and 4˚C. The acetone was removed and the protein pellets were washed with 750 μL cold methanol in 3 alternating cycles of sonication (5 one second pulses) and centrifugation at 6500 g for 5 minutes. The proteins pellets were then dissolved in 650 μL 2.5% SDS in PBS and sonicated for 15 pulses. The samples were then heated for 5 minutes at 60°C followed by centrifugation at 6500 g for 4 minutes to pellet any remaining contaminants. Aliquots of the supernatants were taken for input control after which the samples were mixed with PBS for a final volume of 8 mL.

Streptavidin enrichment

100 μL of streptavidin-agarose beads (ThermoFisher Scientific) were washed with PBS in biospin columns and added to the protein samples, followed by incubation with rotation for 1.5 h at room temperature. The beads were pelleted by centrifugation at 1400 g for 2 minutes, transferred into Biospin columns (Bio-Rad) and washed 3 times with 1% SDS followed by three washes with 6 M urea.

Immunoblotting

Streptavidin beads were washed 3 times with PBS and incubated with 2X SDS-PAGE loading buffer at 95°C for 15 minutes. The resulting eluates were run on a 10% TGX Stain-Free™ FastCast™ Acrylamide gel (Bio-Rad). Proteins were transferred from the gel to a PVDF membrane using the Trans-Blot® Turbo™ Transfer System (Bio-Rad), blocked with 5% milk in TBS-Tween for 1 hour at room temperature and probed with the appropriate primary and secondary antibody dilutions. Imaging for chemiluminescence was performed using the ChemiDoc MP system (Bio-Rad).

Proteomic mass-spectrometry sample preparation

Streptavidin beads were washed once with PBS and 5 times with 50 mM ammonium bicarbonate (ABC), pelleted by centrifugation at 1400 g for 2 minutes, then resuspended in 500 µL of 10 mM DTT in ABC. Samples were heated at 65°C for 15 min and iodoacetamide was added for a final concentration of 25 mM. Samples were rotated at room temperature for 30 min in the dark. Beads were centrifuged and washed with 50 mM triethylammonium bicarbonate (TEAB), pH 8.5. Proteins were digested off the beads overnight with 10 µg/mL trypsin in TEAB at 37°C. Beads were pelleted, the supernatant collected and the protein vacuum dried before dimethyl labelling.

Dimethyl labelling and desalting

Dimethyl labelling was performed based on the method of Boersema *et al*[218]**.** Digested samples were reconstituted in 100 µL of 100 mM TEAB to which 4 µL of 4% (vol/vol) CH_2O (light), CD_2O (medium) or $^{13}CD_2O$ (heavy) were added. Untransfected lysates treated with DMSO were subjected to the "light" condition, control miRNA transfected and FP-biotin-labelled lysates were subjected to the "medium" condition, while miR-185 transfected and FP-biotin-labelled lysates were subjected to the "heavy" condition. Afterwards, 4 µL of 0.6 M $NaBH_3CN$ were added to the light samples and medium samples, and 4 µL of 0.6 M $NaBD_3CN$ were added to the heavy sample. The samples were incubated for 1 h at room temperature while rotating after which, 16 µL of 1%

(vol/vol) ammonia solution and 30 µL of 5% formic acid were mixed in to quench the reaction and acidify the samples. The differentially labelled samples were mixed 1:1, desalted using Pierce C18 spin columns (Thermo Fisher) and vacuum dried.

Proteomic mass-spectrometry and data analysis

MS analysis was performed by Dr. Gleb G. Mirinov, John L. Holmes Mass Spectrometry Facility, Department of Chemistry and Biomolecular Sciences, University of Ottawa. Digested peptides were analyzed by HPLC-MS/MS using a Dionex Ultimate 3000 nano-HPLC system with an Acclaim PepMap RSLC 75 µm ID x 150 mm length separation column (Thermo Scientific, San Jose, CA), coupled with Orbitrap Fusion mass spectrometer (Thermo Scientific, San Jose, CA). 5 µL of sample were injected and separated by the following gradient (solution A: 0.1% formic acid in H_2O; solution B: 80% acetonitrile, 0.1% formic acid in H_2O) with the flow of 200 nL/min, such that 0.0-80.0 min increased between 0-40% B, 80.0-80.1 min rose to 40-80% B, 80.1-90.0 min rose to 80% B, 90.0-90.1 min decreased between 80-2% B, and 90.1-115.0 min maintained 2% B. Peptides were ionized using nano-ESI with spray voltage in positive mode at 2000 V. Ion transfer tube temperature was 275°C and the S-lens RF level was 60. Survey scans were performed on peptide precursors between 300 and 1500 *m*/*z* at 60K resolution (at 200 *m*/*z*). The ion count target was set to 2×10^5 and the maximum injection time 50 ms. Precursor peptides for tandem MS analyses were isolated by quadrupole at 0.7 Th. CID fragmentation was performed with collision energy of 35% and 5% step, and Normal scan MS analysis in the ion trap. The MS^2 ion count target was set to 10^4 and the max injection time was 35 ms. Precursors with charge state 2–6 were sampled for MS^2. The dynamic exclusion duration was set to 60 s with 10 ppm tolerance around a precursor ion and its isotopes. The instrument was run in 4 s cycles in top speed mode. Proteome Discoverer (version 1.4.1.14, Thermo Scientific, San Jose, CA) was used to process the raw data, and MS^2 spectra were searched against a UniProt database for *Homo sapiens (Human)* (http://www.uniprot.org) with SEQUEST HT engine. Peptides were generated from a tryptic

digestion containing up to two missed cleavages. Fixed modifications consisted of carbamidomethylation of cysteines, and variable modifications consisted of oxidation of methionines and protein N-terminal acetylation. Precursor mass tolerance was 10 ppm and product ions were searched at 0.6 Da tolerances. A target decoy validation with FDR of 1% was used to validate peptide spectral matches (PSM). Protein intensities from treated samples were normalized over control transfected samples.

Quantitative PCR

RNA isolation was performed using the RNeasy (Qiagen) isolation kit as per manufacturer's protocol. RNA integrity was confirmed by electrophoresis on 0.8% agarose gel in 1× TBE (Ambion). Reverse transcription was performed using the iScript cDNA Synthesis Kit (Bio-Rad) using 500 ng of RNA as per manufacturer's protocol. Quantitative PCR (qPCR) was performed using SYBR Green Supermix (Bio-Rad) as per manufacturer's protocol on the CFX Real-Time PCR Detection System (Bio-Rad) with the primer sequences are listed in table 7-4. 18S rRNA was used for normalization and expression fold changes relative to mock treatments were calculated using the $2^{-\Delta\Delta Ct}$ method.

HCV subgenomic replicon luciferase assays

Huh7 cells constitutively expressing the HCV sub-genomic replicon linked to a luciferase reporter gene (pFK-I389neo/luc/NS3-3'/5.1) were seeded in 24 well plates at 20000 cells/well. Cells were treated with a serial dilution of WWL113 (Sigma-Aldrich) for final concentrations of 0.024 μM to 25 μM and 1% DMSO for 24 or 72 hours, washed with PBS and lysed with passive lysis buffer (Promega). Luciferase assay was performed in technical triplicates in a 96 well-plate as previously described [256]. Luciferase signal was normalized over protein concentration and mock DMSO treatment.

MJN110 and Fluorophosphonate competitive ABPP

Huh7.5 cells were cultured as described above and one day before treatment, were seeded in 6 well plates at 60000 cells/well. The next day, cells were treated with 1 μM MJN110 or DMSO control. After 72 hours, the cells were harvested with 1% Triton-X 100 in 10 mM PBS and lysed as described above. The samples were diluted at 0.75 ug/μL in 70 μL for FP-TAMRA labelling and 1.5 mg/mL in 1 mL for FP-Biotin. FP-TAMRA (Thermo Fisher) was added for a final concentration of 0.7 μM and incubated at 37°C for one hour, after which the proteins were precipitated with 1 mL acetone for at least 15 minutes at -80°C and centrifuged 5 minutes at 14000 g and 4˚C. The acetone was removed, and the protein pellets were dried and dissolved in 2X SDS-PAGE loading buffer before being loaded on a 10% TGX Stain-Free™ FastCast™ Acrylamide gel (Bio-Rad). The gel was imaged for rhodamine fluorescence using the ChemiDoc MP system (Bio-Rad) after which proteins were transferred to a PVDF membrane and immunoblotting for MGLL and ABHD6 was performed as described above. Labelling with FP-Biotin, streptavidin enrichment, pull-down and immunoblotting were performed as previously described. For the higher resolution gel, labelling of MJN110-treated lysates and gel electrophoresis were performed as previously described for the miR-185-transfected cell lysates.

Samples preparation for analysis of 2-AG and AA levels

Huh7.5 cells were seeded one day prior to treatment in full media (DMEM, 10% FBS, NEAAs) at 60000 cells/well in 6 well plates. Cells were treated with 1 μM MJN110 or DMSO control for 4 hrs, 24 hrs or 72 hrs. Lipid extraction was performed following an acidified Bligh and Dyer method as follows. Cells were washed, trypsinized and lysed in 500 μL cold methanol containing 100nM arachidonic acid-d8 (d8-AA) spike-in (Cayman) to which 1.5 mL of MeOH, 1 mL chloroform and 0.8 mL water were added. The samples were shaken at room temperature at 700 rpm for 1 hour after which 1 mL of water, 50 μL formic acid and 1 mL chloroform were added. The samples were then vortexed and spun at 2000 g and 4 °C for 5 min. The organic layer was separated and vacuum

dried for mass-spectrometry. The remainder fractions were combined with 400 µL MeOH and 600 µL chloroform, vortexed and centrifuged at 2000g for 5min. The top aqueous layer was removed and 2400 µL of MeOH were added. The samples were vortexed and centrifuged at 4500g for 5 min at 4°C after which the supernatants were removed, and the pellets air-dried. The protein pellets were then resuspended in 2X SD-SPAGE loading buffer before being loaded on a 10% TGX Stain-Free™ FastCast™ Acrylamide gel (Bio-Rad) for total protein quantification and immunoblotting.

Lipidomic analysis

Huh7.5 cells were cultured and transfected as described above. Confluent cells were trypsinized, spun down and resuspended in Ca^{2+}, Mg^{2+}-free PBS. Cells were counted and resuspended in PBS before being sent for analysis at Lipotype GmbH. The amounts of the lipid classes were normalized to the total lipid amount to obtain mol % per total lipids. Mol % of the treated samples were divided by their respective control to obtain the mol % ratio.

Microarray analysis

Microarray data was obtained from Singaravelu *et al.*[198]. Data files are available on NCBI GEO depository (GSE73165). Briefly, Huh7.5 cells were cultured and transfected as described above. RNA isolation was performed using the RNeasy (Qiagen) isolation kit as per manufacturer's protocol. Expression profiling was performed in duplicate using Affymetrix Human Gene ST.2.0 arrays. Normalized and analysis was performed using the Affymetrix Expression Console and Transcriptome Analysis Console.

3'UTR luciferase reporter analysis

Huh7.5 cells were seeded in 6 replicates at 40000 cells/well in a 24 well plate. The following day, cells were transfected with 200 ng/well MGLL 3'UTR pEZX-MT06 plasmid (GeneCopoeia) using Lipofectamine 2000 transfection reagent as per manufacturer's protocol (Thermofisher Scientific). After 24 hours, cells were transfected with 100 µM control miRNA, miR-185 or miR-182

(miRVana, ThermoFisher Scientific) using Lipofectamine RNAiMAX transfection reagent (ThermoFisher Scientific) as per manufacturer's protocol. Cells were incubated for 48 hours before being lysed with passive lysis buffer (Promega). Luciferase assay was performed in technical triplicates in a 96 well-plate as previously described [256].

HCV JFH1 infection and MJN110 treatment

Huh7.5 cells were infected with the HCV $JFH1_T$ strain described by Russell *et al.*[310]. Cells were seeded one day prior to infection in full media (DMEM, 10% FBS, NEAAs) at 20000 cells/well in 24 well plates. The next day, the cells were incubated with the virus at MOI 0.1 in serum-free DMEM for 5 hours, after which the infection medium was replaced with full medium containing either 1% DMSO or MJN110 at different dilutions in DMSO. Final MJN110 concentrations ranged from 6.0E-6 μM to 3.1 μM. The cells were incubated for 72 hours after which they were lysed in RL buffer and RNA was isolated using the Norgen Single Cell RNA purification kit (Norgen Biotek) as per manufacturer's protocol. Reverse transcription and qPCR were performed as described above with primers targeting the HCV JFH1 IRES (sequences listed in table 7-4).

Relative analysis of MAG and FFA species

Huh7.5 cells were seeded at $1x10^6$ cells for miR-185 transfection and at 750000 cells for MJN100 treatment in 100mm dishes. Transfection and treatments were performed as described above (100nM miR-185 and 1μM MJN110). After 72 hours, the cells were washed with PBS, scraped, pelleted and flash frozen in liquid nitrogen. Cell pellets were thawed on ice and the total cell metabolome was extracted in 4 mL 2:1:1 $CHCl_3$/MeOH/DPBS (v/v/v) solution containing the internal standard mix (500 pmol 2-AG-d5 and 1 nmol AA-d8). The mixture was vortexed vigorously and centrifuged at 2000g for 5 min at 4 °C. The bottom organic phase was collected, and the remaining aqueous phase was acidified with 20 μL formic acid and re-extracted by the addition of 2 mL $CHCl_3$. Both of the organic phases were pooled, dried down under N2 gas, and reconstituted in 150 μL 2:1 $CHCl_3$/MeOH (v/v) for LC/MS analysis. Metabolites analyzed in this

study were quantified using LC/MS–based multiple reaction monitoring (MRM) methods (Agilent Technologies 6470 Triple Quad). MS analysis was performed using ESI with the following parameters: drying gas temperature, 350 °C; drying gas flow, 9 l/min; nebulizer pressure, 45 Ψ; sheath gas temperature, 375 °C; sheath gas flow, 12 l/min; fragmentor voltage, 100 V; and capillary voltage, 3.5 kV. The MRM transitions for the targeted LC/MS analysis are presented in table 7-5. The separation of metabolites was achieved using a 50 mm × 4.6 mm 5 μm Gemini C18 column (Phenomenex) coupled to a guard column (Gemini: C18: 4 × 3 mm). For negative mode analysis, H_2O:MeOH (95:5, v/v) with 0.1 % NH_4OH (v/v) and iPrOH:MeOH:H_2O (60:35:5, v/v) with 0.1 % NH_4OH (v/v) were used as buffer A and B, respectively. For positive mode analysis, H_2O:MeOH (95:5, v/v) with 0.1 % formic acid (v/v) and iPrOH:MeOH:H_2O (60:35:5, v/v) with 0.1 % formic acid (v/v) were used as buffer A and B, respectively. The LC gradient for negative mode analysis was the following after injection: 20% B at 0.1 mL/min for 5 min; then increase to 85% B at 0.4 mL/min for 15 min; increase to 100% B at 0.5 mL/min for 5 min, run at 100% B at 0.5 mL/min for 2 min; then go back to 20% B and equilibrate at 0.5 mL/min for 5 min. The LC gradient for positive mode analysis was the following after injection: start from 100% A and increase to 60% B at 0.1 mL/min for 5 min; increase to 100% B at 0.4 mL/min for 15 minutes; maintain 100% B at 0.4 mL/min for 13 minutes and then go back to 100% A at 0.4 mL/min and equilibrate for 1 minute. Lipid species were quantified by measuring areas under the curve in comparison to the corresponding internal standards and then normalizing to the cellular protein concentration. Two batches of three biological replicates were performed. Lipid content for each sample was normalized over its total protein content and the results are reported as a percentage of the average control group of each sample respectively.

siRNA knock-down of MGLL and ABHD6 and HCV $JFH1_T$ infection

Huh7.5 cells were seeded at $1.5x10^5$ cells per well in 6 well plates. The following day, siRNA mimic or control siRNA (ThermoFisher Scientific) were combined with 7 μL Lipofectamine

RNAiMAX transfection reagent (ThermoFisher Scientific) in Optimem (Gibco, Life Technologies) medium for a final siRNA concentration of 50 nM in each well. The mixtures were added to the growth media of cells and incubated for 48 hours. For the MJN110 treatments, cells were seeded at $7.5x10^4$ at the same time. After 48 hours of incubation, the media was replaced with serum-free DMEM containing HCV $JFH1_T$ at MOI of 0.1 and the cells were incubated for 5 hours. Following this, the infection media was replaced with full media. For the MJN110 treatments, 1μM MJN110 or DMSO was added at this time. The cells were incubated for either 48 or 72 hours after which they were lysed in RLT buffer and the RNA was isolated using the RNeasy (Qiagen) isolation kit as per manufacturer's protocol. Reverse transcription and qPCR were performed as described above with primers targeting the HCV $JFH1_T$ IRES.

Relative analysis of 2-AG and AA levels using mass-spectrometry

MS analysis was performed by Dr. Zoran Minic, John L. Holmes Mass Spectrometry Facility, Department of Chemistry and Biomolecular Sciences, University of Ottawa. Analysis of arachidonic acid and arachidonic acid-d8 were performed in negative mode. Samples were resuspended in 0.3 mL acetonitrile-water mixture (80:20, v/v) and vortexed for 3 min. The suspension was centrifuged for 30 s at 15000g and the supernatant was used for mass spectrometry analysis. Analysis of 2-arachidonyl glycerol was done in positive mode. Sample preparation was performed as for the negative-ion mode, with the exception that the solubilization solution was acidified with 0.1% formic acid. The obtained samples were analyzed by direct infusion electrospray ionisation (ESI), at a flow rate of 6 μL/min, in an Ion Max API source coupled to Q Exactive Plus MS (ThermoScientific, Bremen, Germany). The instrument was calibrated with Pierce ESI Positive and Negative Ion Calibration solution (Pierce #88323 and #88324). Measurements were carried out in the negative-ion mode with the experimental conditions applied as follows: the ion-spray potential of 3.4 kV and all other parameters (sheath gas flow rate 10, S-lens RF level 50, AGC target 3e6) optimized for maximum molecular ion transmission, and the

transfer capillary temperature at 320 °C. For the positive-ion mode the experimental conditions were set as for the negative-ion mode with a difference that the ion-spray potential was 4.0 kV and sheath gas flow rate of 4. Full scan high resolution mass spectra (R=75000 at m/z 400) were collected at a selected m/z range with a maximum injection time of 100 ms. For data acquisition and data processing, Xcalibur software was used. To obtain stable signals, samples were first electrosprayed for 5 min and then processed at the acquisition time of 1 min. The selected m/z range for analysis of arachidonic acid, arachidonic acid d8 and 2-arachidonoylglycerol were 302-304, 311-313 and 378-381, respectively. The relative intensity of precursor ions at m/z values corresponding to the predicted ratio and previously validated with pure compound were used for relative quantification. Lipid intensities were normalized over the AA-d8 spike-in control and over the densitometric intensity of the protein fractions run on an SDS-PAGE gel.

Statistical analysis

Data analysis was performed in Microsoft Excel and GraphPad Prism software. Fold changes were calculated relative to mock transfected or treated samples. Significance was assessed with two-tailed, unpaired Student's t-test where $p<0.05$ was considered significant.

Table 3-1. Key resources table

REAGENT or RESOURCE	SOURCE	IDENTIFIER
Antibodies		
PTP1D (SHP2)	BD transduction Labs	Cat# 610621; RRID: AB_397953
AADAC (G-12)	Santa-Cruz Biotechnologies	Cat# sc-390591
SCD1	Abcam	Cat# ab19862; RRID: AB_445179
FASN	Santa-Cruz Biotechnologies	Cat# sc-483570
MGLL	Santa-Cruz Biotechnologies	Cat# sc-398942
LIPC (hepatic lipase)	Santa-Cruz Biotechnologies	Cat# sc-21740; RRID: AB_627888
ACOT1/2	Santa-Cruz Biotechnologies	Cat# sc-373917; RRID: AB_10918465
CES1	Kind gift from Dr. Lance Pohl, NIH, Bethesda, MD, USA	N/A

ABHD6	Cell Signalling Technology	Cat# 97573S; RRID: AB_2800281
pAMPK (Thr172)	Cell Signalling Technology	Cat# 2531S; RRID: AB_330330
AMPK	Cell Signalling Technology	Cat# 2532S; RRID: AB_330331
SREBP1	Santa-Cruz Biotechnologies	Cat# Sc-366; RRID: AB_2194229
HRP goat α-mouse	Jackson Immuno-research	Cat# 115-035-062; RRID: AB_2338504
HRP donkey α-rabbit	Jackson Immuno-research	Cat# 711-035-152; RRID: AB_10015282
Bacterial and Virus Strains		
HCV $JFH1_T$	Kind gift from Dr. Rodney Russell, Memorial University, NFL, CA[310]	N/A
Chemicals, Peptides, and Recombinant Proteins		
Lipofectamine RNAiMAX transfection reagent	ThermoFisher Scientific	Cat# 13778150
Lipofectamine 2000 transfection reagent	ThermoFisher Scientific	Cat # 11668019
Fluorophosphonate-biotin	Santa Cruz Biotechnologies	Cat# sc-215056A
ActivX TAMRA-FP Serine Hydrolase Probe	ThermoFisher Scientific	Cat# 88318
Streptavidin-agarose beads	ThermoFisher Scientific	Cat# 20353
WWL113	Sigma-Aldrich	Cat# SML1179
MJN110	Kind gift of Dr. Benjamin Cravatt, Scripps Research Institute[279]	N/A
Arachidonic acid-d8	Cayman	Cat# 390010-1
2-AG-d5	Cayman	Cat# 362162
Critical Commercial Assays		
RNeasy isolation kit	Qiagen	Cat# 74136
10% TGX Stain-Free™ FastCast™ Acrylamide gel	Bio-Rad	Cat# 1610183
Trans-Blot® Turbo™ Transfer System	Bio-Rad	Cat# 1704272
Pierce C18 spin columns	Thermo Fisher	Cat# 89873
iScript cDNA Synthesis Kit	Bio-Rad	Cat# 1708841
SSO advanced SYBR Green Supermix	Bio-Rad	Cat# 1725274
Single Cell RNA purification kit	Norgen Biotek	Cat# 51800
Deposited Data		
miR-185 microarray data	(Singaravelu *et al*., 2015)[198]	NCBI GEO #GSE73165
miR-185 ABPP mass spectrometry data	This paper	Mendeley Data: DOI:10.17632/2h8mf2k3kt.1
Experimental Models: Cell Lines		

Huh7.5	Kind gift from Dr. C.M. Rice, Rockefeller University, NY, USA	RRID: CVCL_7927
E9 (Huh7 pFK-I389neo/luc/NS3-3'/5.1)	(Sagan *et al.* 2006)[308]	N/A
Oligonucleotides		
Primers for 18S, see table 7-4	This paper	N/A
Primers for AADAC, see table 7-4	This paper	N/A
Primers for ABHD6, see table 7-4	This paper	N/A
Primers for ACOT1, see table 7-4	This paper	N/A
Primers for CES1, see table 7-4	This paper	N/A
Primers for FASN, see table 7-4	This paper	N/A
Primers for LIPC, see table 7-4	This paper	N/A
Primers for MGLL, see table 7-4	This paper	N/A
Primers for PPARα, see table 7-4	This paper	N/A
Primers for JFH1 IRES, see table 7-4	This paper	N/A
Recombinant DNA		
mirVana hsa-miRNA-185-5p miRNA mimic, assay ID MC12486	ThermoFisher Scientific	Cat# 4464067
mirVana miRNA Mimic, Negative Control	ThermoFisher Scientific	Cat# 4464060
MGLL 3'UTR pEZX-MT06 plasmid	GeneCopoeia	Cat# HmiT001605-MT06
Silencer™ Select Pre-Designed siRNA (ABHD6)	ThermoFisher Scientific	Cat# 4392420 - s33001
Silencer™ Select Pre-Designed siRNA (MGLL)	ThermoFisher Scientific	Cat# 4390824 - s22379
Software and Algorithms		
Proteome Discoverer	ThermoFisher Scientific	https://www.thermofisher.com/ca/en/home/industrial/mass-spectrometry/liquid-chromatography-mass-spectrometry-lc-ms/lc-ms-software/multi-omics-data-analysis/proteome-discoverer-software.html

Transcriptome Analysis Console	Affymetrix, ThermoFisher Scientific	https://www.thermofisher.com/ca/en/home/life-science/microarray-analysis/microarray-analysis-instruments-software-services/microarray-analysis-software/affymetrix-transcriptome-analysis-console-software.html
Graph Pad Prism	GraphPad Prism Software	https://www.graphpad.com/scientific-software/prism/

Chapter 4: The serine hydrolase LYPLAL1 plays a role in hepatic glucose metabolism

4.1 Statement of contributions

This chapter consists of unpublished data. Contributors to this work include me (Roxana Filip), Étienne Bélanger, Lisa Chen, David Lefebvre and John P. Pezacki. As the main author of this study, I made significant experimental and intellectual contributions. John P. Pezacki and I conceived the project idea. The LYPLAL1 compound and probe were kind gifts of Pfizer Inc. through the Compound Transfer Program. I have performed the majority of the biological experiments. Étienne Bélanger and Lisa Chen aided with the metabolic starvation labelling experiment as well as with primer optimizations for the RT-qPCR analysis. David Lefebvre provided training and supervision for Étienne Bélanger and Lisa Chen while they assisted with the project. Shotgun lipidomics analysis was performed by Lipotype GmbH, Tatzberg, Dresden, Germany. Mouse hepatocyte isolation was performed at the University of Ottawa Heart Institute with the help of Vivian Franklin and Katey Rayner. I performed the data analysis, interpretation and wrote the manuscript. Editing of the manuscript was performed by myself, Étienne Bélanger, David Lefebvre and John P. Pezacki.

4.2 Abstract

The serine hydrolase LYPLAL1 is a poorly characterized enzyme with emerging roles in hepatic metabolism. A multitude of association studies have shown links between variants of this gene locus and metabolic conditions such as obesity and insulin resistance. Additionally, is it known that LYPLAL1 is deferentially expressed in fatty, steatotic, fibrotic and cancerous liver, phenotypes which are associated with hepatitis C virus (HCV) progression. However, the enzyme's function is still unknown. Recent biochemical studies have revealed that it may play a role in hepatic glucose metabolism and that its activity is allosterically regulated. Herein, we use a previously developed selective activity-based probe to delineate LYPLAL1's involvement in hepatic metabolism. We show that the enzyme's activity is modulated during metabolic stress, specifically pointing to a putative role in gluconeogenic processes. We also determine that knock-down of the enzyme does not affect liver lipid profiles and that its activity is modestly but not significantly increased during HCV infection. Finally, we bring forth evidence for insulin-mediated control of LYPLAL1 in HepG2 cells and provide preliminary results for labelling of the enzyme in primary mouse hepatocytes. This improves our understanding regarding the role of this enzyme in glucose metabolism and paves the way for future characterization studies.

4.3 Introduction

LYPLAL1 is a poorly characterized enzyme whose cellular and physiological roles remain elusive. Current understanding of its importance is limited to a handful of genome-wide association studies. Additionally, biochemical characterization has yet to reveal the nature of its endogenous substrate(s). Variants in the gene locus have been linked to obesity[233,311], insulin resistance[311] and non-alcoholic fatty liver disease[312]. More interestingly, results published by Ahn *et al.* suggest this enzyme may be involved in hepatic glucose metabolism. The group developed a specific small-molecule covalent inhibitor of LYPLAL1 as well as a "clickable" alkyne derivative to be used as a probe of enzymatic function. Using these tools, they reported that its inhibition in primary

hepatocytes lead to increased glucose production, pointing to a role for LYPLAL1 in hepatic gluconeogenesis.[313]. The group also showed that the levels of LYPLAL1 mRNA transcripts differ in human fatty, steatotic, fibrotic and cancerous liver extracts. Since these hepatic states are often associated with chronic hepatitis C infection[314], we thought that investigating the role of this enzyme would be of interest in the context of metabolic host-pathogen interactions. Additionally, the availability of the activity-based probe synthesized by this group provided a unique opportunity for applying ABPP to the study of LYPLAL1 function.

Most recently, Kok *et al.* showed that an activity-based activator probe was able to increase the catalytic activity of the enzyme by binding outside of the active site. When used *in vivo*, treatment of insulin-resistant diet-induced obese mice with the activator improved glucose homeostasis[237], further suggesting involvement of LYPLAL1 in glucose metabolism. This study also conclusively demonstrates allosteric control of LYPLAL1's activity, suggesting the existence of endogenous factors which control LYPLAL1 function. Bürger *et al.* solved LYPLAL1's crystal structure and their biochemical analysis of the enzyme revealed it does not have phospholipase nor triacylglycerol lipase activity due to its shallow active site. This result was surprising considering its close sequence homology to the lysophospholipases LYPLA1 and 2 (APT1 and 2)[315]. Furthermore, an initial study of LYPLAL1 knock-out mice reported that the animals did not exhibit altered metabolic phenotypes, maintained normal body weight gain and had regular responses to glucose and insulin dosing[316]. In contrast, a recent pre-print article (BioRxiv, not peer-reviewed) showed that LYPLAL1 KO mice have reduced liver triglycerides and steatosis and that knock-out of the enzyme has sex-specific effects on body fat percentage, white fat mass, and adipocyte diameter[317].

The process of gluconeogenesis in the liver is essential for the preservation of blood glucose levels. The complex regulation of this pathway ensures that glucose is produced to meet the demands of extrahepatic tissues during periods of starvation[103]. Regulation of gluconeogenesis occurs through multiple interlinked mechanisms including metabolite allostery, substrate availability, control of transcription, and cellular redox states. Simultaneous activation of the gluconeogenic enzymes pyruvate carboxylase (PC), phosphoenolpyruvate carboxykinase (PEPCK), fructose-1,6-bisphosphatase (FBPase-1) and glucose-6-phosphatase (G6Pase) coupled with inhibition of glycolytic enzymes prevents the formation of a futile cycle. Hormonal control occurs through glucagon and insulin to activate and repress gluconeogenesis respectively, via induction of protein kinase A (PKA) and protein kinase B (also known as Akt) signalling cascades[318,319].

Herein, we sought to further investigate the implication of LYPLAL1 in hepatic glucose metabolism and gluconeogenesis. Knock-out of LYPLAL1 did not considerably alter the lipid profile of hepatoma cells, further suggesting that the enzyme does not metabolize lipid species. We employed the activity probe (probe 12) developed by Ahn *et al.* to profile changes in LYPLAL1 enzymatic activity under conditions of metabolic stress in cell culture. Interestingly, a significant increase in LYPLAL1 activity was seen under serum and glucose starvation conditions. We also observed a modest increase in the enzymatic activity of LYPLAL1 in cells infected with the hepatitis C virus but inhibition of the enzyme did not affect HCV replication. Insulin treatments decreased LYPLAL1 mRNA in HepG2 cells similarly to the modulation of gluconeogenic enzymes. However, treatment of primary mouse hepatocytes with insulin and glucagon did not alter LYPLAL1 expression levels. Taken together, these results suggest that LYPLAL1 may play an important role in glucose production, possibly acting as an inhibitor of gluconeogenesis, but may function differently in primary versus immortalized cell lines.

4.4 Results

4.4.1 Knock-out of LYPLAL1 does not affect cellular lipid pools

Due to its sequence similarity to phospholipase enzymes, it was initially believed that LYPLAL1 might play a role in metabolizing lipid species. In order to assess whether knock-down of LYPLAL1 affects lipid pools in the liver, we used a CRISPR-Cas9 system to selectively knock-down LYPLAL1 in Huh7.5 cells. This approach allows for a sustained knock-out of the gene as opposed to a transient knock-down which is usually achieved with siRNA. In humans, the enzyme exists as two alternatively spliced isoforms: the dominant form (denoted "202" in ensembl[320]) at 26.3kD, and the lesser expressed form (denoted "201") at 24.4kD (Figure 7-6A). The 16 amino acid difference between isoforms stems from a longer exon 3 in the dominant form of the gene. We designed three guide RNAs targeting exon 3, the exon 2-exon 3 junction as well as exon 4. While the first two guides led to incomplete knock-downs (Figure 7-6B), the guide RNA targeting exon 4 resulted in a complete knock-out of both isoforms (Figure 4-1A). These cells were therefore chosen for subsequent shotgun lipidomics analysis by mass spectrometry to measure the relative levels of major lipid species. This approach revealed little to no change in most major lipid classes, including the phosphatidate (PA), phosphatidylcholine (PC), posphatidylethanolamine (PE), phosphatidylglycerol (PG), phosphatidylinositol (PI) and phosphatidylserine (PS) phospholipids (Figure 4-1B). These results further strengthen the idea that LYPLAL1 is not a lipid metabolizing enzyme, despite its previously reported structural features.

4.4.2 Serum and glucose starvation increase LYPLAL1 activity, but not its abundance

Pharmacological inhibition of LYPLAL1 was shown to result in increased levels of glucose in the growth media of human, rat and mouse primary hepatocytes[313]. This suggests that inhibition of LYPLAL1 activity increases the levels of gluconeogenesis in liver cells, a process which is typically upregulated under starvation conditions. Therefore, we sought to better understand the role of LYPLAL1 under such cellular metabolic stress. To that end, we labelled active LYPLAL1

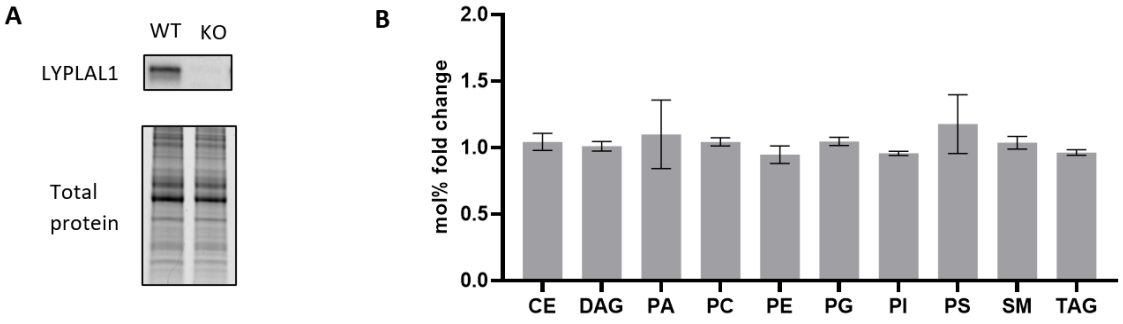

Figure 4-1. LYPLAL1-defecient Huh7.5 cells do not exhibit differential lipid profiles. A. CRISPR-Cas9 mediated knock-out (KO) of LYPLAL1 un Huh7.5 cells shows successful reduction of the enzyme levels via western blotting. **B**. Bar graph depicting the mol% fold change in 10 different lipid categories. The mean of three biological replicates is shown, error bars represent standard deviation. CE: cholesteryl ester, DAG: diacylglycerol, PA: phosphatidate, PC: phosphatidylcholine, PE: phosphatidylethanolamine, PG: phosphatidylglycerol, PI: phosphatidylinositol, PS: phosphatidylserine, SM: sphingomyelin, TAG: triacylglycerol.

in Huh7 hepatoma cells that were starved of glucose, serum and/or pyruvate. The regular growth media of this cell line consists of high glucose DMEM with 10% fetal bovine serum (FBS). For this experiment, the cells were subject to starvation (combinations of low glucose, no serum, no pyruvate) for 48 hours before being treated with probe 12. Labelled LYPLAL1 was then isolated via streptavidin pull-down, electrophoretically separated on an SDS-PAGE gel and transferred to a membrane for immunoblotting. A stronger band for the protein on the blot represents higher levels of active enzyme in the sample. Interestingly, the activity of LYPLAL1 was greatly increased in the most metabolically stressed cells (Figure 4-2A, B). Indeed, a significant increase in the activity of the enzyme is observable in cells grown in low glucose and no serum when compared to cells grown in regular media (high glucose, 10% serum). Removing serum seems to have the strongest effect on the activity of LYPLAL1. RT-qPCR was performed under the same conditions and the levels of LYPLAL1 mRNA were not seen to increase significantly (Figure 4-2C). This suggests that LYPLAL1 is involved in the cellular response to nutrient deprivation and that its activity may allosterically regulated as the changes in activity and expression levels do not correlate.

4.4.3 LYPLAL1 activity is modestly increased by the hepatitis C virus

The hepatitis C virus (HCV) is well known to perturb glucose metabolism and a strong correlation between insulin resistance and HCV has been established[183]. Although the exact mechanisms involved in this modulation are unknown, the NS5 protein of HCV has been shown to increase hepatic gluconeogenesis[321] and HCV positive patients have an increased prevalence of impaired fasting glucose and diabetes[322,323]. Additionally, levels of LYPLAL1 mRNA were shown to be elevated under conditions of steatosis, fibrosis and hepatocellular carcinoma[313], phenotypes which are associated with chronic HCV progression[314]. Therefore, since inhibition of LYPLAL1 was shown to increase glucose production, we sought to investigate whether the virus modulates LYPLAL1 activity. We infected Huh7.5 cells with the JFH1-2a strain of HCV and after 72 hours, performed in situ labelling of the enzyme using probe 12. As shown in figure 4-3, HCV infection

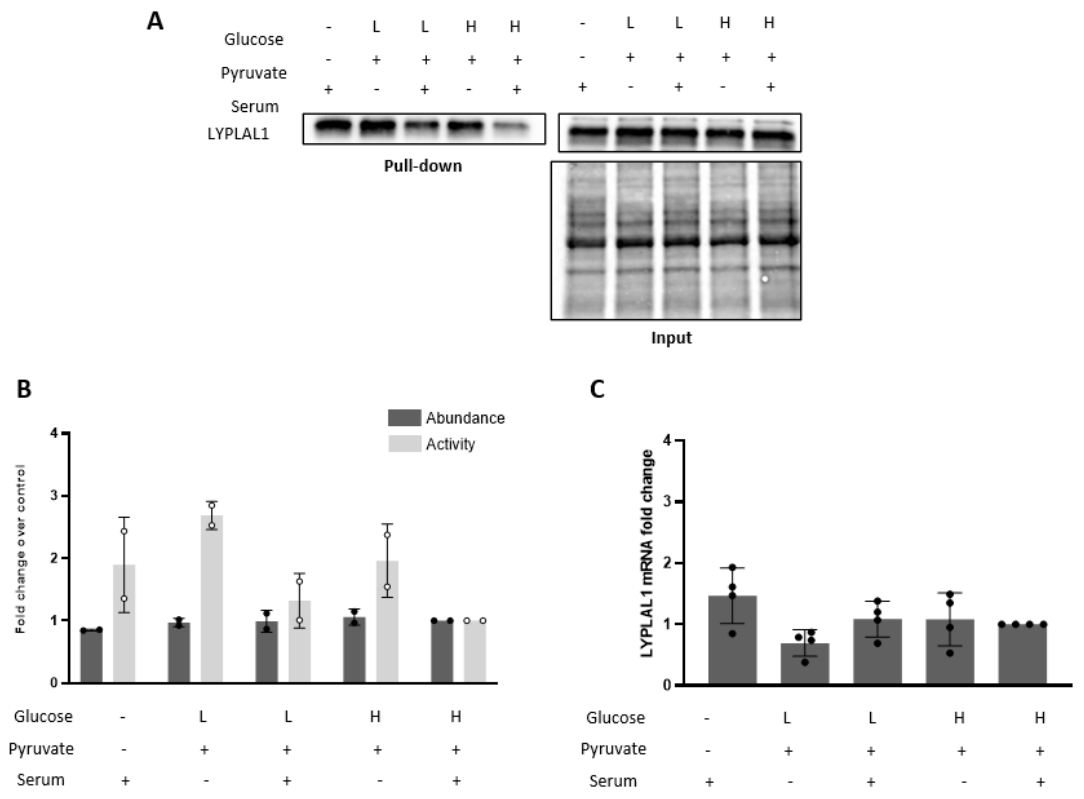

Figure 4-2. Metabolic starvation increases the activity and expression of LYPLAL1 in Huh7 cells. A. Representative western-blot pull-down of active LYPLAL1 grown in high (H, 4.5 mg/ml) or low (L, 1 mg/ml) glucose DMEM, with or without pyruvate and with 10% or no fetal bovine serum. Cells were subject to starvation for 48 hours and then active LYPLAL1 was labelled with probe 12, isolated via streptavidin enrichment and pull-down, run on an SDS-PAGE gel, and blotted. Aliquots of the input samples were collected before the pull-down, run simultaneously, and immunoblotted for LYPLAL1, as shown on the right-side blot. Whole lysate bands for the input are shown as a loading control. **B**. Densitometry analysis of two biological replicates normalized to the regular Huh7 growth medium (high-glucose DMEM with pyruvate and 10% serum) **C**. Relative LYPLAL1 mRNA in samples grown under the same conditions normalized to the regular Huh7 growth medium. The cells were treated for 48 hours, after which they were lysed, and RNA was extracted for reverse transcription. The cDNA levels were probed by quantitative PCR for LYPLAL1, n=4.

led to a slight increase in LYPLAL1 activity, although not significant. However, treatments with compound 11, the LYPLAL1 inhibitor, failed to conclusively inhibit or potentiate HCV JFH1 infection (results not shown). Therefore, LYPLAL1 does not seem to seem to be an important factor in HCV's modulation of cellular glucose metabolism.

4.4.4 Insulin treatment lowers LYPLAL1 transcript abundance in HepG2 cells

Insulin and glucagon are the main reciprocal hormonal controls of glycolysis and gluconeogenesis. Binding of insulin to its receptor in liver cells leads to a repression of gluconeogenesis and downregulation of the gluconeogenic enzymes G6Pase and PEPCK[324,325]. We sought to determine whether LYPLAL1 is similarly regulated by insulin signalling. Huh7 cells were found to not express sufficient levels of G6Pase and PEPCK for detection, therefore, the HepG2 hepatic cell line was used. Treating the cells with 10 nM insulin showed a time-dependent decrease in the expression of G6Pase and PEPCK mRNA (Figure 4-4). After a four-hour treatment of Hep2 cells, we observed a modest but significant downregulation of G6Pase, PEPCK and LYPLAL1 transcript levels. This was not observed after a one-hour treatment. This suggests that LYPLAL1 may be transcriptionally regulated during insulin signalling in HepG2 cells.

4.4.5 Insulin and glucagon treatments do not alter LYPLAL1 mRNA abundance in primary mouse hepatocytes

Although several hepatic cancerous cell lines are responsive to insulin signalling, it is well known that glucose metabolism in these models is not representative of the same processes in healthy cells. Indeed, cancerous cells often exhibit the Warburg effect, whereby the cell prioritizes glucose uptake, glycolysis and subsequent fermentation to lactate to rapidly produce ATP while avoiding utilizing the TCA cycle[326]. This effect also leads to a decrease in the expression of gluconeogenic enzymes, a reduction of gluconeogenesis and a decreased responsiveness to glucagon[327,328]. Indeed, Huh7 cells treated with glucagon did not express measurable levels of G6Pase or PEPCK mRNA, and HepG2 cells demonstrated generally inconsistent changes in the expression of these enzymes

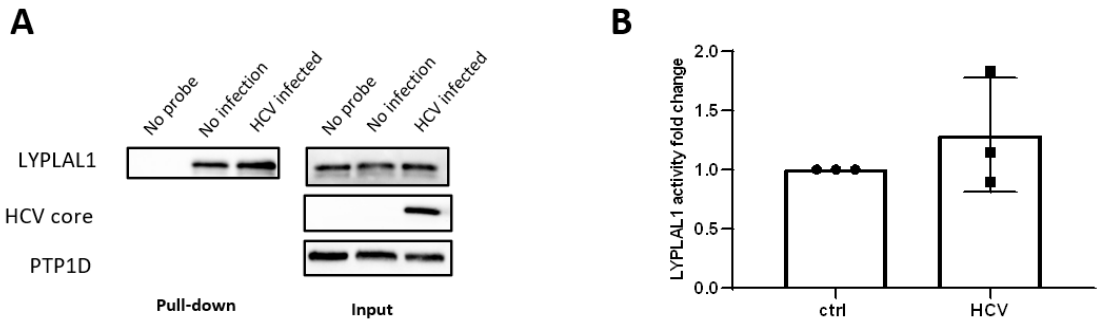

Figure 4-3. HCV infection leads to a small increase in LYPLAL1 activity. A. Representative western blot of the pulled-down active LYPLAL1 and levels of LYPLAL1 abundance in the input control. HCV JFH1-2a infected Huh7.5 cells were labelled with probe 12 and the labelled proteins were conjugated to biotin, isolated with streptavidin beads and run on an SDS-PAGE gel for western blotting. Aliquots of the input samples were collected before the pull-down, run simultaneously, and immunoblotted for LYPLAL1, as shown on the right-side blot. HCV core protein is used to confirm HCV infection and PTP1D is used as a loading control in the input samples. **B.** Densitometric analysis of 3 biological replicates normalized to the no-infection control. Error bars represent standard deviation.

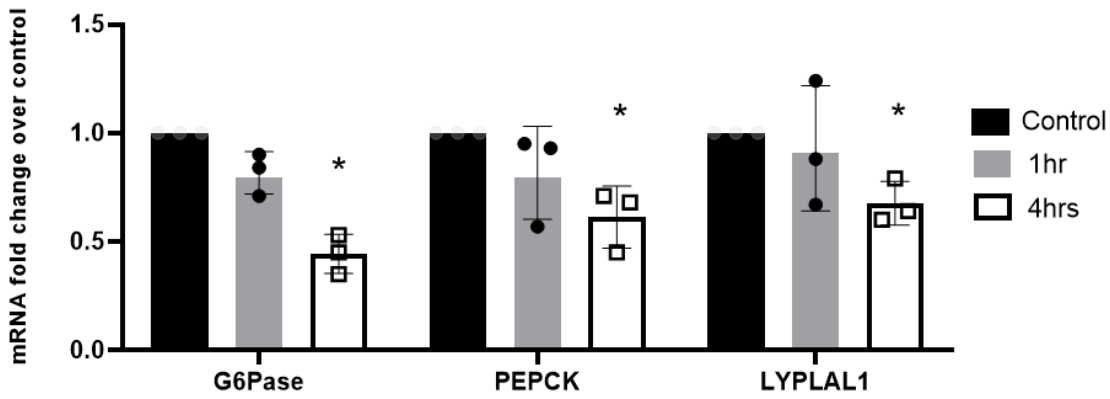

Figure 4-4. Insulin treatment reduces mRNA levels of G6Pase, PEPCK and LYPLAL1. HepG2 cells were treated with 0.01μM of insulin for four hours after which the RNA was extracted and transcript abundance relative to control were measured using RT-qPCR, n=3. Error bars represent standard deviation. Significance assessed with two-tailed, unpaired student's t-test, * = $p<0.05$.

(data not shown). Therefore, we sought to investigate the effects of insulin and glucagon signalling on LYPLAL1 in primary mouse hepatocytes (PMHs). Firstly, we wanted to confirm that the PMHs are responsive to both insulin and glucagon activation. Binding of insulin to its receptor leads to activation of the phosphatidylinositide-3-kinase (PI3K) signalling cascade and phosphorylation of Akt[329] while glucagon signalling acts through an increase in cyclic AMP levels, activation of PKA and phosphorylation of the cAMP response element-binding protein (CREB)[330]. While treatment of both HepG2 cells and PMHs with insulin for 20 minutes resulted in Akt phosphorylation, only PMHs were responsive to glucagon treatments as demonstrated by a dose-dependent phosphorylation of CREB (Figure 4-5A and B). We analyzed the expression levels of G6Pase, PCK1 (mouse PEPCK) and LYPLAL1 mRNA over a range of glucagon and insulin concentrations after one or six hours of treatment. Similarly to our results in HepG2s, insulin signalling had a stronger effect on decreasing the levels of G6Pase and PCK1 after 6 hours (Figure 4-5D), with negligible effects after only one hour (Figure 4-5C). In contrast, glucagon increased the levels of these enzymes to a stronger degree after the first hour of treatment (Figure 4-5E) with some remaining effect on PCK1 after 6 hours (Figure 4-5F). However, as opposed to the downregulation of LYPLAL1 observed after 4 hours of insulin treatment in HEPG2s (Figure 4-4), neither insulin, nor glucagon, significantly changed the levels of LYPLAL1 transcript abundance in the mouse hepatocytes under these conditions. This discrepancy between cell types is possibly due to the metabolic differences between the cancerous cell line and the primary cells and/or regulatory differences in the mouse model versus human cells.

4.4.6 Active LYPLAL1 can be labelled in primary mouse hepatocytes

As previously demonstrated during serum starvation, the activity of LYPLAL1 can be modulated independently of its expression levels. This is consistent with Kok e*t al.*'s observation that the enzyme possesses an allosteric regulatory site and that its activity can be pharmacologically increased with a small molecule activator[237]. Therefore, we sought to label active LYPLAL1 in

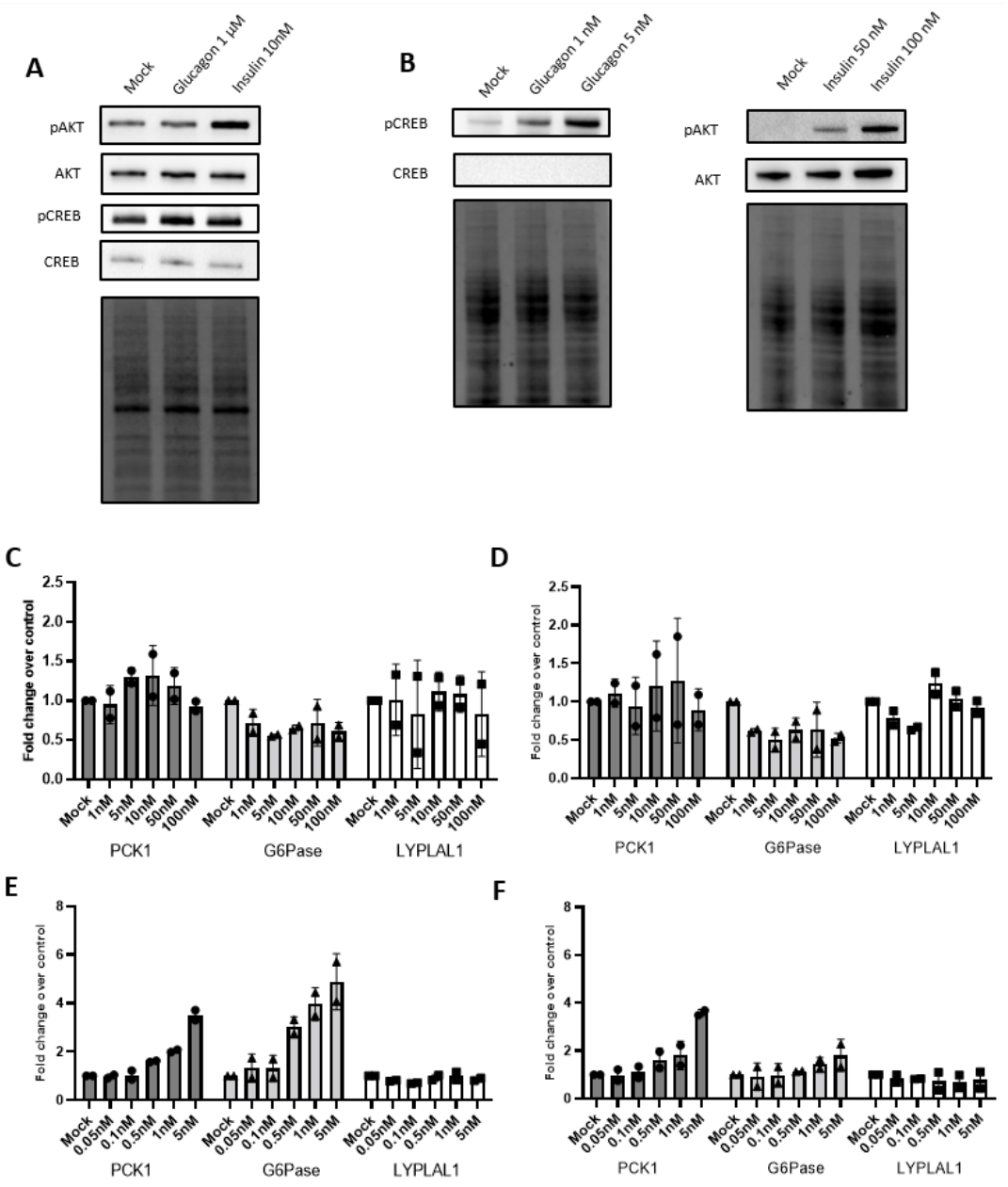

Figure 4-5. Glucagon and Insulin treatments have different effects in HepG2 cells and primary mouse hepatocytes. A. HepG2 cells are responsive to insulin, but not glucagon. Cells were treated with either 1 μM glucagon, 10 nM insulin or mock for 20 minutes, lysed and the lysates were run on a SDS-PAGE blot for immunoblotting. Whole lysate bands are shown as a loading control. **B.** Primary mouse hepatocytes are responsive to both glucagon and insulin, showing dose-dependent phosphorylation of CREB and Akt, respectively. [caption continued on next page]

[Figure 4-5. caption continued]

Non-phosphorylated CREB was not detected in the mouse hepatocyte lysates. **C.** Fold changes in the expression of PCK1, G6Pase and LYPLAL1 after one hour of insulin treatment at various concentrations in PMHs, n=2. Error bars represent standard deviation. D. Fold changes after six hours of insulin treatment. **E.** Fold changes after one hour of glucagon treatments. **F.** Fold changes after six hours of glucagon treatment.

mouse hepatocytes to determine whether the activity of the enzyme is changed with insulin and glucagon treatments. Preliminary labelling experiments showed that the active enzyme can be labelled and observed by western blotting following a similar protocol to that of cancerous cells. However, the levels of LYPLAL1 in primary hepatocytes were lower than those in Huh7.5 cells and the labelling efficiency was much lower (Figure 4-6). Therefore, future work should aim to optimize LYPLAL1 labelling in these cells and to determine whether insulin and glucagon signalling modulate its enzymatic activity in primary liver cells.

4.5 Discussion

Although multiple association studies have linked LYPLAL1 to metabolic disorders, the role of the enzyme in metabolism is still poorly understood. Ahn *et al.* developed a potent pharmacological inhibitor and probe of LYPLAL1 enzymatic activity (probe 12). Using these tools, they determined that inhibition of LYPLAL1 in liver cells leads to an increase in glucose secretion[313]. This points to a role for LYPLAL1 in inhibiting gluconeogenesis. More recently, LYPLAL1 was shown to possess an allosteric regulation site which can be targeted pharmacologically to increase the enzyme's activity, suggesting the possibly of endogenous allosteric regulation[237]. In light of the limited knowledge relating to LYPLAL1's function, we sought to bring forth further evidence to support its involvement in hepatic glucose metabolism and gluconeogenesis.

Firstly, we investigated the possibility of LYPLAL1 acting as a phospholipase. The enzyme possesses sequence similarity to LYPLA1 and LYPLA2, which have thioesterase and lysophospholipase activity[331,332]. A previous study used an *in vitro* biochemical approach and concluded that LYPLAL1's shallow active site does not accommodate phospholipids[333]. However, this was not tested in a cellular environment. Therefore, we sought to determine whether knocking out the enzyme influences cellular lipid pools. Using a CRISPR-Cas9 system, stable LYPLAL1

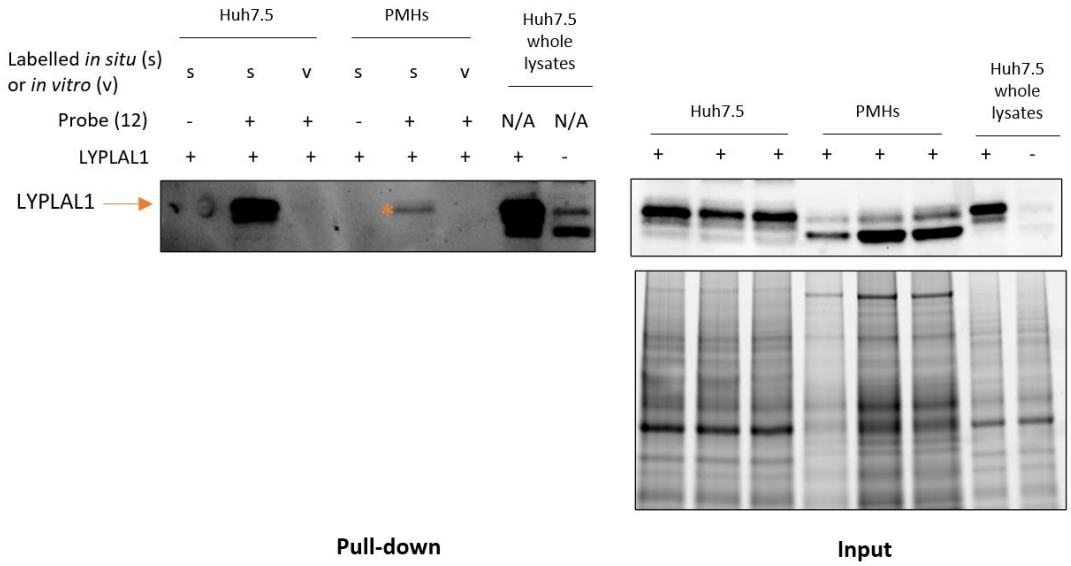

Figure 4-6. LYPLAL1 is labelled by probe 12 in primary mouse hepatocytes, but to a lower degree than in Huh7.5 cells. Huh7.5s cells or primary mouse hepatocytes (PMHs) were either labelled in culture (*in situ*) or lysed and labelled (*in vitro*) with probe 12 or DMSO. Labelled LYPLAL1 was pulled down using streptavidin enrichment and run on an SDS-PAGE gel alongside whole Huh7.5 lysates from wild-type or LYPLAL1 KO cells for immunoblotting. The orange * denotes labelled mouse LYPLAL1. Aliquots of the input samples were collected before the pull-down, run simultaneously, and immunoblotted for LYPLAL1, as shown on the right-side blot. Whole lysate bands for the input are shown as a loading control.

knock-out cells were generated, and their lipid profiles were determined using mass spectrometry lipidomic analysis. No changes were observed in the levels of lipid species, including phospholipids, di and triglycerides, cholesteryl esters and sphingomyelins. This supports the hypothesis that LYPLAL1 is not a lipid metabolizing enzyme and may play a role in alternative energy metabolism pathways.

Gluconeogenesis is often considered as "glycolysis in reverse" and is a process used by liver cells to generate glucose during periods of starvation[103]. Since inhibition of LYPLAL1 led to an increase in glucose production[232], we sought to mimic conditions of gluconeogenic activation to determine whether LYPLAL1 may be involved in regulating gluconeogenesis. Using the LYPLAL1 activity probe 12, we observed a strong increase in LYPLAL1 activity under various levels of starvation in hepatocellular carcinoma cells. Interestingly, the cells grown in media reduced in glucose and lacking serum had the strongest upregulation of LYPLAL1 activity. It is possible that as a homeostatic response, LYPLAL1 acts as an inhibitor of gluconeogenesis and has increased activity when the pathway is activated. However, the mechanism through which this occurs still needs to be investigated. Control of gene expression during fasting is complex, involving epigenetic regulation as well as modified cellular signalling. Since the activity, but not the expression of LYPLAL1 was increased under these conditions, it is possibly the result of an increase in an allosteric activator of the enzyme. This endogenous activator may be a protein or metabolite whose levels are increased in low serum or glucose conditions. In future experiments, subjecting cells to metabolic stress could be a useful tool in identifying the endogenous regulator of LYPLAL1 activity.

Based on the strong links between the hepatitis C virus and glucose metabolism, we sought to understand if LYPLAL1 played a role in HCV host-pathogen interactions. Our results show a

modest increase in LYPLAL1 activity during HCV infection. Although the effect is minimal, the virus is known to increase gluconeogenesis similarly to starvation conditions, once again suggesting that LYPLAL1 is activated when the gluconeogenic pathway is stimulated. However, inhibiting the enzyme did not affect HCV levels, suggesting it may not play an important role in HCV host-pathogen interactions under these conditions.

Hormonal control of gluconeogenesis occurs through insulin and glucagon signalling. Specifically, insulin treatment of liver cells reduces the expression of the rate limiting gluconeogenic enzymes G6Pase and PEPCK. We tested whether LYPLAL1 was under similar hormonal control and observed a decrease in the levels of LYPLAL1 mRNA in HepG2 cells treated with insulin for 4 hours. The regulation of G6Pase and PEPCK expression occurs in major part through modulation of transcription factor binding to response elements in the promoter regions of these genes[104,334,335]. Under fasting conditions, the FOXO1 transcription factor is bound on insulin response elements (IREs) to activate gene expression. At the same time, the CREB transcription factor is phosphorylated by active PKA, and binds CRE response elements. These events increase expression of G6Pase and PEPCK[336]. During insulin signalling, activated Akt phosphorylates FOXO1 and prevents its nuclear localization, thereby repressing G6Pase and PEPCK gene expression[115,337]. We analyzed the LYPLAL1 promoter and enhancer regions upstream of the gene as denoted in Ensembl[320] and did not find the CRE consensus sequence (5'TGACGTCA3'[338]), but were able to identify four possible FOXO1 binding sites (5'T(G/A)TTT(T/G)(G/T)3'[338]) in the promoter directly upstream of the LYPLAL1 transcription start site (Figure 7-7). Whether these sites allow for insulin-mediated repression of transcription would need to be validated experimentally. Interestingly, expression of PEPCK and G6Pase was not increased by glucagon in these cells and was undetectable in Huh7 cells. This points towards dysregulated hormonal signalling in cancerous cell lines.

To bypass the complications induced by perturbed metabolic pathways in cancerous cells lines, we sought to investigate LYPLAL1 expression and activity in primary mouse hepatocytes during insulin and glucagon signalling. We observed that the PMHs are indeed responsive to both insulin and glucagon signalling, which was not the case for the HepG2 cells. As opposed to effects in HepG2s, insulin did not consistently decrease LYPLAL1 levels; neither did the levels of the enzyme increase with glucagon treatment. This discrepancy between models may be due to the cancerous phenotype of the HepG2 cells or to differences in gene regulation between the mouse and human LYPLAL1 genes. The transcriptional regulation of LYPLAL1 has indeed not been studied and differences between mouse and human LYPLAL1 have not been thoroughly investigated. Such differences can be seen in the comparison of LYPLAL1 labelling with probe 12 between Huh7.5 cells and PMHs. For the same amount of starting material, there is significantly less LYPLAL1 expression and labeling in PMHs. Furthermore, mouse LYPLAL1 is only expressed in one isoform with 77% amino acid sequence similarity to the dominant human LYPLAL1. The implications of these differences on the role of the enzyme in various models should be taken into consideration in future studies.

Overall, this study brought forth new evidence for LYPLAL1's involvement in glucose metabolic pathways. Lipidomic analysis confirmed that the enzyme does not influence cellular lipid pools and activity-based protein profiling showed activation of its enzymatic activity during starvation. Although the enzyme did not seem to play an important role in HCV's modulation of gluconeogenesis, the downregulation of LYPLAL1 expression in HepG2 cells treated with insulin seem to suggest that the enzyme may be under hormonal control. The role of LYPLAL1 in mouse hepatocytes still need to be investigated but preliminary work showed that the Ahn. *et al*. probe 12 is capable of reporting on mouse LYPLAL1 activity. Future work would include investigating the activity of LYPLAL1 under insulin and glucagon stimulation in the PMHs. Other avenues for

demystifying LYPLAL1's role could include probing the enzyme's activity under other conditions such as treatments with the glycolysis inhibitor 2-deoxy-D-glucose or the gluconeogenesis inhibitor Metformin. Additionally, profiling protein-protein interactions using mass spectrometry proteomics or investigating changes in the metabolome with LYPLAL1 overexpression or knock-down could provide valuable insight into the enzyme's endogenous interacting partners. Understanding the role of LYPLAL1 in metabolism may be challenging, but could lead to the enzyme being a novel pharmacological target in metabolic diseases for which inhibitors, as wells as activators, have already been developed.

4.6 Materials and methods

Cell culture

Human hepatoma cells (Huh7 and Huh7.5) were grown at 37°C in DMEM (Gibco, Thermo Fisher) with 10% FBS and 10 mM non-essential amino acids. HepG2 cells were grown in 37°C in MEM (Gibco, Thermo Fisher) with 10% FBS.

Generation of LYPLAL1 knock-out Huh7.5 cells

Huh7.5 cells were used to generate knock-outs of LYPLAL1 using the method published by Sanjana *et al.*[339]. Briefly, the lentiCas9-Blast, pSPAX2 and pMD2 plasmids were transfected in Hek293T cells to generate lentivirus particles. Huh7.5 cells were transduced and stably expressing cells were selected using Blasticidin resistance. Guide RNA sequences (Figure 7-6) against LYPLAL1 were cloned into the lentiGuide-Puro plasmid using *BsmB*I digestion and this plasmid was used to transfect Hek293T cells in conjunction with the pSPAX2 and pMD2 packaging plasmids. The resulting lentivirus particles were used to transduce the previously generated Huh7.5-Cas9 cells and puromycin resistance was used for selection. Successful knock-out of LYPLAL1 was validated by western blotting using an anti-LYPLAL1 primary (Sigma Prestige Antibodies) and a Donkey anti-rabbit secondary antibody (Jackson Immuno-research).

Lipidomics

Huh7.5 cells were cultured as described above. Confluent control cells and LYPLAL1 knock-out cells were trypsinized, spun down and resuspended in Ca^{2+}, Mg^{2+}-free PBS. Cells were counted and resuspended in PBS before being sent for analysis at Lipotype GmbH. The amounts of the lipid classes were normalized to the total lipid amount to obtain mol % per total lipids. Mol % of the treated samples were divided by their respective control to obtain the mol % ratio.

Cell starvation and labelling

For the activity-based protein profiling of starved cells, Huh7 cells were seeded in 100 mm plates at $1.5x10^6$ cells per plate in full medium. After 24 hours, the cells were washed with PBS and the appropriate medium was added: high glucose (4.5g/L) DMEM with pyruvate, low glucose (1g/L) DMEM with pyruvate, and no glucose DMEM without pyruvate (Gibco, Thermo Fisher). Each condition was added with or without 10% FBS. The cells were incubated for 48 hours, after which the medium was changed for fresh medium containing 50 nM of probe 12^{313}. The cells were incubated with the probe for 5 hours after which they were lysed in 1 mL of PBS with 1% Triton-X.

Click-chemistry on LYPLAL1 probe and clean-up

The cells were lysed by sonication (15 one second pulses) and centrifuged at 20000g, 4°C for 5 min. A DC protein assay (Bio-Rad) was used to quantify protein content and supernatants were stored at -80°C. On the day of labelling, the lysates were diluted to 1 mg/mL and split into two 500 µL aliquots. To each of those aliquots, the following were added in order followed by vortexing: biotin azide (Sigma) for a final concentration of 0.09 µM, TCEP (BioShop) for a final concentration of 0.9 µM, TBTA (Sigma) for a final concentration of 0.09 µM and copper sulfate for a final concentration of 0.9 µM. The samples were rotated at room temperature for 2 hours. Proteins were precipitated in 5X volume of acetone for at least 15 minutes at -80°C and centrifuged 5 minutes at 6500 g, 4˚C. The acetone was removed, and the protein pellets were washed with 750 µL cold

methanol in 3 alternating cycles of sonication (5 one second pulses) and centrifugation at 6500 g for 5 minutes. The proteins pellets were then dissolved in 650 μL 2.5% SDS in PBS and sonicated for 15 pulses. The samples were then heated for 5 minutes at 60°C followed by centrifugation at 6500 g for 4 minutes to pellet any remaining contaminants. Aliquots of the supernatants (20μL) were taken for input control after which the remaining samples were mixed with PBS for a final volume of 8 mL.

Streptavidin enrichment

100 μL of streptavidin-agarose beads (ThermoFisher Scientific) were washed with PBS in biospin columns and added to the protein samples, followed by incubation with rotation for 1.5 h at room temperature. The beads were pelleted by centrifugation at 1400 g for 2 minutes, transferred into biospin columns (Bio-Rad) and washed 3 times with 1% SDS followed by three washes with 6 M urea.

Western blotting

For the pull-down samples, streptavidin beads were washed 3 times with PBS and incubated with 40μL of 2X SDS-PAGE loading buffer at 95°C for 15 minutes after which the buffer was pipetted off the beads. For the input samples, 4μL of 6x SDS-PAGE buffer was added to previously collected 20μL aliquots. The pull-down and input samples were run on a 10% TGX Stain-Free™ FastCast™ Acrylamide gel (Bio-Rad). Proteins were transferred from the gel to a PVDF membrane using the Trans-Blot® Turbo™ Transfer System (Bio-Rad), blocked with 5% milk in TBS-Tween for 1 hour at room temperature and probed with the primary (anti-LYPLAL1, Sigma Prestige Antibodies) and secondary antibody (Donkey anti-rabbit, Jackson Immuno-research) dilutions. For the HCV experiments, the input control was probed for HCV core (abcam) and PTP1D (BD transduction labs) For the western blotting of insulin and glucagon treated cells, the cells were lysed in SDS lysis buffer and protein content was quantified via DC protein assay (Bio-Rad). A volume corresponding to 20 μg of protein was mixed with the appropriate volume of gel loading buffer and

the samples were run as described above. The blots were probed with the primaries anti-phospho Akt (Cell Signalling), anti-Akt (Cell Signalling), anti-phospho CREB (Cell Signalling), anti-CREB (Cell Signalling) and the secondaries Donkey anti-rabbit or goat anti-mouse (Jackson Immuno-research) as appropriate.

RT-qPCR

The RNeasy (Qiagen) isolation kit was used to perform RNA isolation as per manufacturer's protocol. Reverse transcription was performed using the iScript cDNA Synthesis Kit (Bio-Rad) using 500 ng of RNA as per manufacturer's protocol. Quantitative PCR (qPCR) was performed using SYBR Green Supermix (Bio-Rad) as per manufacturer's protocol on the CFX Real-Time PCR Detection System (Bio-Rad). Primer sequences used in this study are as follows: human LYPLAL1 (fwrd 5' ATAGCGCCTCTCTGATCTTCC 3', rev 5' AAAACCTGCTTGATCCACATTCT 3'), human G6Pase, catalytic subunit (fwrd 5' GTGTCCGTGATCGCAGACC 3', rev 5' GACGAGGTTGAGCCAGTCTC 3'), human PEPCK (fwrd 5' TTGAGAAAGCGTTCAATGCCA 3', rev 5' CACGTAGGGTGAATCCGTCAG 3'), mouse LYPLAL1 (fwrd 5' TGTCAAGTGCTCAGTGGATTG 3', rev 5' CCACATCTGGGTGACTTCTGTA 3'), mouse G6Pase (fwrd 5' CGACTCGCTATCTCCAAGTGA 3', rev 5' GTTGAACCAGTCTCCGACCA 3'), mouse PCK1 (fwrd 5' CTGCATAACGGTCTGGACTTC 3', rev 5' CAGCAACTGCCCGTACTCC 3'). 18S rRNA was used for normalisation and expression fold changes relative to mock treatments were calculated using the $2^{-\Delta\Delta Ct}$ method.

HCV infection

Huh7.5 cells were infected with the HCV JFH1T strain described by Russell *et al.*[310]. Cells were seeded one day prior to infection in full medium (DMEM, 10% FBS, NEAAs) in 100 mm plates. The next day, the cells were incubated with the virus at MOI 0.1 in serum-free DMEM for 5 hours, after which the infection medium was replaced with full medium. The cells for incubated for 72

hours after which they were labelled for 4 hours with 50 nM of probe 12 and subsequently lysed in 1mL of PBS with 1% Triton-X.

Insulin treatments

HepG2 cells were seeded at 500000 cells/well in 6 well plates in full medium. The day after seeding, insulin (Sigma) or PBS mock were added to the wells for a final concentration of 0.01μM. The cells were incubated for 1 or 4 hours and lysed in RL buffer. The RNeasy (Qiagen) isolation kit was used to perform RNA isolation as per manufacturer's protocol.

Mouse hepatocyte extraction and culture

Mouse care was performed as per the Canada Council on Animal Care guidelines and approved by the University of Ottawa Animal Care Committee. Male C57BL/6 wild-type mice were purchased from Charles River. On the day of the extraction, one mouse was euthanized with 0.12 mL of pentabarbitol prior to laparotomy of the abdomen. The liver was perfused with 50 ml of 0.5 mM EGTA solution in HEPES at a flow rate of 8 mL/min followed by 50 mL of 5.4 mM collagenase type IV (Sigma) in HEPES at 6mL/min. The liver was removed and transferred to a dish containing Williams' Medium E (Gibco) in which the hepatocytes were gently removed from the hepatic sac. The cells were centrifuged twice at 1000 rpm for 5-7 minutes and the supernatant was discarded. The hepatocytes were resuspended in 20 mL of complete medium (Williams' medium with 10% FBS and 1% antibiotic/antimycotic mixture) (Gibco), plated in fibronectin coated plates and left to attach overnight.

Mouse hepatocyte treatments and labelling

For the insulin and glucagon treatments of mouse hepatocytes, the cells were plated in 6 well plates at confluency. The next day, they were treated with mock vehicle (PBS for insulin, 0.05 M acetic acid for glucagon), insulin (50 nM and 100 nM) or glucagon (1 nM and 5 nM) in fresh full medium for 20 minutes, after which they were lysed with SDS protein lysis buffer for Western blotting and

processed as indicated above. For gene expression analysis, the cells were treated with mock vehicle (PBS for insulin, 0.05 M acetic acid for glucagon), insulin (1n M, 5 nM, 10 nM, 50 nM and 100 nM) or glucagon (0.05 nM, 0.1 nM, 0.5 nM, 1 nM and 5 nM) in fresh full media for one hour or 6 hours after which they were lysed in RL buffer and the RNeasy (Qiagen) isolation kit was used to perform RNA isolation as per manufacturer's protocol. For the probe labelling samples, the mouse hepatocytes were plated for confluency in a 100 mm plate. For *in situ* labelling, the cells were labelled with 50 nM probe 12 in 3 mL of media for 5 hours and then lysed in 1% Triton X in PBS. For *in vitro* labelling, the cells were lysed in 1% Triton X in PBS, quantified with DC assay (Bio-Rad) and labelled with 10 μM probe 12 at 1 mg/mL in 1mL lysis buffer. Both *in situ* and *in vitro* samples were then processed for click-chemistry and pull-down as indicated above.

Chapter 5: General discussion and future perspectives

Characterizing molecular factors which modulate metabolic pathways and immunity is essential for the study of host-pathogen interactions. Deconvoluting the actors in these complex networks allows for the subsequent development and evaluation of therapeutic strategies. This thesis made use of chemical biology approaches to better understand the roles of a fungal xenobiotic, an immunometabolic microRNA and a poorly characterized enzyme in this context. The following discussion summarizes the key findings of each chapter and explores further investigative avenues for each project.

5.1 Activation of the aryl-hydrocarbon receptor by schizocommunin

Chapter 2 of this thesis demonstrated activation of the aryl-hydrocarbon receptor (AhR) pathway in liver and lung cells treated with an alkaloid compound extracted from a sample of *Schizophyllum commune* fungus found in the lungs of a Japanese woman. Activation of the pathway was shown to increase the expression of the metabolic enzymes CYP1A1, CYP1B1, ALDH3A1 and UGT1A in these cell models. Over the last 30 years, an increasing number of invasive infections with this fungus have been described, affecting both the respiratory and nervous systems[141–146,340]. The incidence of these diagnostics is set to become more frequent as sequencing and mass spectrometry tools become more readily available to allow for accurate identification of the pathogen in the clinic. Therefore, there is an imperative to better understand the manifestations and physiological consequences of such infections for the development of fast diagnosis tools and effective treatments.

Activation of the AhR pathway by a fungal pathogen has been previously reported. The Malassezia genus yeasts are a type of skin-dwelling opportunistic fungi which have been linked to skin abnormalities such as pityriasis versicolor, seborrheic dermatitis, atopic eczema and psoriasis[341].

These organisms have been shown to produce an array of AhR ligands using tryptophan from sweat as their nitrogen source[342]. One of these ligands, malassezin, cyclizes to form indolo[3,2-b]carbazole (ICZ), a close analogue of the potent AhR activator 6-formylindolo[3,2-b]carbazole (FICZ)[341,343]. Malassezin by itself is also an AhR agonist and was shown to cause apoptosis of primary human melanocytes[254]. ICZ as well as indirubin, another Malassezia AhR-activating metabolite, decreased human monocyte-derived dendritic cells response to immune activation[344]. Indirubin was also shown to increase the expression of proinflammatory chemokines and cytokines from normal human keratinocyte[345]. There is therefore precedent for fungal metabolites activating the AhR pathway and modulating host immune responses. *Candida albicans* is another well-known opportunistic fungus which forms part of the normal human skin flora. However, uncontrolled infections with this pathogen can be life-threatening, especially in immunocompromised individuals[346]. It was recently determined that infection with *C. albicans* activates the aryl hydrocarbon receptor and promotes endocytosis of the fungus in oral epithelial cells through a phosphorylation cascade and activation of the epidermal growth factor receptor (EGFR). Interestingly, treatment of mice with an AhR inhibitor reduced fungal infection in this model of oropharyngeal candidiasis[347]. However, in a model of vulvovaginal candidiasis also caused by *C. albicans*, agonism of AhR using indole-3-aldehyde protected mice against infection by promoting IL-22 and IL-18 production[348]. This suggests that targeting AhR for therapeutic purposes can be challenging. This is not surprising, considering the pathway's many tissue and ligand-specific functions.

To fully understand the implications of AhR activation by schizocommunin, further biochemical and immunological analysis would need to be performed. Many questions remain regarding the effects of schizocommunin-mediated AhR signalling and the link with the allergic manifestations of the fungal infection. In our study, we showed increased expression of xenobiotic metabolism

genes in cancerous liver and lung cell lines. However, there is significant evidence that the AhR pathway controls immune cell activation, differentiation and signalling in a ligand-specific manner, especially in Th17 helper T cells[24,25,246]. Th17 cells express high levels of AhR and have been associated with chronic lung inflammation via activation of macrophages and neutrophils[349]. Therefore, it would be of interest to study the effects of schizocommunin on various immune cell lineages, with emphasis on Th17 lung-resident cells. In addition, we showed that schizocommunin and its analogue exhibit low-micromolar cytotoxicity against Huh7 liver hepatoma cells. The mechanism for this effect, the reason for the difference between the two compounds, as well as the effects on primary cells all remain to be addressed. More importantly, an increase in the levels of the cytochrome drug-metabolizing enzymes suggests potential transformation of schizocommunin into various metabolites within the cells. It is therefore possible that some of the biological effects of the molecule are mediated by its transformation products. An analytical study of the metabolism of schizocommunin by purified CYP1A1, CYP1B1, ALDH3A1 and UGT1A would therefore be of interest.

Overall, this study is the first report of a *Schizophyllum commune* natural product acting as an aryl-hydrocarbon receptor agonist. It sets the stage for further biological studies which should aim to reinforce the currently poorly understood link between xenobiotic metabolism and the immune response in the context of host-pathogen interactions. As outlined in the introduction, in addition to fungi, viruses and bacterial pathogen also interact with AhR. These interactions can be both detrimental and beneficial to the host; however, in most cases, activation of AhR is linked to immunosuppression and increases pathogen virulence. Considering that the pathway can also be activated by environmental pollutants, it begs the question as to whether air quality affects our ability to fight such respiratory infections, especially in light of the recent Covid-19 pandemic.

Overall, there is considerable room for expanding our knowledge of AhR, its target metabolic genes and intersecting signalling pathways.

5.2 Functional effects of microRNA-185 as determined by activity-based protein profiling

Chapter 3 of this thesis makes use of activity-based protein profiling (ABPP) to determine the effects of miR-185, an immunometabolic small RNA, on the regulation of metabolic enzymes. These results, together with transcriptomic and lipidomic analysis, allowed for a better understanding of how miR-185 reshapes the cellular environment in liver cells to be unfavourable to HCV infection. This is done through regulation of the expression and/or activity of various serine hydrolase enzymes including fatty acid synthase (FASN), arylacetamide deacetylase (AADAC), acyl-coenzyme A (CoA) thioesterase 1 (ACOT1), lipase C (LIPC), monoacylglyceride lipase (MGLL), alpha/beta-hydrolase domain containing protein 6 (ABHD6), and carboxylesterase 1 (CES1). These enzymes have roles in both lipid and endocannabinoid metabolism. We also determined that miR-185 targets the PPARα transcription factor, thereby affecting downstream processes such as beta oxidation and triglyceride hydrolysis. Interestingly, we identified monoacylglyceride lipase as a new pharmacological target whose inhibition and downregulation hinder HCV propagation. This study was both broad in its scope of characterizing microRNA function and specific in its analysis of enzymatic modulators of metabolism. There are therefore many avenues which can be further explored to enrich our understanding of metabolic processes in host-pathogen interactions and their respective regulatory mechanisms. The following sections will discuss the value of using -omics approaches to studying microRNA function, the utility of ABPP probes for investigating direct and indirect microRNA targets, and the evolving link between the hepatitis C virus and endocannabinoid metabolism.

microRNAs, metabolism and -omics

microRNAs have the inherent ability to target multiple genes, often with an overarching physiological goal. Their diverse roles in metabolic pathways have come to light in recent years, making them attractive therapeutic agents and valuable research tools. However, there is still a need for developing methods to fully understand the functional roles of these endogenous regulators. For instance, microRNA-122 is well known for its direct interaction with the HCV genome and pro-viral role. However, this microRNA's canonical function is in triglyceride synthesis, cholesterol metabolism, and tumor suppression[350]. Indeed, the small RNA has been shown to target genes such as AGPAT1, AGPAT3 and DGAT1 as well as members of the phosphatidic acid phosphatase (PAP) family, and mouse lacking the *Mir122* gene develop hepatosteatosis[351]. Additionally, it has been shown that levels of miR-122 are reduced in hepatocellular carcinoma and that this loss of miR-122 increases cancerous cell migration and invasion[352]. A miR-122-specific inhibitor, miravirsen, was developed for the treatment of HCV infection and reached phase II clinical trials, showing broad anti-HCV activity in patients[353]. However, the drug has yet to reach the market and there is concern about the long-term effects of miR-122 depletion in the liver considering its endogenous roles[354]. Therefore, there is an imperative to fully characterize the biological effects of microRNAs before they can be considered for therapeutic interventions.

In chapter 3 of this thesis, we uncovered direct and indirect targets of miR-185. Our focus was on the modulation of serine hydrolases, but the addition of transcriptomic and lipidomic analysis allowed the contextualization of these changes within lipid metabolic pathways and lipoparticle formation. This complementation of data from broad screens and hypothesis-based experiments allows the bridging of information between effector and effect, and the deconvolution of complex regulatory pathways such as the ones modulated by microRNAs. Such systematic analysis is the basis for the emerging field of "multi-omics" in systems biology. This approach makes use of multiple large-scale screens such as genomics, epigenomics, transcriptomics, proteomics,

lipidomics and metabolomics to generate an interconnected, layered picture of biological states[355]. The use of multiple -omics methods to analyze changes in RNA transcripts and protein levels have been previously used to study microRNA function[356,357]; however, such studies rarely include lipidomic, epigenetic or metabolomic data. Since the involvement of miR-185 in metabolic pathways is well established, it would be of interest to perform metabolomic analysis in the context of miR-185 overexpression and knock-down. This could provide confirmation of changes in intermediate species and identify areas where the metabolic flux is differentially modulated by the microRNA. For instance, Bi *et al.* used mass-spectrometry metabolomics to identify N-methylnicotinamide, l-carnitine, isobutyryl-carnitine and isovaleryl-carnitine as metabolites elevated in miR-1291-expressing human pancreatic carcinoma cells, linking the microRNA to nicotinamide and fatty acid metabolism[358]. Ideally, such analyses should be performed in primary hepatocytes or tissues from genetically modified model organisms since cancerous cell line have dysregulated metabolism. Generally, the use of multi-omics analysis could be applied to the study of other metabolic or oncogenic microRNAs, especially microRNAs with potential therapeutic applications.

ABPP for the study of microRNA function

Activity-based protein profiling is a proteomic method which provides valuable end-point functional data for a subset of the proteome. In our investigation of miR-185 function, we used the fluorophosphonate activity-based probe to report on the activity of serine hydrolases. Recently, our group applied a similar workflow to probe metabolic serine hydrolases differentially regulated by microRNA-27b and identified lipase C (LIPC) as an enzyme central to the microRNA's effects on lipid metabolism. Regulation of the enzyme was also shown to be dependent on miR-27b's targeting of the transcription factors Jun, PPARα and HNF4α[359]. These studies show the practicality of ABPP as a tool to investigate microRNA function; however, fluorophosphate is just one probe out of an arsenal of molecules which can be applied to microRNA studies. For instance, the

Wortmannin probe has been previously applied by our group to identify kinases that displayed differential activity in cells expressing the full genomic replicon of HCV[360]. Alternatively, nucleotide acyl phosphate probes have been shown to label at least 75% of the known human protein kinases at the ATP binding site[361]. Targeting kinases provides valuable functional information since these proteins are involved in major signalling pathways and are often post-translationally regulated[362]. In addition, while Wortmannin and acyl phosphate probes are useful for broad studies of the kinome, more targeted probes have also been developed for the specific labeling of central kinases such as the c-Jun N-terminal kinases (JNK)[363], phosphatidylinositol 4-kinases B (PI4KB)[364] and protein kinase A (PKA)[365]. These may be of particular use in the study of oncogenic microRNAs which can regulate cell division and growth signalling. Another ABPP-targetable enzymatic group of interest is that of deubiquitylating enzymes (DUBs). These enzymes can hydrolyze peptide, amide, ester or thioester bonds at the C-terminus of ubiquitin and thereby regulate cellular processes such as proteolysis and protein trafficking[366]. MicroRNAs such as let-7b and let-7c have been shown to target deubiquitylation as part of their tumor-suppressive functions[367] and a variety of probes have been designed to target this class of enzymes[368,369]. Therefore, probing the activity of DUBs could report on the state of protein turnover downstream of microRNA signalling. Similarly, ABPP probes have been developed to target the proteasome[370–372]. This complex of proteases is the main mechanism for protein degradation in the cell and plays an important role in cellular growth, damage repair and immunity[373]. Our group has previously used an Orlistat-based probe to interrogate proteosome activity during HCV infection, demonstrating that the virus influences protein degradation[374]. Such an approach could be taken to determine if the direct or interact effects of microRNAs lead to changes in protein catabolism. In addition to the previously mentioned pathways, ABPP probes exist which able to report on the activity of glycosidases[375], poly(ADP-ribose) polymerases[376,377], histone deacetylases[378], and

methyltransferases[379], amongst many other classes of enzymes. Therefore, the field of chemical biology has a lot to offer for profiling cellular pathways in response to microRNA signalling.

Endocannabinoid metabolism and HCV

A surprising result of our investigation into miR-185's regulation of serine hydrolases was its modulation of multiple enzymes which metabolize the 2-AG endocannabinoid. Indeed, we saw changes in the activities of MGLL, ABHD6 and CES1, all enzymes known to break-down this signalling lipid. Furthermore, pharmacological inhibition and siRNA knock-down of MGLL showed potent antiviral effects against HCV. Although some links have been made between endocannabinoid metabolism and the hepatitis C virus, the mechanism through which downregulation of MGLL is antiviral is not straightforward. The enzyme catalyzes the conversion of 2-AG to arachidonic acid and glycerol, therefore, a lower activity of MGLL should increase 2-AG levels and activate the CB1 receptor. Shahidi *et al*. showed that antagonism of CB1 with the AM251 inhibitor inhibited HCV replication and infectivity[380]. This is counterintuitive to our results as we expect activation of CB1 with higher 2-AG levels. However, a more in-depth look at genes downstream of CB1, such as AMPK and SREBP1 revealed no effect on the pathway. We therefore hypothesized that MGLL's antiviral effect may be mediated by its modulation of lipid species other than 2-AG. A targeted lipid analysis revealed that both miR-185 and the MGLL inhibitor increased the levels of 18:1 MAG, also known as 1-monoolein. Further studies should investigate whether this lipid species has biological effects relevant to the HCV life cycle. This may be done by treatments with the lipid in viral infectivity assays. In a separate experiment, we observed that inhibition of MGLL did not affect the replication of the HCV subgenomic replicon, a model deficient in the production of viral particles. This suggests that the antiviral effect may be a result of decreased virion production. This could be assessed by measuring the levels of secreted virus in the supernatant of MGLL-deficient infected cells. Additionally, immunofluorescence experiments could be performed to determine whether HCV proteins are deferentially localized when the

activity of MGLL is reduced. The virus requires recruitment of its nonstructural proteins by core to lipid droplets to form its replication complexes[381], a step which is crucial to the formation of infectious particles. Overall, further investigation of the effects of MGLL depletion is cells is warranted to better understand its antiviral effect whether there is a link with the endocannabinoid system.

5.3 Role of LYPLAL1 in glucose metabolism

Chapter 4 of this thesis aims to understand the role of the LYPLAL1 serine hydrolase in glucose metabolism. Although multiple genetic association studies have linked the enzyme to metabolic phenotypes, its endogenous role is still unknown. We firstly determined that LYPLAL1 knock-out does not affect cellular lipid pools. Subsequently, we employed the activity-based probe developed by *Ahn et al.* to assess changes in the enzyme's activity in cell culture and observed that LYPLAL1 is more active under conditions of serum starvation. We also observed a modest but not statistically significant increase in the activity of the enzyme with HCV infection. Treatment of HepG2 cells with insulin showed a decrease in the levels of the gluconeogenic enzymes G6Pase and PEPCK as well as in LYPLAL1. However, a similar treatment of primary mouse hepatocytes with both insulin and glucagon did not change LYPLAL1 mRNA levels. Finally, preliminary labelling of LYPLAL1 in mouse hepatocytes revealed that the expression of the enzyme is reduced in these cells when compared to immortalized hepatocellular carcinoma cells.

Numerous questions remain to be answered to explain our observations and conclusively link LYPLAL1 to glucose metabolism. Firstly, the mechanism through which the enzyme's activity increase with serum starvation is not clear. It is possible that the allosteric activator of LYPLAL1 is an intermediary metabolite produced in greater quantities due to the metabolic reprograming that occurs during nutrient deficiency. For instance, multiple enzymes in glycolysis are under metabolic

regulation such as the activation of phosphofructokinase-1 by fructose 2,6-bisphosphate or the inhibition of pyruvate kinase by acetyl-CoA and ATP[382]. Testing changes to the enzyme's activity in the presence of elevated concentrations of such metabolic intermediates may be of interest to try and identify its endogenous activator. Alternatively, it is possible that the enzyme's activity is mediated by protein-protein interactions. For example, the mature active form of the Cathepsin D protease is composed of two interacting peptides linked by non-covalent interactions[383]. Such interactions could be captured by immunoprecipitation experiments. In this specific case, the availability of the activity probe 12 provides a unique opportunity to use the small molecule as a tool for affinity pull-down of interacting partners. Indeed, once the enzyme is labelled in cell culture, interacting proteins can be cross-linked to LYPLAL1 using agents such as formaldehyde[384]. The probe-labelled and cross-linked proteins could then be isolated using the same protocol as the one used in our study, and interacting partners could be identified using gel electrophoresis and/or mass-spectrometry[385]. These interactions could then be validated via traditional immunoprecipitation. Such experiments could be done in cells overexpressing the enzyme or under conditions of serum starvation which we have shown to increase LYPLAL1 activity.

Despite initial clues in the literature suggesting that LYPLAL1 may be of interest in the context of HCV infection, we did not observe a significant change in the enzyme's activity in our infection system. In addition, inhibition of LYPLAL1 did not affect HCV replication. LYPLAL1 was shown to be differentially expressed in fatty, steatotic and fibrotic livers, conditions which occur with chronic HCV infection. Since our system mimics more closely an acute infection with a short incubation time, it is possible that we were not able to capture HCV's true long-term effects on LYPLAL1. Inhibition of the enzyme was also shown to increase glucose production in hepatocytes, suggesting it may be involved in regulating gluconeogenesis. As discussed previously, the hepatitis C virus modulates hepatic gluconeogenesis. Taking together the available evidence, a

link may exist between LYPLAL1 expression and activity, glucose processing and the virus. However, this link is still hypothetical, and more evidence is needed to establish this correlation. Assessment of LYPLAL1 activity using probe 12 in a mouse model of chronic hepatitis C infection may provide a more accurate picture of the enzyme's role.

One of the main challenges of studying the role of this enzyme in glucose metabolism is the dysregulated metabolic phenotype of cancerous cells. Ideally, the activity of the enzyme should be consistently probed in primary hepatocytes which regulate glycolysis, gluconeogenesis and insulin/glucagon signalling most similarly to *in vivo* conditions[386,387]. However, as discussed in chapter 4, there are considerable differences between mouse and human LYPLAL1, the consequences of which have not been defined. Obtaining, culturing, and treating/modifying primary cells is also more challenging and requires more resources than traditional cancerous cell culture. These limitations will have to be considered in future studies of the enzyme's function. However, despite these constraints, we confirmed that knock-out of the enzyme does not affect lipid metabolism and showed that its activity is increased under conditions of cell starvation, further confirming the idea that LYPLAL1 may be involved in regulating, and/or may be regulated by, glucose metabolism.

5.4 Concluding remarks

Although diverse in nature, the work presented herein provides insight into the complex interactions between metabolic and immune pathways. The perspectives on xenobiotic metabolism, lipid metabolism and glucose metabolism presented in this thesis complement current knowledge and open the door for further studies in host-pathogen interactions and enzymatic function while highlighting valuable methods in chemical biology. In particular, the utility of activity-based protein profiling to study changes enzymatic activity was demonstrated in chapters 3 and 4. To our

knowledge, we are the first to apply ABPP to the study of microRNA function. By using this approach, we were able to identify new unpredicted targets of the small non-coding RNA, contextualize its function in lipid metabolism and identify an enzyme which once inhibited can recapitulate the microRNA's antiviral effect. This outcome has important implications for using ABPP as a tool to deconvolute the effects of non-coding RNAs in the cell, a valuable approach in the design of microRNA therapeutics. Overall, all three projects presented herein provide steppingstones for exciting new avenues of research in metabolism, immunity and host-pathogen interactions.

Chapter 6: References

1. Martín-Acebes, M. A., Vázquez-Calvo, Á. & Saiz, J. C. Lipids and flaviviruses, present and future perspectives for the control of dengue, Zika, and West Nile viruses. *Progress in Lipid Research* **64**, 123–137 (2016).
2. Danielson, P. B. The Cytochrome P450 Superfamily: Biochemistry, Evolution and Drug Metabolism in Humans. *Current Drug Metabolism* **3**, 561–597 (2002).
3. Nelson, D. R. Cytochrome P450: Structure, Mechanism, and Biochemistry. *Journal of the American Chemical Society* **127**, 12147–12148 (2005).
4. Hubacek, J. A. & Bobkova, D. Role of cholesterol 7α-hydroxylase (CYP7A1) in nutrigenetics and pharmacogenetics of cholesterol lowering. *Molecular Diagnosis and Therapy* **10**, 93–100 (2006).
5. Isoherranen, N. & Zhong, G. Biochemical and physiological importance of the CYP26 retinoic acid hydroxylases. *Pharmacology and Therapeutics* **204**, 107400 (2019).
6. Porubek, D. CYP17A1: A Biochemistry, Chemistry, and Clinical Review. *Current Topics in Medicinal Chemistry* **13**, 1364–1384 (2013).
7. Meunier, B., de Visser, S. P. & Shaik, S. Mechanism of oxidation reactions catalyzed by cytochrome P450 enzymes. *Chemical Reviews* **104**, 3947–3980 (2004).
8. Ma, Q. Induction of CYP1A1. The AhR / DRE Paradigm Transcription, Receptor Regulation, and Expanding Biological Roles. *Current Drug Metabolism* **2**, 149–164 (2005).
9. Brown, C. M., Reisfeld, B. & Mayeno, A. N. *Cytochromes P450: A structure-based summary of biotransformations using representative substrates*. *Drug Metabolism Reviews* **40**, (2008).
10. Mescher, M. & Haarmann-Stemmann, T. Modulation of CYP1A1 metabolism: From adverse health effects to chemoprevention and therapeutic options. *Pharmacology and Therapeutics* **187**, 71–87 (2018).
11. Mukerjee, D. Health impact of polychlorinated dibenzo-p-dioxins: A critical review. *Journal of the Air and Waste Management Association* **48**, 157–165 (1998).
12. Bock, K. W. & Köhle, C. Ah receptor: Dioxin-mediated toxic responses as hints to deregulated physiologic functions. *Biochemical Pharmacology* **72**, 393–404 (2006).
13. Rowland, A., Miners, J. O. & Mackenzie, P. I. The UDP-glucuronosyltransferases: Their role in drug metabolism and detoxification. *International Journal of Biochemistry and Cell Biology* **45**, 1121–1132 (2013).
14. Strange, R. C., Spiteri, M. A., Ramachandran, S. & Fryer, A. A. Glutathione-S-transferase family of enzymes. *Mutation Research - Fundamental and Molecular Mechanisms of Mutagenesis* **482**, 21–26 (2001).
15. Ross, D. & Siegel, D. Functions of NQO1 in cellular protection and CoQ10 metabolism and its potential role as a redox sensitive molecular switch. *Frontiers in Physiology* **8**, 1–10 (2017).
16. Voulgaridou, G. P. *et al.* Human aldehyde dehydrogenase 3A1 (ALDH3A1) exhibits chaperone-like function. *International Journal of Biochemistry and Cell Biology* **89**, 16–24 (2017).
17. Weiss, C. *et al.* TCDD induces c-jun expression via a novel Ah (dioxin) receptor-mediated p38-MAPK-dependent pathway. *Oncogene* **24**, 4975–4983 (2005).
18. Madhukar, B. V. *et al.* 2,3,7,8-Tetrachlorodibenzo-p-dioxin causes an increase in protein kinases growth hepatic associated with epidermal factor receptor in the plasma membrane. *Journal of Biochemical Toxicology* **3**, 261–277 (1988).
19. Enan, E., El-Sabeawy, F., Scott, M., Overstreet, J. & Lasley, B. Alterations in the Growth Factor Signal Transduction Pathways and Modulators of the Cell Cycle in Endocervical Cells from Macaques Exposed to TCDD. *Toxicology and Applied Pharmacology* **151**, 283–293 (1998).
20. Tian, Y., Ke, S., Denison, M. S., Rabson, A. B. & Gallo, M. A. Ah receptor and NF-κB interactions, a potential mechanism for dioxin toxicity. *Journal of Biological Chemistry* **274**, 510–515 (1999).

21. Serasanambati, M. & Chilakapati, S. R. Function of Nuclear Factor Kappa B (NF-kB) in Human Diseases-A Review. *South Indian Journal of Biological Sciences* **2**, 368 (2016).
22. Kimura, A., Naka, T., Nohara, K., Fujii-Kuriyama, Y. & Kishimoto, T. Aryl hydrocarbon receptor regulates Stat1 activation and participates in the development of Th17 cells. *Proceedings of the National Academy of Sciences* **105**, 9721–9726 (2008).
23. Kimura, A. *et al.* Aryl hydrocarbon receptor in combination with Stat1 regulates LPS-induced inflammatory responses. *The Journal of Experimental Medicine* **206**, 2027–2035 (2009).
24. Quintana, F. J. *et al.* Control of Tregand TH17 cell differentiation by the aryl hydrocarbon receptor. *Nature* **453**, 65–71 (2008).
25. Hao, N. & Whitelaw, M. L. The emerging roles of AhR in physiology and immunity. *Biochemical Pharmacology* **86**, 561–570 (2013).
26. Sibilano, R., Pucillo, C. E. & Gri, G. Allergic responses and aryl hydrocarbon receptor novel pathway of mast cell activation. *Molecular Immunology* **63**, 69–73 (2015).
27. Burleson, G. R. *et al.* Effect of 2,3,7,8-tetrachlorodibenzo-p-dioxin (TCDD) on influenza virus host resistance in mice. *Fundamental and Applied Toxicology* **29**, 40–47 (1996).
28. Giovannoni, F. *et al.* AHR is a Zika virus host factor and a candidate target for antiviral therapy. *Nature Neuroscience* **23**, 939–951 (2020).
29. Giovannoni, F. *et al.* AHR signaling is induced by infection with coronaviruses. *Nature Communications* **12**, (2021).
30. Pernomian, L., Duarte-Silva, M. & de Barros Cardoso, C. R. The Aryl Hydrocarbon Receptor (AHR) as a Potential Target for the Control of Intestinal Inflammation: Insights from an Immune and Bacteria Sensor Receptor. *Clinical Reviews in Allergy and Immunology* **59**, 382–390 (2020).
31. Scott, S. A., Fu, J. & Chang, P. V. Microbial tryptophan metabolites regulate gut barrier function via the aryl hydrocarbon receptor. *Proceedings of the National Academy of Sciences of the United States of America* **117**, 19376–19387 (2020).
32. Smith, S., Witkowski, A. & Joshi, A. K. Structural and functional organization of the animal fatty acid synthase. *Progress in Lipid Research* **42**, 289–317 (2003).
33. Pietrocola, F., Galluzzi, L., Bravo-San Pedro, J. M., Madeo, F. & Kroemer, G. Acetyl coenzyme A: A central metabolite and second messenger. *Cell Metabolism* **21**, 805–821 (2015).
34. Shi, L. & Tu, B. P. Acetyl-CoA and the regulation of metabolism: Mechanisms and consequences. *Current Opinion in Cell Biology* **33**, 125–131 (2015).
35. Hunkeler, M. *et al.* Structural basis for regulation of human acetyl-CoA carboxylase. *Nature* **558**, 470–474 (2018).
36. Brownsey, R. W., Boone, A. N., Elliott, J. E., Kulpa, J. E. & Lee, W. M. Regulation of acetyl-CoA carboxylase. *Biochemical Society Transactions* **34**, 223–227 (2006).
37. Leibundgut, M., Maier, T., Jenni, S. & Ban, N. The multienzyme architecture of eukaryotic fatty acid synthases. *Current Opinion in Structural Biology* **18**, 714–725 (2008).
38. Bond, L. M., Miyazaki, M., O'Neill, L. M., Ding, F. & Ntambi, J. M. Fatty Acid Desaturation and Elongation in Mammals. in *Biochemistry of Lipids, Lipoproteins and Membranes* 185–208 (Elsevier, 2016). doi:10.1016/B978-0-444-63438-2.00006-7
39. Ehehalt, R. *et al.* Translocation of long chain fatty acids across the plasma membrane - Lipid rafts and fatty acid transport proteins. *Molecular and Cellular Biochemistry* **284**, 135–140 (2006).
40. Wilburn, K. M., Fieweger, R. A. & VanderVen, B. C. Cholesterol and fatty acids grease the wheels of Mycobacterium tuberculosis pathogenesis. *Pathogens and disease* **76**, 1–14 (2018).
41. Yao, J. & Rock, C. O. How bacterial pathogens eat host lipids: Implications for the development of fatty acid synthesis therapeutics. *Journal of Biological Chemistry* **290**, 5940–5946 (2015).
42. Ohol, Y. M., Wang, Z., Kemble, G. & Duke, G. Direct inhibition of cellular fatty acid synthase impairs replication of respiratory syncytial virus and other respiratory viruses. *PLoS ONE* **10**, 1–20 (2015).
43. Chu, J. *et al.* Pharmacological inhibition of fatty acid synthesis blocks SARS-CoV-2 replication.

Nature Metabolism **3**, 1466–1475 (2021).

44. Yang, W. *et al.* Fatty acid synthase is up-regulated during hepatitis C virus infection and regulates hepatitis C virus entry and production. *Hepatology* **48**, 1396–1403 (2008).
45. Alves-Bezerra, M. & Cohen, D. E. Triglyceride metabolism in the liver. *Comprehensive Physiology* **8**, 1–22 (2018).
46. Wendel, A. A., Lewin, T. M. & Coleman, R. A. Glycerol-3-phosphate acyltransferases: Rate limiting enzymes of triacylglycerol biosynthesis. *Biochimica et Biophysica Acta (BBA) - Molecular and Cell Biology of Lipids* **1791**, 501–506 (2009).
47. Takeuchi, K. & Reue, K. Biochemistry, physiology, and genetics of GPAT, AGPAT, and lipin enzymes in triglyceride synthesis. *American Journal of Physiology - Endocrinology and Metabolism* **296**, (2009).
48. Vance, J. E. Phospholipid Synthesis and Transport in Mammalian Cells. *Traffic* **16**, 1–18 (2015).
49. Martin-Sanz, P., Hopewell, R. & Brindley, D. N. Long-chain fatty acids and their acyl-CoA esters cause the translocation of phosphatidate phosphohydrolase from the cytosolic to the microsomal fraction of rat liver. *FEBS Letters* **175**, 284–288 (1984).
50. Reue, K. & Zhang, P. The lipin protein family: Dual roles in lipid biosynthesis and gene expression. *FEBS Letters* **582**, 90–96 (2008).
51. Finck, B. N. *et al.* Lipin 1 is an inducible amplifier of the hepatic PGC-1α/PPARα regulatory pathway. *Cell Metabolism* **4**, 199–210 (2006).
52. Manmontri, B. *et al.* Glucocorticoids and cyclic AMP selectively increase hepatic lipin-1 expression, and insulin acts antagonistically. *Journal of Lipid Research* **49**, 1056–1067 (2008).
53. Yen, C. L. E., Stone, S. J., Koliwad, S., Harris, C. & Farese, R. V. DGAT enzymes and triacylglycerol biosynthesis. *Journal of Lipid Research* **49**, 2283–2301 (2008).
54. Sahini, N. & Borlak, J. Recent insights into the molecular pathophysiology of lipid droplet formation in hepatocytes. *Progress in Lipid Research* **54**, 86–112 (2014).
55. Miyanari, Y. *et al.* The lipid droplet is an important organelle for hepatitis C virus production. *Nature Cell Biology* **9**, 1089–1097 (2007).
56. Kumar, Y., Cocchiaro, J. & Valdivia, R. H. The Obligate Intracellular Pathogen Chlamydia trachomatis Targets Host Lipid Droplets. *Current Biology* **16**, 1646–1651 (2006).
57. Herker, E. & Ott, M. Emerging role of lipid droplets in host/pathogen interactions. *Journal of Biological Chemistry* **287**, 2280–2287 (2012).
58. Russell, D. W. Cholesterol biosynthesis and metabolism. *Cardiovascular Drugs and Therapy* **6**, 103–110 (1992).
59. Burg, J. S. & Espenshade, P. J. Regulation of HMG-CoA reductase in mammals and yeast. *Progress in Lipid Research* **50**, 403–410 (2011).
60. Brown, M. S. & Goldstein, J. L. The SREBP pathway: Regulation of cholesterol metabolism by proteolysis of a membrane-bound transcription factor. *Cell* **89**, 331–340 (1997).
61. Espenshade, P. J. & Hughes, A. L. Regulation of sterol synthesis in eukaryotes. *Annual Review of Genetics* **41**, 401–427 (2007).
62. Song, B. L., Sever, N. & DeBose-Boyd, R. A. Gp78, a membrane-anchored ubiquitin ligase, associates with Insig-1 and couples sterol-regulated ubiquitination to degradation of HMG CoA reductase. *Molecular Cell* **19**, 829–840 (2005).
63. Tobert, J. A. Lovastatin and beyond: The history of the HMG-CoA reductase inhibitors. *Nature Reviews Drug Discovery* **2**, 517–526 (2003).
64. Chang, T. Y., Chang, C. C. Y. & Cheng, D. Acyl-coenzyme A: Cholesterol acyltransferase. *Annual Review of Biochemistry* **66**, 613–638 (1997).
65. Rogers, M. A. *et al.* Acyl-CoA:cholesterol acyltransferases (ACATs/SOATs): Enzymes with multiple sterols as substrates and as activators. *Journal of Steroid Biochemistry and Molecular Biology* **151**, 102–107 (2015).

66. Ono, A. & Freed, E. O. Plasma membrane rafts play a critical role in HIV-1 assembly and release. *Proceedings of the National Academy of Sciences of the United States of America* **98**, 13925–13930 (2001).

67. Takeda, M., Leser, G. P., Russell, C. J. & Lamb, R. A. Influenza virus hemagglutinin concentrates in lipid raft microdomains for efficient viral fusion. *Proceedings of the National Academy of Sciences of the United States of America* **100**, 14610–14617 (2003).

68. Ilnytska, O. *et al.* Enteroviruses harness the cellular endocytic machinery to remodel the host cell cholesterol landscape for effective viral replication. *Cell Host and Microbe* **14**, 281–293 (2013).

69. Olofsson, S. O., Asp, L. & Borén, J. The assembly and secretion of apolipoprotein B-containing lipoproteins. *Current Opinion in Lipidology* **10**, 341–346 (1999).

70. Hussain, M. M., Shi, J. & Dreizen, P. Microsomal triglyceride transfer protein and its role in apoB-lipoprotein assembly. *Journal of Lipid Research* **44**, 22–32 (2003).

71. Gibbons, G. F., Wiggins, D., Brown, A. M. & Hebbachi, A. M. Synthesis and function of hepatic very-low-density lipoprotein. *Biochemical Society Transactions* **32**, 59–64 (2004).

72. Han, S. *et al.* Hepatic insulin signaling regulates VLDL secretion and atherogenesis in mice. *Journal of Clinical Investigation* **119**, 1029–1041 (2009).

73. Brown, A. M. & Gibbons, G. F. Insulin inhibits the maturation phase of VLDL assembly via a phosphoinositide 3-kinase-mediated event. *Arteriosclerosis, Thrombosis, and Vascular Biology* **21**, 1656–1661 (2001).

74. Haas, M. E., Attie, A. D. & Biddinger, S. B. The regulation of ApoB metabolism by insulin. *Trends in Endocrinology and Metabolism* **24**, 391–397 (2013).

75. Tiwari, S. & Siddiqi, S. A. Intracellular trafficking and secretion of VLDL. *Arteriosclerosis, Thrombosis, and Vascular Biology* **32**, 1079–1086 (2012).

76. Mead, J. R., Irvine, S. A. & Ramji, D. P. Lipoprotein lipase: Structure, function, regulation, and role in disease. *Journal of Molecular Medicine* **80**, 753–769 (2002).

77. Connelly, P. W. The role of hepatic lipase in lipoprotein metabolism. *Clinica Chimica Acta* **286**, 243–255 (1999).

78. Quiroga, A. D. & Lehner, R. Liver triacylglycerol lipases. *Biochimica et Biophysica Acta - Molecular and Cell Biology of Lipids* **1821**, 762–769 (2012).

79. Quiroga, A. D. & Lehner, R. Pharmacological intervention of liver triacylglycerol lipolysis: The good, the bad and the ugly. *Biochemical Pharmacology* **155**, 233–241 (2018).

80. Dubuquoy, C. *et al.* Distinct regulation of adiponutrin/PNPLA3 gene expression by the transcription factors ChREBP and SREBP1c in mouse and human hepatocytes. *Journal of Hepatology* **55**, 145–153 (2011).

81. Zechner, R. *et al.* FAT SIGNALS - Lipases and lipolysis in lipid metabolism and signaling. *Cell Metabolism* **15**, 279–291 (2012).

82. Taschler, U. *et al.* Monoglyceride lipase deficiency in mice impairs lipolysis and attenuates diet-induced insulin resistance. *The Journal of biological chemistry* **286**, 17467–77 (2011).

83. Labar, G., Wouters, J. & Lambert, D. M. A Review on the Monoacylglycerol Lipase: At the Interface Between Fat and Endocannabinoid Signalling. *Current Medicinal Chemistry* **17**, 2588–2607 (2010).

84. Sonnweber, T., Pizzini, A., Nairz, M., Weiss, G. & Tancevski, I. Arachidonic acid metabolites in cardiovascular and metabolic diseases. *International Journal of Molecular Sciences* **19**, (2018).

85. Bononi, G. *et al.* An updated patent review of monoacylglycerol lipase (MAGL) inhibitors (2018-present). *Expert Opinion on Therapeutic Patents* **31**, 153–168 (2021).

86. Gil-Ordóñez, A., Martín-Fontecha, M., Ortega-Gutiérrez, S. & López-Rodríguez, M. L. Monoacylglycerol lipase (MAGL) as a promising therapeutic target. *Biochemical Pharmacology* **157**, 18–32 (2018).

87. Rakhshandehroo, M. *et al.* Comprehensive analysis of PPARα-dependent regulation of hepatic lipid metabolism by expression profiling. *PPAR Research* **2007**, (2007).

88. Varga, T., Czimmerer, Z. & Nagy, L. PPARs are a unique set of fatty acid regulated transcription factors controlling both lipid metabolism and inflammation. *Biochimica et Biophysica Acta - Molecular Basis of Disease* **1812**, 1007–1022 (2011).

89. Bougarne, N. *et al.* Molecular actions of PPARα in lipid metabolism and inflammation. *Endocrine Reviews* **39**, 760–802 (2018).

90. Pawlak, M., Lefebvre, P. & Staels, B. Molecular mechanism of PPARα action and its impact on lipid metabolism, inflammation and fibrosis in non-alcoholic fatty liver disease. *Journal of Hepatology* **62**, 720–733 (2015).

91. Kota, B. P., Huang, T. H. W. & Roufogalis, B. D. An overview on biological mechanisms of PPARs. *Pharmacological Research* **51**, 85–94 (2005).

92. Kerner, J. & Hoppel, C. Fatty acid import into mitochondria. *Biochimica et Biophysica Acta - Molecular and Cell Biology of Lipids* **1486**, 1–17 (2000).

93. Indiveri, C. *et al.* The mitochondrial carnitine/acylcarnitine carrier: Function, structure and physiopathology. *Molecular Aspects of Medicine* **32**, 223–233 (2011).

94. Schulz, H. Beta oxidation of fatty acids & its Regulation. *Biochimica et Biophysica Acta* **1081**, 109–120 (1991).

95. Foster, D. W. Malonyl-CoA: The regulator of fatty acid synthesis and oxidation. *Journal of Clinical Investigation* **122**, 1958–1959 (2012).

96. Amako, Y. *et al.* Hepatitis C Virus Attenuates Mitochondrial Lipid β-Oxidation by Downregulating Mitochondrial Trifunctional-Protein Expression. *Journal of Virology* **89**, 4092–4101 (2015).

97. Kao, Y. T. *et al.* Japanese Encephalitis Virus Nonstructural Protein NS5 Interacts with Mitochondrial Trifunctional Protein and Impairs Fatty Acid β-Oxidation. *PLoS Pathogens* **11**, 1–26 (2015).

98. van Liempd, S. *et al.* Impaired beta-oxidation increases vulnerability to influenza A infection. *Journal of Biological Chemistry* **297**, 101298 (2021).

99. Thorens, B. GLUT2, glucose sensing and glucose homeostasis. *Diabetologia* **58**, 221–232 (2015).

100. Wilson, J. E. Isozymes of mammalian hexokinase: Structure, subcellular localization and metabolic function. *Journal of Experimental Biology* **206**, 2049–2057 (2003).

101. Massa, M. L., Gagliardino, J. J. & Francini, F. Liver glucokinase: An overview on the regulatorymechanisms of its activity. *IUBMB Life* **63**, 1–6 (2011).

102. Adeva-Andany, M. M., Pérez-Felpete, N., Fernández-Fernández, C., Donapetry-García, C. & Pazos-García, C. Liver glucose metabolism in humans. *Bioscience Reports* **36**, 1–15 (2016).

103. Hue, L. Gluconeogenesis and its regulation. *Diabetes/Metabolism Reviews* **3**, 111–126 (1987).

104. Yabaluri, N. & Bashyam, M. D. Hormonal regulation of gluconeogenic gene transcription in the liver. *Journal of Biosciences* **35**, 473–484 (2010).

105. Achari, A., Marshall, S. E., Muirhead, H., Palmieri, R. H. & Noltmann, E. A. Glucose-6-phosphate isomerase. *Philosophical transactions of the Royal Society of London. Series B, Biological sciences* **293**, 145–157 (1981).

106. Jenkins, C. M., Yang, J., Sims, H. F. & Gross, R. W. Reversible high affinity inhibition of phosphofructokinase-1 by Acyl-CoA: A mechanism integrating glycolytic flux with lipid metabolism. *Journal of Biological Chemistry* **286**, 11937–11950 (2011).

107. Herzog, B., Waltner-Law, M., Scott, D. K., Eschrich, K. & Granner, D. K. Characterization of the human liver fructose-1,6-bisphosphatase gene promoter. *Biochemical Journal* **351**, 385–392 (2000).

108. Pilkis, S. J. & Claus, T. H. Hepatic Gluconeogenesis/Glycolysis: Regulation and Structure/Function Relationships of Substrate Cycle Enzymes. *Annual Review of Nutrition* **11**, 465–515 (1991).

109. Taylor, C. B. & Bailey, E. Activation of liver pyruvate kinase by fructose 1,6-diphosphate. *The Biochemical journal* **102**, 32C-33C (1967).

110. Israelsen, W. J. & Vander Heiden, M. G. Pyruvate kinase: Function, regulation and role in cancer. *Seminars in Cell and Developmental Biology* **43**, 43–51 (2015).

111. Jitrapakdee, S. *et al.* Structure, mechanism and regulation of pyruvate carboxylase. *Biochemical Journal* **413**, 369–387 (2008).

112. Hanson, R. W. Thematic minireview series: A perspective on the biology of phosphoenolpyruvate carboxykinase 55 years after its discovery. *Journal of Biological Chemistry* **284**, 27021–27023 (2009).

113. Christ, B., Nath, A., Bastian, H. & Jungermann, K. Regulation of the expression of the phosphoenolpyruvate carboxykinase gene in cultured rat hepatocytes by glucagon and insulin. *European Journal of Biochemistry* **178**, 373–379 (1988).

114. Hubbard, S. R. The insulin receptor: Both a prototypical and atypical receptor tyrosine kinase. *Cold Spring Harbor Perspectives in Biology* **5**, (2013).

115. Barthel, A. & Schmoll, D. Novel concepts in insulin regulation of hepatic gluconeogenesis. *American Journal of Physiology - Endocrinology and Metabolism* **285**, (2003).

116. Vanhaesebroeck, B. & Alessi, D. R. The PI3K-PBK1 connection: More than just a road to PKB. *Biochemical Journal* **346**, 561–576 (2000).

117. Liao, J., Barthel, A., Nakatani, K. & Roth, R. A. Activation of protein kinase B/Akt is sufficient to repress the glucocorticoid and cAMP induction of phosphoenolpyruvate carboxykinase gene. *Journal of Biological Chemistry* **273**, 27320–27324 (1998).

118. Manning, B. D. & Toker, A. AKT/PKB Signaling: Navigating the Network. *Cell* **169**, 381–405 (2017).

119. Quinn, P. G. & Yeagley, D. Insulin regulation of PEPCK gene expression: A model for rapid and reversible modulation. *Current Drug Targets: Immune, Endocrine and Metabolic Disorders* **5**, 423–437 (2005).

120. Mattedi, G., Acosta-Gutiérrez, S., Clark, T. & Gervasio, F. L. A combined activation mechanism for the glucagon receptor. *Proceedings of the National Academy of Sciences of the United States of America* **117**, 15414–15422 (2020).

121. Mayr, B. & Montminy, M. Transcriptional regulation by the phosphorylation-dependent factor creb. *Nature Reviews Molecular Cell Biology* **2**, 599–609 (2001).

122. Janah, L. *et al.* Glucagon receptor signaling and glucagon resistance. *International Journal of Molecular Sciences* **20**, (2019).

123. Watford, M. Starvation: Metabolic Changes. in *eLS* 1–7 (Wiley, 2015). doi:10.1002/9780470015902.a0000642.pub2

124. Weber, G., Singhal, R. L. & Srivastava, S. K. Effect of nutritional state on hormonal regulation of liver enzymes. *Canadian journal of biochemistry* **43**, 1549–1563 (1965).

125. Hsieh, W. C. *et al.* Glucose starvation induces a switch in the histone acetylome for activation of gluconeogenic and fat metabolism genes. *Molecular Cell* **82**, 60-74.e5 (2022).

126. Liu, Y. *et al.* A fasting inducible switch modulates gluconeogenesis via activator/coactivator exchange. *Nature* **456**, 269–273 (2008).

127. Wang, Z. & Dong, C. Gluconeogenesis in Cancer: Function and Regulation of PEPCK, FBPase, and G6Pase. *Trends in Cancer* **5**, 30–45 (2019).

128. Grasmann, G., Smolle, E., Olschewski, H. & Leithner, K. Gluconeogenesis in cancer cells – Repurposing of a starvation-induced metabolic pathway? *Biochimica et Biophysica Acta - Reviews on Cancer* **1872**, 24–36 (2019).

129. Annibaldi, A. & Widmann, C. Glucose metabolism in cancer cells. *Current Opinion in Clinical Nutrition and Metabolic Care* **13**, 466–470 (2010).

130. Lugus, J. J., Walsh, K., Shoelson, S. E. & Cantrell, D. A. Immunometabolism: an emerging frontier. *Nature Publishing Group* **11**, 81–83 (2011).

131. Boothby, M. & Rickert, R. C. Metabolic Regulation of the Immune Humoral Response. *Immunity* **46**, 743–755 (2017).

132. Mouton, A. J., Li, X., Hall, M. E. & Hall, J. E. Obesity, hypertension, and cardiac dysfunction novel roles of immunometabolism in macrophage activation and inflammation. *Circulation*

Research 789–806 (2020). doi:10.1161/CIRCRESAHA.119.312321

133. Ayres, J. S. Immunometabolism of infections. *Nature Reviews Immunology* **20**, 79–80 (2020).
134. Brown, G. D. *et al.* Hidden killers: Human fungal infections. *Science Translational Medicine* **4**, 1–10 (2012).
135. Weerasinghe, H. & Traven, A. Immunometabolism in fungal infections: the need to eat to compete. *Current Opinion in Microbiology* **58**, 32–40 (2020).
136. Tucey, T. M. *et al.* Glucose Homeostasis Is Important for Immune Cell Viability during Candida Challenge and Host Survival of Systemic Fungal Infection. *Cell Metabolism* **27**, 988-1006.e7 (2018).
137. Cheng, S.-C. *et al.* Candida albicans Dampens Host Defense by Downregulating IL-17 Production . *The Journal of Immunology* **185**, 2450–2457 (2010).
138. Rosa, R. L. *et al.* Proteomics of Rat Lungs Infected by Cryptococcus gattii Reveals a Potential Warburg-like Effect. *Journal of Proteome Research* **18**, 3885–3895 (2019).
139. Akoumianaki, T. *et al.* Aspergillus Cell Wall Melanin Blocks LC3-Associated Phagocytosis to Promote Pathogenicity. *Cell Host and Microbe* **19**, 79–90 (2016).
140. Ohm, R. A. *et al.* Genome sequence of the model mushroom Schizophyllum commune. *Nature Biotechnology* **28**, 957–963 (2010).
141. Kim, H. *et al.* Pneumonia due to Schizophyllum commune in a Patient with Acute Myeloid Leukemia: Case Report and Literature Review. *Infection and Chemotherapy* **53**, 195–201 (2021).
142. Kamei, K. *et al.* Allergic Bronchopulmonary Mycosis Caused by the Basidiomycetous Fungus Schizophyllum commune. *Clinical Infectious Diseases* **18**, 305–309 (1994).
143. Won, E. J. *et al.* Molecular identifcation of Schizophyllum commune as a cause of allergic fungal sinusitis. *Annals of Laboratory Medicine* **32**, 375–379 (2012).
144. Swain, B., Panigrahy, R. & Panigrahi, D. Schizophyllum commune sinusitis in an immunocompetent host. *Indian Journal of Medical Microbiology* **29**, 439–442 (2011).
145. Kaur, M. *et al.* Sino-orbital infection caused by Schizophyllum commune - rare presentation of a basidiomycetous fungus. *Journal de Mycologie Medicale* **30**, 30–32 (2020).
146. Rihs, J. D., Padhye, A. A. & Good, C. B. Brain abscess caused by Schizophyllum commune: an emerging basidiomycete pathogen. *Journal of Clinical Microbiology* **34**, 1628–1632 (1996).
147. Sanchez, E. L. & Lagunoff, M. Viral activation of cellular metabolism. *Virology* **479**–**480**, 609–618 (2015).
148. Fritsch, S. D. & Weichhart, T. Effects of interferons and viruses on metabolism. *Frontiers in Immunology* **7**, 1–13 (2016).
149. Thaker, S. K., Ch'ng, J. & Christofk, H. R. Viral hijacking of cellular metabolism. *BMC biology* **17**, 59 (2019).
150. Munger, J., Bajad, S. U., Coller, H. A., Shenk, T. & Rabinowitz, J. D. Dynamics of the cellular metabolome during human cytomegalovirus infection. *PLoS Pathogens* **2**, 1165–1175 (2006).
151. Abrantes, J. L. *et al.* Herpes simplex type 1 activates glycolysis through engagement of the enzyme 6-phosphofructo-1-kinase (PFK-1). *Biochimica et Biophysica Acta - Molecular Basis of Disease* **1822**, 1198–1206 (2012).
152. Fontaine, K. A., Sanchez, E. L., Camarda, R. & Lagunoff, M. Dengue Virus Induces and Requires Glycolysis for Optimal Replication. *Journal of Virology* **89**, 2358–2366 (2015).
153. Diamond, D. L. *et al.* Temporal proteome and lipidome profiles reveal hepatitis C virus-associated reprogramming of hepatocellular metabolism and bioenergetics. *PLoS Pathogens* **6**, (2010).
154. Yang, F. *et al.* Expression of hepatitis B virus proteins in transgenic mice alters lipid metabolism and induces oxidative stress in the liver. *Journal of Hepatology* **48**, 12–19 (2008).
155. Alvisi, G., Madan, V. & Bartenschlager, R. Hepatitis C virus and host cell lipids: An intimate connection. *RNA Biology* **8**, (2011).
156. Heaton, N. S. & Randall, G. Dengue virus-induced autophagy regulates lipid metabolism. *Cell Host*

and Microbe **8**, 422–432 (2010).

157. Delgado, T., Sanchez, E. L., Camarda, R. & Lagunoff, M. Global Metabolic Profiling of Infection by an Oncogenic Virus: KSHV Induces and Requires Lipogenesis for Survival of Latent Infection. *PLoS Pathogens* **8**, (2012).
158. Shepard, C. W., Finelli, L. & Alter, M. J. Global epidemiology of hepatitis C virus infection. *The Lancet Infectious Diseases* **5**, 558–567 (2005).
159. Popescu, C.-I. *et al.* Hepatitis C Virus Life Cycle and Lipid Metabolism. *Biology* **3**, 892–921 (2014).
160. Lerat, H. *et al.* Hepatitis C virus induces a prediabetic state by directly impairing hepatic glucose metabolism in mice. *Journal of Biological Chemistry* **292**, 12860–12873 (2017).
161. Shoji, I., Deng, L. & Hotta, H. Molecular mechanism of hepatitis C virus-induced glucose metabolic disorders. *Frontiers in Microbiology* **2**, 1–5 (2012).
162. Li, Q. *et al.* Cellular microRNA networks regulate host dependency of hepatitis C virus infection. *Nature Communications* **8**, 1789 (2017).
163. El-Diwany, R. *et al.* Acute Hepatitis C Virus Infection Induces Consistent Changes in Circulating MicroRNAs That Are Associated with Nonlytic Hepatocyte Release. *Journal of Virology* **89**, 9454–9464 (2015).
164. Dienes, H. P., Popper, H., Arnold, W. & Lobeck, H. Histologic Observations in Human Hepatitis Non-A, Non-B. *Hepatology* **2**, 562S-571S (1982).
165. Modaresi Esfeh, J. & Ansari-Gilani, K. Steatosis and hepatitis C. *Gastroenterology Report* **4**, gov040 (2015).
166. Andréo, U. *et al.* Lipoprotein lipase mediates hepatitis C virus (HCV) cell entry and inhibits HCV infection. *Cellular Microbiology* **9**, 2445–2456 (2007).
167. Gerold, G., Moeller, R. & Pietschmann, T. Hepatitis c virus entry: Protein interactions and fusion determinants governing productive hepatocyte invasion. *Cold Spring Harbor Perspectives in Medicine* **10**, (2020).
168. Suzuki, R., Suzuki, T., Ishii, K., Matsuura, Y. & Miyamura, T. Processing and functions of hepatitis C virus proteins. *Intervirology* **42**, 145–152 (1999).
169. Egger, D. *et al.* Expression of Hepatitis C Virus Proteins Induces Distinct Membrane Alterations Including a Candidate Viral Replication Complex. *Journal of Virology* **76**, 5974–5984 (2002).
170. Reiss, S. *et al.* Recruitment and activation of a lipid kinase by hepatitis C virus NS5A is essential for integrity of the membranous replication compartment. *Cell Host and Microbe* **9**, 32–45 (2011).
171. Bishé, B., Syed, G. & Siddiqui, A. Phosphoinositides in the hepatitis C virus life cycle. *Viruses* **4**, 2340–2358 (2012).
172. Meng, Z., Liu, Q., Sun, F. & Qiao, L. Hepatitis C virus nonstructural protein 5A perturbs lipid metabolism by modulating AMPK/SREBP-1c signaling. *Lipids in Health and Disease* **18**, 1–13 (2019).
173. Oem, J. K. *et al.* Activation of sterol regulatory element-binding protein 1c and fatty acid synthase transcription by hepatitis C virus non-structural protein 2. *Journal of General Virology* **89**, 1225–1230 (2008).
174. Herker, E. *et al.* Efficient hepatitis C virus particle formation requires diacylglycerol acyltransferase-1. *Nature Medicine* **16**, 1295–1298 (2010).
175. Read, S. A., Tay, E., Shahidi, M., George, J. & Douglas, M. W. Hepatitis C virus infection mediates cholesteryl ester synthesis to facilitate infectious particle production. *Journal of General Virology* **95**, 1900–1910 (2014).
176. Liefhebber, J. M. P., Hague, C. V., Zhang, Q., Wakelam, M. J. O. & McLauchlan, J. Modulation of triglyceride and cholesterol ester synthesis impairs assembly of infectious hepatitis C virus. *Journal of Biological Chemistry* **289**, 21276–21288 (2014).
177. Masaki, T. *et al.* Involvement of Hepatitis C Virus NS5A Hyperphosphorylation Mediated by Casein Kinase I-α in Infectious Virus Production. *Journal of Virology* **88**, 7541–7555 (2014).

178. Menzel, N. *et al.* MAP-kinase regulated cytosolic phospholipase A2 activity is essential for production of infectious Hepatitis C virus particles. *PLoS Pathogens* **8**, 21 (2012).

179. Grassi, G. *et al.* Hepatitis C virus relies on lipoproteins for its life cycle. *World Journal of Gastroenterology* **22**, 1953–1965 (2016).

180. Huang, H. *et al.* Hepatitis C virus production by human hepatocytes dependent on assembly and secretion of very low-density lipoproteins. *Proceedings of the National Academy of Sciences* **104**, 5848–5853 (2007).

181. Coller, K. E. *et al.* Molecular determinants and dynamics of hepatitis C virus secretion. *PLoS Pathogens* **8**, (2012).

182. Desbois, A. C. & Cacoub, P. Diabetes mellitus, insulin resistance and hepatitis C virus infection: A contemporary review. *World Journal of Gastroenterology* **23**, 1697–1711 (2017).

183. Alaei, M. & Negro, F. Hepatitis C virus and glucose and lipid metabolism. *Diabetes & metabolism* **34**, 692–700 (2008).

184. Zhu, S. *et al.* p38MAPK plays a critical role in induction of a pro-inflammatory phenotype of retinal Müller cells following Zika virus infection. *Antiviral Research* **145**, 70–81 (2017).

185. Yu, J. W. *et al.* Hepatitis C virus core protein induces hepatic metabolism disorders through down-regulation of the SIRT1-AMPK signaling pathway. *International Journal of Infectious Diseases* **17**, e539–e545 (2013).

186. Parvaiz, F. *et al.* Hepatitis C virus nonstructural protein 5A favors upregulation of gluconeogenic and lipogenic gene expression leading towards insulin resistance: A metabolic syndrome. *Archives of Virology* **159**, 1017–1025 (2014).

187. Rottiers, V. & Näär, A. M. MicroRNAs in metabolism and metabolic disorders. *Nature reviews. Molecular cell biology* **13**, 239–50 (2012).

188. Zhu, S., Pan, W. & Qian, Y. MicroRNA in immunity and autoimmunity. *Journal of Molecular Medicine* **91**, 1039–1050 (2013).

189. Gulyaeva, L. F. & Kushlinskiy, N. E. Regulatory mechanisms of microRNA expression. *Journal of Translational Medicine* **14**, 1–10 (2016).

190. Trobaugh, D. W. & Klimstra, W. B. MicroRNA Regulation of RNA Virus Replication and Pathogenesis. *Trends in Molecular Medicine* **23**, 80–93 (2017).

191. Jopling, C. L., Yi, M. K., Lancaster, A. M., Lemon, S. M. & Sarnow, P. Molecular biology: Modulation of hepatitis C virus RNA abundance by a liver-specific MicroRNA. *Science* **309**, 1577–1581 (2005).

192. Mortimer, S. A. & Doudna, J. A. Unconventional miR-122 binding stabilizes the HCV genome by forming a trimolecular RNA structure. *Nucleic Acids Research* **41**, 4230–4240 (2013).

193. Luna, J. M. *et al.* Hepatitis C virus RNA functionally sequesters miR-122. *Cell* **160**, 1099–1110 (2015).

194. Shrivastava, S., Steele, R., Ray, R. & Ray, R. B. MicroRNAs: Role in hepatitis C virus pathogenesis. *Genes and Diseases* **2**, 35–45 (2015).

195. Forster, S. C., Tate, M. D. & Hertzog, P. J. MicroRNA as type I interferon-regulated transcripts and modulators of the innate immune response. *Frontiers in Immunology* **6**, 1–9 (2015).

196. Pedersen, I. M. *et al.* Interferon modulation of cellular microRNAs as an antiviral mechanism. *Nature* **449**, 919–922 (2007).

197. Shirasaki, T. *et al.* MicroRNA-27a Regulates Lipid Metabolism and Inhibits Hepatitis C Virus Replication in Human Hepatoma Cells. *Journal of Virology* **87**, 5270–5286 (2013).

198. Singaravelu, R. *et al.* MicroRNAs regulate the immunometabolic response to viral infection in the liver. *Nature Chemical Biology* **11**, 988–993 (2015).

199. Wang, X.-C., Zhan, X.-R., Li, X.-Y., Yu, J.-J. & Liu, X.-M. MicroRNA-185 regulates expression of lipid metabolism genes and improves insulin sensitivity in mice with non-alcoholic fatty liver disease. *World journal of gastroenterology : WJG* **20**, 17914–23 (2014).

200. Yang, M. *et al.* Identification of miR-185 as a regulator of de novo cholesterol biosynthesis and

low density lipoprotein uptake. *Journal of Lipid Research* **55**, 226–238 (2014).

201. Anderson, N. L. & Anderson, N. G. Proteome and proteomics: New technologies, new concepts, and new words. *Electrophoresis* **19**, 1853–1861 (1998).
202. Gygi, S. P. & Aebersold, R. Mass spectrometry and proteomics. *Current Opinion in Chemical Biology* **4**, 489–494 (2000).
203. Westermeier, R. & Marouga, R. Protein detection methods in proteomics research. *Bioscience Reports* **25**, 19–32 (2005).
204. Qian, W. J., Jacobs, J. M., Liu, T., Camp, D. G. & Smith, R. D. Advances and challenges in liquid chromatography-mass spectrometry-based proteomics profiling for clinical applications. *Molecular and Cellular Proteomics* **5**, 1727–1744 (2006).
205. Harborth, J., Elbashir, S. M., Bechert, K., Tuschl, T. & Weber, K. Identification of essential genes in cultured mammalian cells using small interfering RNAs. *Journal of Cell Science* **114**, 4557–4565 (2001).
206. Urnov, F. D., Rebar, E. J., Holmes, M. C., Zhang, H. S. & Gregory, P. D. Genome editing with engineered zinc finger nucleases. *Nature Reviews Genetics* **11**, 636–646 (2010).
207. Minghua Deng, Kui Zhang, Mehta, S., Ting Chen & Fengzhu Sun. Prediction of protein function using protein-protein interaction data. in *Proceedings. IEEE Computer Society Bioinformatics Conference* **3037**, 197–206 (IEEE Comput. Soc, 2004).
208. Watson, J. D., Laskowski, R. A. & Thornton, J. M. Predicting protein function from sequence and structural data. *Current Opinion in Structural Biology* **15**, 275–284 (2005).
209. Berger, A. B., Vitorino, P. M. & Bogyo, M. Activity-based protein profiling: applications to biomarker discovery, in vivo imaging and drug discovery. *American Journal of Pharmacogenetics* **4**, 371–381 (2004).
210. Cravatt, B. F., Wright, A. T. & Kozarich, J. W. Activity-Based Protein Profiling: From Enzyme Chemistry to Proteomic Chemistry. *Annual Review of Biochemistry* **77**, 383–414 (2008).
211. Jessani, N. & Cravatt, B. F. The development and application of methods for activity-based protein profiling. *Current Opinion in Chemical Biology* **8**, 54–59 (2004).
212. Sieber, S. A. & Cravatt, B. F. Analytical platforms for activity-based protein profiling - Exploiting the versatility of chemistry for functional proteomics. *Chemical Communications* 2311–2319 (2006). doi:10.1039/b600653c
213. Cardoza, J. D., Parikh, J. R., Ficarro, S. B. & Marto, J. A. Mass spectrometry-based proteomics: Qualitative identification to activity-based protein profiling. *Wiley Interdisciplinary Reviews: Systems Biology and Medicine* **4**, 141–162 (2012).
214. Sap, K. A. & Demmers, J. A. Labeling Methods in Mass Spectrometry Based Quantitative Proteomics. in *Integrative Proteomics* (InTech, 2012). doi:10.5772/32489
215. Xie, F., Liu, T., Qian, W. J., Petyuk, V. A. & Smith, R. D. Liquid chromatography-mass spectrometry-based quantitative proteomics. *Journal of Biological Chemistry* **286**, 25443–25449 (2011).
216. Abdel-Daim, A., Ohura, K. & Imai, T. A novel quantification method for serine hydrolases in cellular expression system using fluorophosphonate-biotin probe. *European Journal of Pharmaceutical Sciences* **114**, 267–274 (2018).
217. Hsu, J. L., Huang, S. Y., Chow, N. H. & Chen, S. H. Stable-Isotope Dimethyl Labeling for Quantitative Proteomics. *Analytical Chemistry* **75**, 6843–6852 (2003).
218. Boersema, P. J., Raijmakers, R., Lemeer, S., Mohammed, S. & Heck, A. J. R. Multiplex peptide stable isotope dimethyl labeling for quantitative proteomics. *Nature Protocols* **4**, 484–494 (2009).
219. Boersema, P. J., Aye, T. T., Van Veen, T. A. B., Heck, A. J. R. & Mohammed, S. Triplex protein quantification based on stable isotope labeling by peptide dimethylation applied to cell and tissue lysates. *Proteomics* **8**, 4624–4632 (2008).
220. Bachovchin, D. A. & Cravatt, B. F. The pharmacological landscape and therapeutic potential of serine hydrolases. *Nature Reviews Drug Discovery* **11**, 52–68 (2012).

221. Simon, G. M. & Cravatt, B. F. Activity-based proteomics of enzyme superfamilies: Serine hydrolases as a case study. *Journal of Biological Chemistry* **285**, 11051–11055 (2010).

222. Long, J. Z. & Cravatt, B. F. The metabolic serine hydrolases and their functions in mammalian physiology and disease. *Chemical Reviews* **111**, 6022–6063 (2011).

223. Jensen-Urstad, A. P. L. & Semenkovich, C. F. Fatty acid synthase and liver triglyceride metabolism: Housekeeper or messenger? *Biochimica et Biophysica Acta (BBA) - Molecular and Cell Biology of Lipids* **1821**, 747–753 (2012).

224. Satoh, T. & Hosokawa, M. Structure, function and regulation of carboxylesterases. *Chemico-Biological Interactions* **162**, 195–211 (2006).

225. Kirkby, B., Roman, N., Kobe, B., Kellie, S. & Forwood, J. K. Functional and structural properties of mammalian acyl-coenzyme A thioesterases. *Progress in Lipid Research* **49**, 366–377 (2010).

226. Blais, D. R. *et al.* Activity-based Protein Profiling Identifies a Host Enzyme, Carboxylesterase 1, Which Is Differentially Active during Hepatitis C Virus Replication. *Journal of Biological Chemistry* **285**, 25602–25612 (2010).

227. Faucher, F., Bennett, J. M., Bogyo, M. & Lovell, S. Strategies for Tuning the Selectivity of Chemical Probes that Target Serine Hydrolases. *Cell Chemical Biology* **27**, 937–952 (2020).

228. Speers, A. E. & Cravatt, B. F. Profiling Enzyme Activities In Vivo Using Click Chemistry Methods. *Chemistry & Biology* **11**, 535–546 (2004).

229. Speers, A. E., Adam, G. C. & Cravatt, B. F. Activity-Based Protein Profiling in Vivo Using a Copper (I) -Catalyzed Azide-Alkyne [3 + 2] Cycloaddition. **4**, 4686–4687 (2003).

230. Nasheri, N. *et al.* Modulation of Fatty Acid Synthase Enzyme Activity and Expression during Hepatitis C Virus Replication. *Chemistry & Biology* **20**, 570–582 (2013).

231. Tsai, C. S. *et al.* Cell-permeable probe for identification and imaging of sialidases. *Proceedings of the National Academy of Sciences of the United States of America* **110**, 2466–2471 (2013).

232. Ahn, K. *et al.* Discovery of a Selective Covalent Inhibitor of Lysophospholipase-like 1 (LYPLAL1) as a Tool to Evaluate the Role of this Serine Hydrolase in Metabolism. *ACS Chemical Biology* **11**, 2529–2540 (2016).

233. Hernández-Tobías, E.-A. *et al.* PPARG-LYPLAL1 Multi-Allelic Combination Associated with Obesity and Overweight in Mexican Adolescent Females. *Ethnicity & Disease* **26**, 477 (2016).

234. Hotta, K. *et al.* Polymorphisms in NRXN3, TFAP2B, MSRA, LYPLAL1, FTO and MC4R and their effect on visceral fat area in the Japanese population. *Journal of Human Genetics* **55**, 738–742 (2010).

235. Speliotes, E. K. *et al.* Genome-wide association analysis identifies variants associated with nonalcoholic fatty liver disease that have distinct effects on metabolic traits. *PLoS Genetics* **7**, (2011).

236. Bille, D. S. *et al.* Implications of central obesity-related variants in LYPLAL1, NRXN3, MSRA, and TFAP2B on quantitative metabolic traits in adult danes. *PLoS ONE* **6**, (2011).

237. Kok, B. P. *et al.* Discovery of small-molecule enzyme activators by activity-based protein profiling. *Nature Chemical Biology* **16**, 997–1005 (2020).

238. Wong, C. K., Leung, K. N., Fung, K. P. & Choy, Y. M. Immunomodulatory and Anti-Tumour Polysaccharides from Medicinal Plants. *Journal of International Medical Research* **22**, 299–312 (1994).

239. Hosoe, T. *et al.* Isolation of a new potent cytotoxic pigment along with indigotin from the pathogenic basidiomycetous fungus Schizophyllum commune. *Mycopathologia* **146**, 9–12 (1999).

240. Uehata, K. *et al.* Total synthesis of schizocommunin and revision of its structure. *Journal of Natural Products* **76**, 2034–2039 (2013).

241. Esser, C. Biology and function of the aryl hydrocarbon receptor: Report of an international and interdisciplinary conference. *Archives of Toxicology* **86**, 1323–1329 (2012).

242. Mimura, J. & Fujii-Kuriyama, Y. Functional role of AhR in the expression of toxic effects by TCDD. *Biochimica et Biophysica Acta - General Subjects* **1619**, 263–268 (2003).

243. Nebert, D. W., Puga, A. & Vasilis, V. Role of the Ah Receptor and the Dioxin-Inducible [Ah] Gene Battery in Toxicity, Cancer, and Signal Transduction. *Annals of the New York Academy of Sciences* **685**, 624–640 (1993).

244. Denison, M. S. & Nagy, S. R. Activation of the aryl hydrocarbon receptor by structurally diverse exogenous and endogenous chemicals. *Annual Review of Pharmacology and Toxicology* **43**, 309–334 (2003).

245. Beischlag, T. V, Luis Morales, J., Hollingshead, B. D. & Perdew, G. H. The aryl hydrocarbon receptor complex and the control of gene expression. *Critical reviews in eukaryotic gene expression* **18**, 207–50 (2008).

246. Esser, C., Rannug, A. & Stockinger, B. The aryl hydrocarbon receptor in immunity. *Trends in Immunology* **30**, 447–454 (2009).

247. Kerkvliet, N. I. Recent advances in understanding the mechanisms of TCDD immunotoxicity. *International Immunopharmacology* **2**, 277–291 (2002).

248. Veldhoen, M. *et al.* The aryl hydrocarbon receptor links TH17-cell-mediated autoimmunity to environmental toxins. *Nature* **453**, 106–109 (2008).

249. Kawasaki, H. *et al.* A tryptophan metabolite, kynurenine, promotes mast cell activation through aryl hydrocarbon receptor. *Allergy: European Journal of Allergy and Clinical Immunology* **69**, 445–452 (2014).

250. Danelli, L. *et al.* The Aryl Hydrocarbon Receptor Modulates Acute and Late Mast Cell Responses. *The Journal of Immunology* **189**, 120–127 (2012).

251. Iyer, S. S. *et al.* Dietary and Microbial Oxazoles Induce Intestinal Inflammation by Modulating Aryl Hydrocarbon Receptor Responses. *Cell* **173**, 1123-1134.e11 (2018).

252. Moura-Alves, P. *et al.* AhR sensing of bacterial pigments regulates antibacterial defence. *Nature* **512**, 387–392 (2014).

253. Carney, P. R. *et al.* Aryl hydrocarbon receptor-dependent apoptotic cell death induced by the flavonoid chrysin in human colorectal cancer cells. *Cancer Letters* **370**, 91–99 (2015).

254. Krämer, H. J. *et al.* Malassezin, a novel agonist of the aryl hydrocarbon receptor from the yeast Malassezia furfur, induces apoptosis in primary human melanocytes. *ChemBioChem* **6**, 860–865 (2005).

255. Chopra, M. & Schrenk, D. Dioxin toxicity, aryl hydrocarbon receptor signaling, and apoptosis-Persistent pollutants affect programmed cell death. *Critical Reviews in Toxicology* **41**, 292–320 (2011).

256. Dyer, B. W., Ferrer, F. A., Klinedinst, D. K. & Rodriguez, R. A noncommercial dual luciferase enzyme assay system for reporter gene analysis. *Analytical Biochemistry* **282**, 158–161 (2000).

257. Scaria, V., Hariharan, M., Maiti, S., Pillai, B. & Brahmachari, S. K. Host-virus interaction: a new role for microRNAs. *Retrovirology* **3**, 68 (2006).

258. John, B. *et al.* Human MicroRNA targets. *PLoS biology* **2**, e363 (2004).

259. Lewis, B. P., Shih, I., Jones-Rhoades, M. W., Bartel, D. P. & Burge, C. B. 33-Prediction of Mammalian MicroRNA Targets. *Cell* **115**, 787–798 (2003).

260. Didiano, D. & Hobert, O. Perfect seed pairing is not a generally reliable predictor for miRNA-target interactions. *Nature structural & molecular biology* **13**, 849–851 (2006).

261. Chi, S. W., Zang, J. B., Mele, A. & Darnell, R. B. Argonaute HITS-CLIP decodes microRNA-mRNA interaction maps. *Nature* **460**, 479–486 (2009).

262. Merkel, M., Eckel, R. H. & Goldberg, I. J. Lipoprotein lipase. *Journal of Lipid Research* **43**, 1997–2006 (2002).

263. Thomas, G. *et al.* The Serine Hydrolase ABHD6 Is a Critical Regulator of the Metabolic Syndrome. *Cell Reports* **5**, 508–520 (2013).

264. Pham, C. T. N. Neutrophil serine proteases: specific regulators of inflammation. *Nature Reviews Immunology* **6**, 541–550 (2006).

265. Liu, Y., Patricelli, M. P. & Cravatt, B. F. Activity-based protein profiling: The serine hydrolases.

Proceedings of the National Academy of Sciences of the United States of America **96**, 14694–14699 (1999).

266. Chang, S. & Borensztajn, J. Hepatic lipase function and the accumulation of beta-very-low- density lipoproteins in the plasma of cholesterol-fed rabbits. *Biochemical Journal* **293**, 745–750 (1993).

267. Hunt, M. C., Tillander, V. & Alexson, S. E. H. Regulation of peroxisomal lipid metabolism: The role of acyl-CoA and coenzyme A metabolizing enzymes. *Biochimie* **98**, 45–55 (2014).

268. Lo, V. *et al.* Arylacetamide deacetylase attenuates fatty-acid-induced triacylglycerol accumulation in rat hepatoma cells. *Journal of Lipid Research* **51**, 368–377 (2010).

269. Maier, T. *et al.* The crystal structure of a mammalian fatty acid synthase. *Science (New York, N.Y.)* **321**, 1315–22 (2008).

270. Sun, L. J. *et al.* Endocannabinoid system activation contributes to glucose metabolism disorders of hepatocytes and promotes hepatitis C virus replication. *International Journal of Infectious Diseases* **23**, 75–81 (2014).

271. Chanda, D. *et al.* Activation of cannabinoid receptor type 1 (Cb1r) disrupts hepatic insulin receptor signaling via cyclic AMP-response element-binding protein H (Crebh)-mediated induction of Lipin1 gene. *The Journal of biological chemistry* **287**, 38041–9 (2012).

272. Patsenker, E. *et al.* Elevated Levels of Endocannabinoids in Chronic Hepatitis C May Modulate Cellular Immune Response and Hepatic Stellate Cell Activation. *International Journal of Molecular Sciences* **16**, 7057–7076 (2015).

273. Di Marzo, V., Bifulco, M. & De Petrocellis, L. The endocannabinoid system and its therapeutic exploitation. *Nature Reviews Drug Discovery* **3**, 771–784 (2004).

274. Dharancy, S., Lemoine, M., Mathurin, P., Serfaty, L. & Dubuquoy, L. Peroxisome Proliferator-Activated Receptors in HCV-Related Infection. *PPAR Research* **2009**, 1–5 (2009).

275. Dongol, B., Shah, Y., Kim, I., Gonzalez, F. J. & Hunt, M. C. The acyl-CoA thioesterase I is regulated by PPARα and HNF4α via a distal response element in the promoter. *Journal of Lipid Research* **48**, 1781–1791 (2007).

276. Jones, R. D., Taylor, A. M., Tong, E. Y. & Repa, J. J. Carboxylesterases Are Uniquely Expressed among Tissues and Regulated by Nuclear Hormone Receptors in the Mouse. *Drug Metabolism and Disposition* **41**, 40–49 (2013).

277. Kersten, S. & Stienstra, R. The role and regulation of the peroxisome proliferator activated receptor alpha in human liver. *Biochimie* **136**, 75–84 (2017).

278. Jones, D. M. & McLauchlan, J. Hepatitis C virus: Assembly and release of virus particles. *Journal of Biological Chemistry* **285**, 22733–22739 (2010).

279. Niphakis, M. J. *et al.* Evaluation of NHS carbamates as a potent and selective class of endocannabinoid hydrolase inhibitors. *ACS Chemical Neuroscience* **4**, 1322–1332 (2013).

280. Ibsen, M. S., Connor, M. & Glass, M. Cannabinoid CB 1 and CB 2 Receptor Signaling and Bias . *Cannabis and Cannabinoid Research* **2**, 48–60 (2017).

281. Mihaylova, M. M. & Shaw, R. J. The AMPK signalling pathway coordinates cell growth, autophagy and metabolism. *Nature Cell Biology* **13**, 1016–1023 (2011).

282. Gainetdinov, R. R., Premont, R. T., Bohn, L. M., Lefkowitz, R. J. & Caron, M. G. Desensitization of G Protein–Coupled Receptors and Neuronal Functions. *Annual Review of Neuroscience* **27**, 107–144 (2004).

283. Martin, B. R., Sim-Selley, L. J. & Selley, D. E. Signaling pathways involved in the development of cannabinoid tolerance. *Trends in Pharmacological Sciences* **25**, 325–330 (2004).

284. Schlosburg, J. E. *et al.* Chronic monoacylglycerol lipase blockade causes functional antagonism of the endocannabinoid system. *Nature Neuroscience* **13**, 1113–1119 (2010).

285. Wang, L. *et al.* MicroRNAs 185, 96, and 223 Repress Selective High-Density Lipoprotein Cholesterol Uptake through Posttranscriptional Inhibition. *Molecular and Cellular Biology* **33**, 1956–1964 (2013).

286. Nourbakhsh, M. *et al.* Arylacetamide deacetylase: A novel host factor with important roles in the

lipolysis of cellular triacylglycerol stores, VLDL assembly and HCV production. *Journal of Hepatology* (2013). doi:10.1016/j.jhep.2013.03.022

287. Shimizu, Y. *et al.* Lipoprotein lipase and hepatic triglyceride lipase reduce the infectivity of hepatitis C virus (HCV) through their catalytic activities on HCV-associated lipoproteins. *Virology* **407**, 152–159 (2010).

288. Shinohara, Y. *et al.* Hepatic triglyceride lipase plays an essential role in changing the lipid metabolism in genotype 1b hepatitis C virus replicon cells and hepatitis C patients. *Hepatology Research* **43**, 1190–1198 (2013).

289. Ben-Zeev, O. & Doolittle, M. H. Maturation of hepatic lipase: Formation of functional enzyme in the endoplasmic reticulum is the rate-limiting step in its secretion. *Journal of Biological Chemistry* **279**, 6171–6181 (2004).

290. Savinainen, J. R., Saario, S. M. & Laitinen, J. T. The serine hydrolases MAGL, ABHD6 and ABHD12 as guardians of 2-arachidonoylglycerol signalling through cannabinoid receptors. *Acta Physiologica* **204**, 267–276 (2012).

291. Marrs, W. R. *et al.* The serine hydrolase ABHD6 controls the accumulation and efficacy of 2-AG at cannabinoid receptors. *Nature Neuroscience* **13**, 951–957 (2010).

292. Ross, M. K., Streit, T. M., Herring, K. L. & Xie, S. Carboxylesterases: dual roles in lipid and pesticide metabolism. *Journal of Pesticide Science* **35**, 257–264 (2010).

293. Xie, S. *et al.* Inactivation of lipid glyceryl ester metabolism in human THP1 monocytes/macrophages by activated organophosphorus insecticides: Role of carboxylesterases 1 and 2. *Chemical Research in Toxicology* **23**, 1890–1904 (2010).

294. Gilham, D. *et al.* Inhibitors of hepatic microsomal triacylglycerol hydrolase decrease very low density lipoprotein secretion. *The FASEB journal : official publication of the Federation of American Societies for Experimental Biology* **17**, 1685–1687 (2003).

295. Auboeuf, D. *et al.* Tissue Distribution and Quantification of the Expression of mRNAs of Peroxisome Proliferator-Activated Receptors and Liver X Receptor-a in Humans. *Diabetes* **46**, 1319–1327 (1997).

296. Rakic, B. *et al.* Peroxisome proliferator-activated receptor α antagonism inhibits hepatitis C virus replication. *Chemistry and Biology* **13**, 23–30 (2006).

297. Franklin, M. P., Sathyanarayan, A. & Mashek, D. G. Acyl-CoA thioesterase 1 (ACOT1) regulates PPARα to couple fatty acid flux with oxidative capacity during fasting. *Diabetes* **66**, 2112–2123 (2017).

298. Xu, J. *et al.* Hepatic carboxylesterase 1 is essential for both normal and farnesoid X receptor-controlled lipid homeostasis. *Hepatology* **59**, 1761–1771 (2014).

299. Loizides-Mangold, U. *et al.* HCV 3a core protein increases lipid droplet cholesteryl ester content via a mechanism dependent on sphingolipid biosynthesis. *PLoS ONE* **9**, 1–24 (2014).

300. Barneda, D., Cosulich, S., Stephens, L. & Hawkins, P. How is the acyl chain composition of phosphoinositides created and does it matter? *Biochemical Society Transactions* **47**, 1291–1305 (2019).

301. Lyn, R. K. *et al.* Stearoyl-CoA desaturase inhibition blocks formation of hepatitis C virus-induced specialized membranes. *Scientific Reports* **4**, 1–11 (2014).

302. Nomura, D. K. *et al.* Monoacylglycerol Lipase Regulates a Fatty Acid Network that Promotes Cancer Pathogenesis. *Cell* **140**, 49–61 (2010).

303. Bassendine, M. F., Sheridan, D. A., Bridge, S. H., Felmlee, D. J. & Neely, R. D. G. Lipids and HCV. *Seminars in Immunopathology* **35**, 87–100 (2013).

304. Kapadia, S. B. & Chisari, F. V. Hepatitis C virus RNA replication is regulated by host geranylgeranylation and fatty acids. *Proceedings of the National Academy of Sciences of the United States of America* **102**, 2561–2566 (2005).

305. Cho, K. H., Hong, J. H. & Lee, K. T. Monoacylglycerol (MAG)-oleic acid has stronger antioxidant, anti-atherosclerotic, and protein glycation inhibitory activities than MAG-palmitic acid. *Journal of*

Medicinal Food **13**, 99–107 (2010).

306. Tsukimoto, A. *et al.* A new role for PGA1 in inhibiting hepatitis C virus-IRES-mediated translation by targeting viral translation factors. *Antiviral Research* **117**, 1–9 (2015).
307. Blight, K. J., McKeating, J. A. & Rice, C. M. Highly Permissive Cell Lines for Subgenomic and Genomic Hepatitis C Virus RNA Replication. *Journal of Virology* **76**, 13001–13014 (2002).
308. Sagan, S. M. *et al.* The influence of cholesterol and lipid metabolism on host cell structure and hepatitis C virus replication. *Biochemistry and Cell Biology* **84**, 67–79 (2006).
309. Barglow, K. T. & Cravatt, B. F. Activity-based protein profiling for the functional annotation of enzymes. *Nature Methods* **4**, 822–827 (2007).
310. Russell, R. S. *et al.* Advantages of a single-cycle production assay to study cell culture-adaptive mutations of hepatitis C virus. *Proceedings of the National Academy of Sciences of the United States of America* **105**, 4370–4375 (2008).
311. Bille, D. S. *et al.* Implications of Central Obesity-Related Variants in LYPLAL1, NRXN3, MSRA, and TFAP2B on Quantitative Metabolic Traits in Adult Danes. *PLoS ONE* **6**, e20640 (2011).
312. Sliz, E. *et al.* NAFLD risk alleles in PNPLA3, TM6SF2, GCKR and LYPLAL1 show divergent metabolic effects. *Human Molecular Genetics* **27**, 2214–2223 (2018).
313. Ahn, K. *et al.* Discovery of a Selective Covalent Inhibitor of Lysophospholipase-like 1 (LYPLAL1) as a Tool to Evaluate the Role of this Serine Hydrolase in Metabolism. *ACS Chemical Biology* (2016). doi:10.1021/acschembio.6b00266
314. Hajarizadeh, B., Grebely, J. & Dore, G. J. Epidemiology and natural history of HCV infection. *Nature Reviews Gastroenterology and Hepatology* **10**, 553–562 (2013).
315. Bürger, M. *et al.* Crystal structure of the predicted phospholipase LYPLAL1 reveals unexpected functional plasticity despite close relationship to acyl protein thioesterases. *Journal of Lipid Research* **53**, 43–50 (2012).
316. Watson, R. A. *et al.* Lyplal1 is dispensable for normal fat deposition in mice. *DMM Disease Models and Mechanisms* **10**, 1481–1488 (2017).
317. Vohnoutka, R. B. *et al.* Knockout of murine Lyplal1 confers sex-specific protection against diet-induced obesity. *bioRxiv* 2021.08.05.455257 (2021). doi:10.1101/2021.08.05.455257
318. Petersen, M. C., Vatner, D. F. & Shulman, G. I. Regulation of hepatic glucose metabolism in health and disease. *Nature Reviews Endocrinology* **13**, 572–587 (2017).
319. Radziuk, J. & Pye, S. Hepatic glucose uptake, gluconeogenesis and the regulation of glycogen synthesis. *Diabetes/Metabolism Research and Reviews* **17**, 250–272 (2001).
320. Cunningham, F. *et al.* Ensembl 2022. *Nucleic Acids Research* **50**, D988–D995 (2022).
321. Kuo, Y. C. *et al.* Hepatitis C virus NS5A protein enhances gluconeogenesis through upregulation of Akt-/JNK-PEPCK signalling pathways. *Liver International* **34**, 1358–1368 (2014).
322. Lecube, A. *et al.* High Prevalence of Glucose Abnormalities in Patients with Hepatitis C Virus Infection: A multivariate analysis considering the liver injury. *Diabetes Care* **27**, 1171–1175 (2004).
323. Chen, Y. *et al.* Different Hepatitis C Virus Infection Statuses Show a Significant Risk of Developing Type 2 Diabetes Mellitus: A Network Meta-Analysis. *Digestive Diseases and Sciences* **65**, 1940–1950 (2020).
324. Granner, D., Andreone, T., Sasaki, K. & Beale, E. Inhibition of transcription of the phosphoenolpyruvate carboxykinase gene by insulin. *Nature* **305**, 549–551 (1983).
325. Streeper, R. S. *et al.* A multicomponent insulin response sequence mediates a strong repression of mouse glucose-6-phosphatase gene transcription by insulin. *Journal of Biological Chemistry* **272**, 11698–11701 (1997).
326. Heiden, M. G. V., Cantley, L. C. & Thompson, C. B. Understanding the warburg effect: The metabolic requirements of cell proliferation. *Science* **324**, 1029–1033 (2009).
327. Khan, M. *et al.* mTORC2 controls cancer cell survival by modulating gluconeogenesis. *Cell Death Discovery* **1**, 1–12 (2015).

328. Ma, R. *et al.* Switch of glycolysis to gluconeogenesis by dexamethasone for treatment of hepatocarcinoma. *Nature Communications* **4**, (2013).

329. Saltiel, A. R. & Kahn, C. R. Insulin signalling and the regulation of glucose and lipid metabolism. *Nature* **414**, 799–806 (2001).

330. Habegger, K. M. *et al.* The metabolic actions of glucagon revisited. *Nature Reviews Endocrinology* **6**, 689–697 (2010).

331. Hirano, T. *et al.* Thioesterase activity and subcellular localization of acylprotein thioesterase 1/lysophospholipase 1. *Biochimica et Biophysica Acta - Molecular and Cell Biology of Lipids* **1791**, 797–805 (2009).

332. Manna, J. D. *et al.* Identification of the major prostaglandin glycerol ester hydrolase in human cancer cells. *Journal of Biological Chemistry* **289**, 33741–33753 (2014).

333. Bürger, M. *et al.* Crystal structure of the predicted phospholipase LYPLAL1 reveals unexpected functional plasticity despite close relationship to acyl protein thioesterases. *Journal of Lipid Research* **53**, 43–50 (2012).

334. Kooi, B. T. Vander *et al.* The Three Insulin Response Sequences in the Glucose-6-phosphatase Catalytic Subunit Gene Promoter Are Functionally Distinct *. *Journal of Biological Chemistry* **278**, 11782–11793 (2003).

335. Ayala, J. E. *et al.* Conservation of an insulin response unit between mouse and human glucose-6-phosphatase catalytic subunit gene promoters: transcription factor FKHR binds the insulin response sequence. *Diabetes* **48**, 1885–1889 (1999).

336. Oh, K. J., Han, H. S., Kim, M. J. & Koo, S. H. CREB and FoxO1: Two transcription factors for the regulation of hepatic gluconeogenesis. *BMB Reports* **46**, 567–574 (2013).

337. He, L., Li, Y., Zeng, N. & Stiles, B. L. Regulation of basal expression of hepatic PEPCK and G6Pase by AKT2. *Biochemical Journal* **477**, 1021–1031 (2020).

338. Carlezon, W. A., Duman, R. S. & Nestler, E. J. The many faces of CREB. *Trends in Neurosciences* **28**, 436–445 (2005).

339. Sanjana, N. E., Shalem, O. & Zhang, F. Improved vectors and genome-wide libraries for CRISPR screening. *Nature Methods* **11**, 783–784 (2014).

340. Cavanna, C. *et al.* Human infections due to Schizophyllum commune: Case report and review of the literature. *Journal de Mycologie Medicale* **29**, 365–371 (2019).

341. Gaitanis, G. *et al.* AhR ligands, malassezin, and indolo[3,2-b]carbazole are selectively produced by Malassezia furfur strains isolated from seborrheic dermatitis. *Journal of Investigative Dermatology* **128**, 1620–1625 (2008).

342. Gaitanis, G., Velegraki, A., Magiatis, P., Pappas, P. & Bassukas, I. D. Could Malassezia yeasts be implicated in skin carcinogenesis through the production of aryl-hydrocarbon receptor ligands? *Medical Hypotheses* **77**, 47–51 (2011).

343. Wille, G. *et al.* Malassezin - A novel agonist of the Arylhydrocarbon receptor from the yeast Malassezia furfur. *Bioorganic and Medicinal Chemistry* **9**, 955–960 (2001).

344. Vlachos, C., Schulte, B. M., Magiatis, P., Adema, G. J. & Gaitanis, G. Malassezia-derived indoles activate the aryl hydrocarbon receptor and inhibit Toll-like receptor-induced maturation in monocyte-derived dendritic cells. *British Journal of Dermatology* **167**, 496–505 (2012).

345. Sato, Y. *et al.* Malassezia-derived aryl hydrocarbon receptor ligands enhance the CCL20/Th17/soluble CD163 pathogenic axis in extra-mammary Paget's disease. *Experimental Dermatology* **28**, 933–939 (2019).

346. Mayer, F. L., Wilson, D. & Hube, B. Candida albicans pathogenicity mechanisms. *Virulence* **4**, 119–128 (2013).

347. Solis, N. V., Swidergall, M., Bruno, V. M., Gaffen, S. L. & Filler, S. G. The aryl hydrocarbon receptor governs epithelial cell invasion during oropharyngeal candidiasis. *mBio* **8**, (2017).

348. Borghi, M. *et al.* Targeting the Aryl Hydrocarbon Receptor With Indole-3-Aldehyde Protects From Vulvovaginal Candidiasis via the IL-22-IL-18 Cross-Talk. *Frontiers in Immunology* **10**, 1–10

(2019).

349. Nembrini, C., Marsland, B. J. & Kopf, M. IL-17-producing T cells in lung immunity and inflammation. *Journal of Allergy and Clinical Immunology* **123**, 986–994 (2009).

350. Wen, J. & Friedman, J. R. miR-122 regulates hepatic lipid metabolism and tumor suppression. *Journal of Clinical Investigation* **122**, 2773–2776 (2012).

351. Hsu, S. *et al.* Essential metabolic, anti-inflammatory, and anti-tumorigenic functions of miR-122 in liver. *Journal of Clinical Investigation* **122**, 2871–2883 (2012).

352. Coulouarn, C., Factor, V. M., Andersen, J. B., Durkin, M. E. & Thorgeirsson, S. S. Loss of miR-122 expression in liver cancer correlates with suppression of the hepatic phenotype and gain of metastatic properties. *Oncogene* **28**, 3526–3536 (2009).

353. Ottosen, S. *et al.* In Vitro antiviral activity and preclinical and clinical resistance profile of miravirsen, a novel anti-hepatitis C virus therapeutic targeting the human factor miR-122. *Antimicrobial Agents and Chemotherapy* **59**, 599–608 (2015).

354. Thakral, S. & Ghoshal, K. miR-122 is a Unique Molecule with Great Potential in Diagnosis, Prognosis of Liver Disease, and Therapy Both as miRNA Mimic and Antimir. *Current Gene Therapy* **15**, 142–150 (2015).

355. Hasin, Y., Seldin, M. & Lusis, A. Multi-omics approaches to disease. *Genome Biology* **18**, 1–15 (2017).

356. Liu, Q. *et al.* Integrative omics analysis reveals the importance and scope of translational repression in microRNA-mediated regulation. *Molecular and Cellular Proteomics* **12**, 1900–1911 (2013).

357. Lin, Y. C. D. *et al.* Multi-omics profiling reveals microRNA-mediated insulin signaling networks. *BMC Bioinformatics* **21**, 1–19 (2020).

358. Bi, H. C. *et al.* N-methylnicotinamide and nicotinamide N-methyltransferase are associated with microRNA-1291-altered pancreatic carcinoma cell metabolome and suppressed tumorigenesis. *Carcinogenesis* **35**, 2264–2272 (2014).

359. Desrochers, G. F., Filip, R., Bastianelli, M., Stern, T. & Pezacki, J. P. microRNA-27b regulates hepatic lipase enzyme LIPC and reduces triglyceride degradation during hepatitis C virus infection. *Journal of Biological Chemistry* **298**, 101983 (2022).

360. Desrochers, G. F. *et al.* Profiling Kinase Activity during Hepatitis C Virus Replication Using a Wortmannin Probe. *ACS Infectious Diseases* **1**, 443–452 (2016).

361. Patricelli, M. P. *et al.* Functional interrogation of the kinome using nucleotide acyl phosphates. *Biochemistry* **46**, 350–358 (2007).

362. Gesellchen, F., Bertinetti, O. & Herberg, F. W. Analysis of posttranslational modifications exemplified using protein kinase A. *Biochimica et Biophysica Acta - Proteins and Proteomics* **1764**, 1788–1800 (2006).

363. Qian, L. *et al.* Live-cell imaging and profiling of c-Jun N-terminal kinases using covalent inhibitor-derived probes. *Chemical Communications* **55**, 1092–1095 (2019).

364. Desrochers, G. F., Cornacchia, C., McKay, C. S. & Pezacki, J. P. Activity-Based Phosphatidylinositol Kinase Probes Detect Changes to Protein-Protein Interactions during Hepatitis C Virus Replication. *ACS Infectious Diseases* **4**, 752–757 (2018).

365. Stolze, S. C. *et al.* Photo-crosslinking of clinically relevant kinases using H89-derived photo-affinity probes. *Molecular BioSystems* **12**, 1809–1817 (2016).

366. Singhal, S., Taylor, M. C. & Baker, R. T. Deubiquitylating enzymes and disease. *BMC Biochemistry* **9**, 1–8 (2008).

367. Spolverini, A., Fuchs, G., Bublik, D. R. & Oren, M. Let-7b and let-7c microRNAs promote histone H2B ubiquitylation and inhibit cell migration by targeting multiple components of the H2B deubiquitylation machinery. *Oncogene* **36**, 5819–5828 (2017).

368. Ekkebus, R., Flierman, D., Geurink, P. P. & Ovaa, H. Catching a DUB in the act: Novel ubiquitin-based active site directed probes. *Current Opinion in Chemical Biology* **23**, 63–70 (2014).

369. Harrigan, J. & Jacq, X. Monitoring Target Engagement of Deubiquitylating Enzymes Using

Activity Probes: Past, Present, and Future. in *Methods in Molecular Biology* **1449**, 395–410 (2016).

370. Hewings, D. S., Flygare, J. A., Wertz, I. E. & Bogyo, M. Activity-based probes for the multicatalytic proteasome. *FEBS Journal* **284**, 1540–1554 (2017).
371. Li, N. *et al.* Relative quantification of proteasome activity by activity-based protein profiling and LC-MS/MS. *Nature Protocols* **8**, 1155–1168 (2013).
372. de Bruin, G. *et al.* A Set of Activity-Based Probes to Visualize Human (Immuno)proteasome Activities. *Angewandte Chemie International Edition* **55**, 4199–4203 (2016).
373. Adams, J. The proteasome: Structure, function, and role in the cell. *Cancer Treatment Reviews* **29**, 3–9 (2003).
374. Nasheri, N. *et al.* Activity-based profiling of the proteasome pathway during hepatitis C virus infection. *Proteomics* (2015). doi:10.1002/pmic.201500169
375. Kallemeijn, W. W. *et al.* Novel activity-based probes for broad-spectrum profiling of retaining β-exoglucosidases in situ and in vivo. *Angewandte Chemie - International Edition* **51**, 12529–12533 (2012).
376. Howard, R. T. *et al.* Structure-Guided Design and In-Cell Target Profiling of a Cell-Active Target Engagement Probe for PARP Inhibitors. *ACS Chemical Biology* **15**, 325–333 (2020).
377. Jiang, H., Kim, J. H., Frizzell, K. M., Kraus, W. L. & Lin, H. Clickable NAD analogues for labeling substrate proteins of poly(ADP-ribose) polymerases. *Journal of the American Chemical Society* **132**, 9363–9372 (2010).
378. Xie, Y. *et al.* Fluorescent Probes for Single-Step Detection and Proteomic Profiling of Histone Deacetylases. *Journal of the American Chemical Society* **138**, 15596–15604 (2016).
379. Horning, B. D. *et al.* Chemical Proteomic Profiling of Human Methyltransferases. *Journal of the American Chemical Society* **138**, 13335–13343 (2016).
380. Shahidi, M. *et al.* Endocannabinoid CB1 antagonists inhibit hepatitis C virus production, Providing a novel class of antiviral host-targeting agents. *Journal of General Virology* **95**, 2468–2479 (2014).
381. Bartenschlager, R., Penin, F., Lohmann, V. & André, P. Assembly of infectious hepatitis C virus particles. *Trends in Microbiology* **19**, 95–103 (2011).
382. Chandel, N. S. Glycolysis. *Cold Spring Harbor perspectives in biology* **13**, 1–12 (2021).
383. Benes, P., Vetvicka, V. & Fusek, M. Cathepsin D-Many functions of one aspartic protease. *Critical Reviews in Oncology/Hematology* **68**, 12–28 (2008).
384. Sutherland, B. W., Toews, J. & Kast, J. Utility of formaldehyde cross-linking and mass spectrometry in the study of protein–protein interactions. *Journal of Mass Spectrometry* **43**, 699–715 (2008).
385. Sinz, A. Investigation of protein-protein interactions in living cells by chemical crosslinking and mass spectrometry. *Analytical and Bioanalytical Chemistry* **397**, 3433–3440 (2010).
386. Molinaro, A., Becattini, B. & Solinas, G. Insulin signaling and glucose metabolism in different hepatoma cell lines deviate from hepatocyte physiology toward a convergent aberrant phenotype. *Scientific Reports* 1–10 (2020). doi:10.1038/s41598-020-68721-9
387. Nagarajan, S. R. *et al.* Lipid and glucose metabolism in hepatocyte cell lines and primary mouse hepatocytes: A comprehensive resource for in vitro studies of hepatic metabolism. *American Journal of Physiology - Endocrinology and Metabolism* **316**, E578–E589 (2019).
388. Donnelly, P. S., Zanatta, S. D., Zammit, S. C., White, J. M. & Williams, S. J. 'Click' cycloaddition catalysts: Copper(I) and copper(II) tris(triazolylmethyl)amine complexes. *Chemical Communications* **233**, 2459–2461 (2008).

Chapter 7: Appendix

7.1 Supplemental material for chapter 3

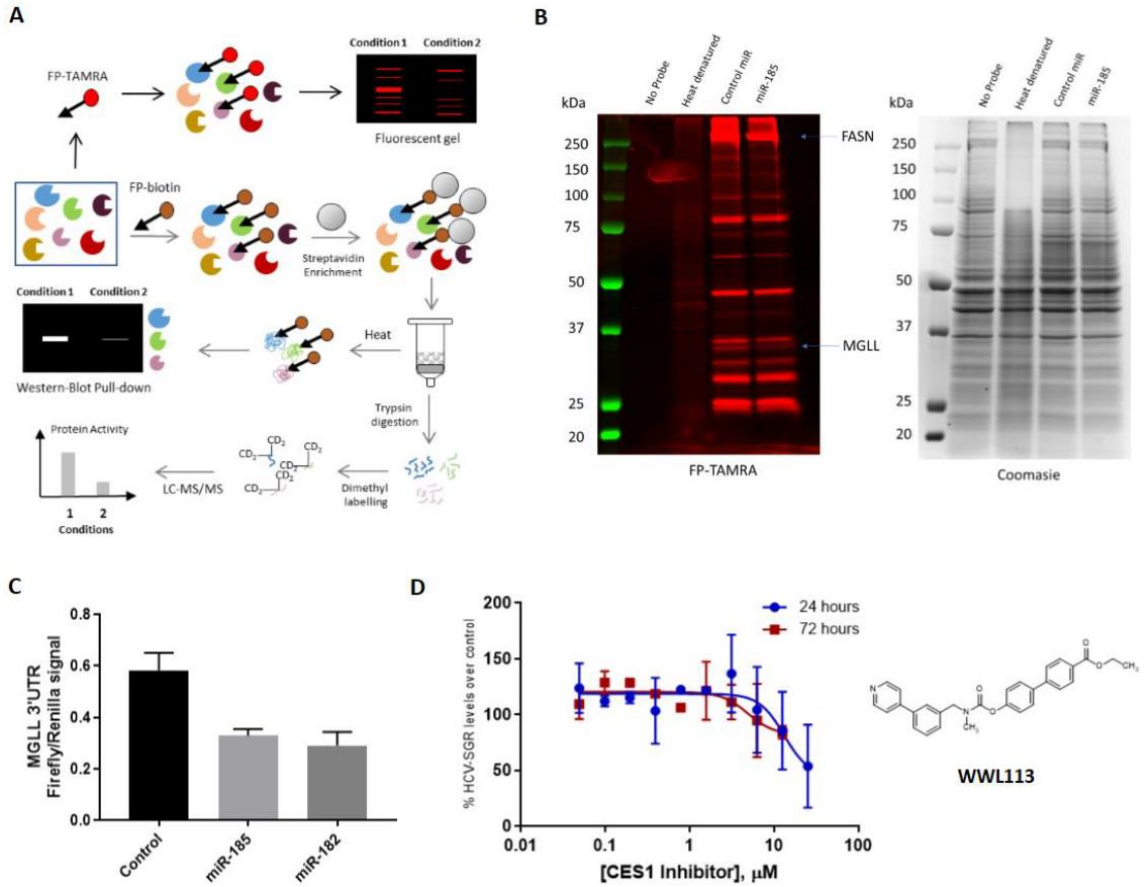

Figure 7-1. Activity-based protein profiling identifies targets of microRNA-185. Related to Figure 3-1 and Figure 3-2. **A.** Schematic representation of an ABPP workflow. The active proteome is labelled with either FP-TAMRA or FP-Biotin. The fluorescently labelled proteome is separated on an SDS-PAGE gel and imaged. The biotinylated proteome is enriched with streptavidin, isolated and subsequently analyzed with either western-blotting or mass-spectrometry. **B.** FP-TAMRA labeling of miR-185-transfected cell lysates shows differential activity of certain serine hydrolases. [caption continued on next page]

[Figure 7-1. Caption continued]

The bands for FASN and MGLL are indicated and can be seen to decrease in intensity. The Coomasie stain image on the right shows whole protein content. Cells were transfected with miR-185, incubated for 72 hours and lysed for labelling with the FP-TAMRA probe. Heat denaturation was performed before probe addition and acts as control for labelling of active serine hydrolase enzymes. **C.** miR-185 directly targets the MGLL 3'UTR. The MGLL 3'UTR construct bearing a luciferase gene was transfected into Huh7.5 cells followed by miRNA transfection 24 hours later. miR-182 was strongly predicted to bind the 3'UTR of MGLL and was used as a positive control. Renilla signal was used for normalisation. n=2, error bars represent the standard deviation. **D.** Pharmacological inhibition of miR-185 target CES1 leads to a 50% reduction in the levels of virus in a HCV sub-genomic replicon model linked to a luciferase reporter gene. Cells were treated for WWL113 final concentrations of 0.024μM to 25μM and signal was normalized over protein concentration (significant toxicity was observed at 25μM after 72hours). n=2, error bars represent the standard deviation.

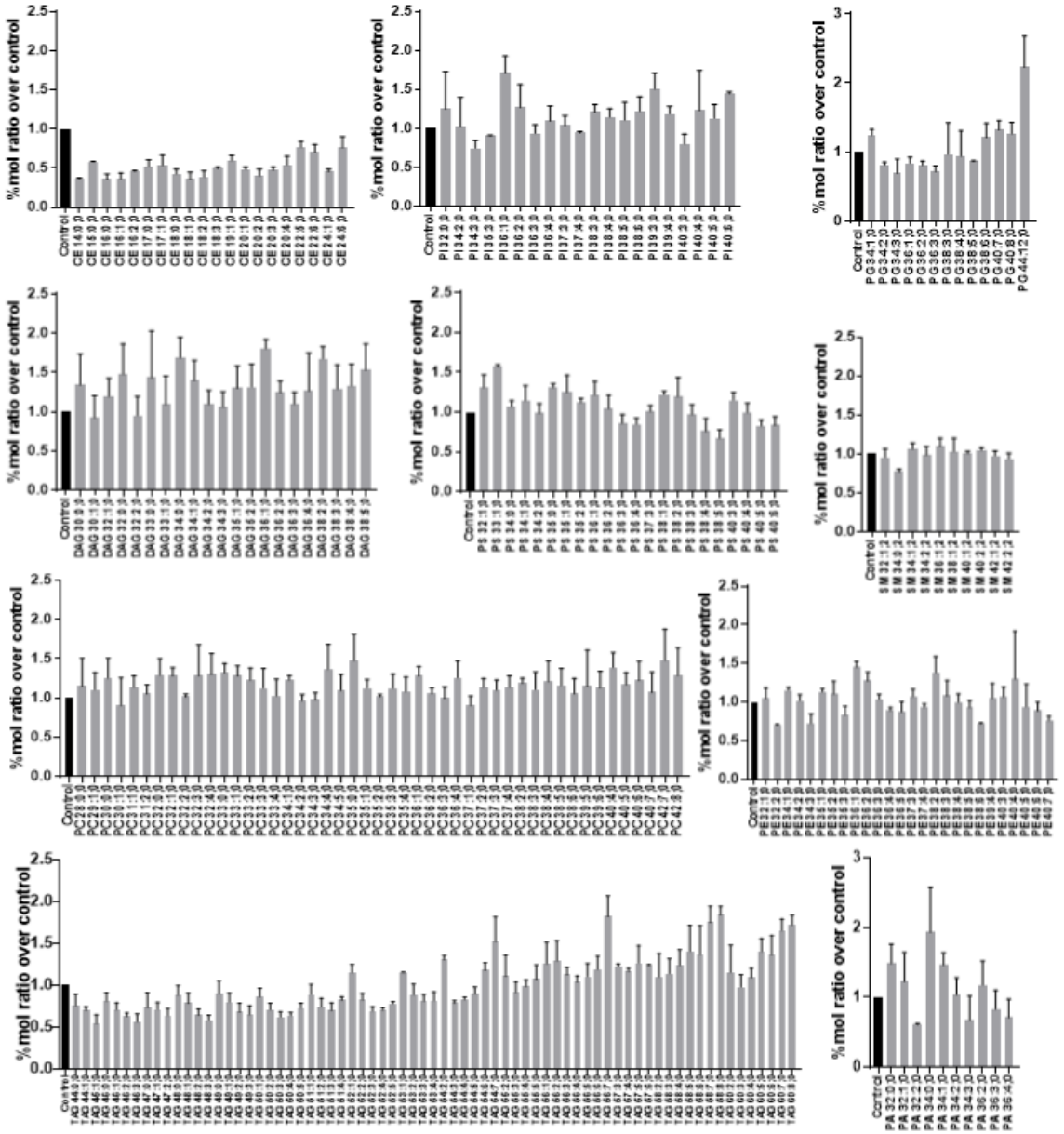

Figure 7-2. Graphical representation of the changes in each lipid species by category. Related to Figure 3-3 and Figure 3-4. CE: cholesteryl ester, PG: phosphatidylglycerol, DAG: diacylglycerol, SM: sphingomyelin, PS: phosphatidylserine, PI: phosphatidylinositol, PE: phosphatidylethanolamine, PA: phosphatidate, PC: phosphatidylcholine, TAG: triacylglycerol. Fold change is shown as the % mol ratio of miR-185 treated cells over control miRNA treated cells. Error bars represent standard deviation, n=3.

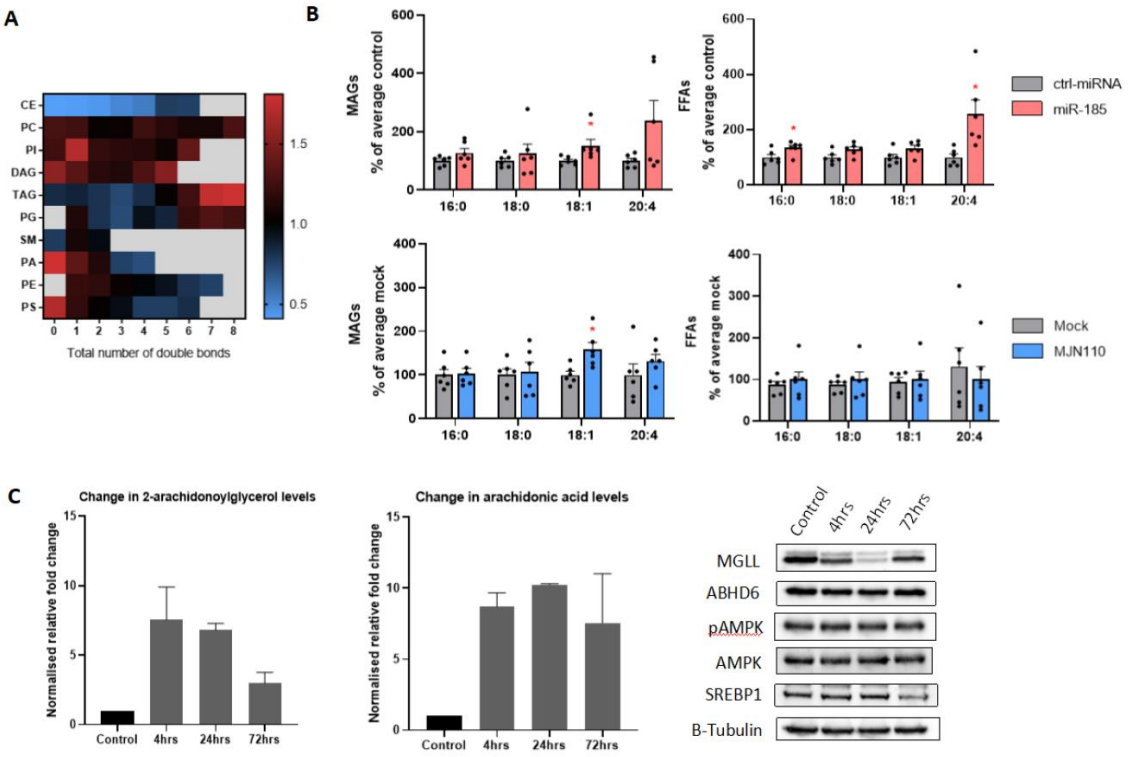

Figure 7-3. Analysis of changes to lipid species reveals modifications caused by miR-185 and MJN110. Related to Figure 3-5. **A.** Heat map showing the mol % ratio of lipids in each category based on their total number of double bonds in the acyl chains. Grey squares denote where no data was obtained. Fold changes for each lipid species by category can be found in Fig. 7-2. CE: cholesteryl ester, TAG: triacylglycerol, PC: phosphatidylcholine, PI: phosphatidylinositol, DAG: diacylglycerol, PA: phosphatidate, PE: phosphatidylethanolamine, PG: phosphatidylglycerol, PS: phosphatidylserine, SM: sphingomyelin. **B**. Transfection with miR-185 and treatment with MJN110 lead to changes in monoacylglycerol (MAG) and free fatty acid (FFA) species. Cells were transfected with 100nM miR-185 for 72 hours. Significant changes were observed in 18:1 MAGs, 16:0 FFAs and 20:4 FFAs. Cells were treated with MJN110 at 1μM for 72 hours. Significant changes were observed in 18:1 MAGs. Lipids were extracted using a chloroform-methanol extraction method and analyzed on a triple-quadrupole mass spectrometer. Lipid content was normalized over total protein content. Data shown is that of two sets of experiments with n=3 each, where each treatment is shown as a percentage of the average of its respective control group. Significance assessed with two-tailed, unpaired student's t-test, * = $p<0.05$. Error bars represent the standard error of the mean. [caption continued on next page]

[Figure 7-3. Caption continued]

C. Pharmacological inhibition of MGLL leads to an increase in both 2-arachidonylglycerol levels and arachidonic acid levels. Cells were treated with 1μM of MJN110 for 4, 24 or 72hours before being lysed in methanol. Lipids were extracted using an acidified Bligh and Dyer method and levels were analyzed via LC-MS/MS. Lipid intensities were normalized over a deuterated spike-in control and over the densitometric intensity of the protein fractions run on an SDS-PAGE gel. n=2, error bars represent the standard deviation of two biological replicates. Western blot of the protein fractions of each sample probed for various targets. Representative blot of one of the biological replicates is shown.

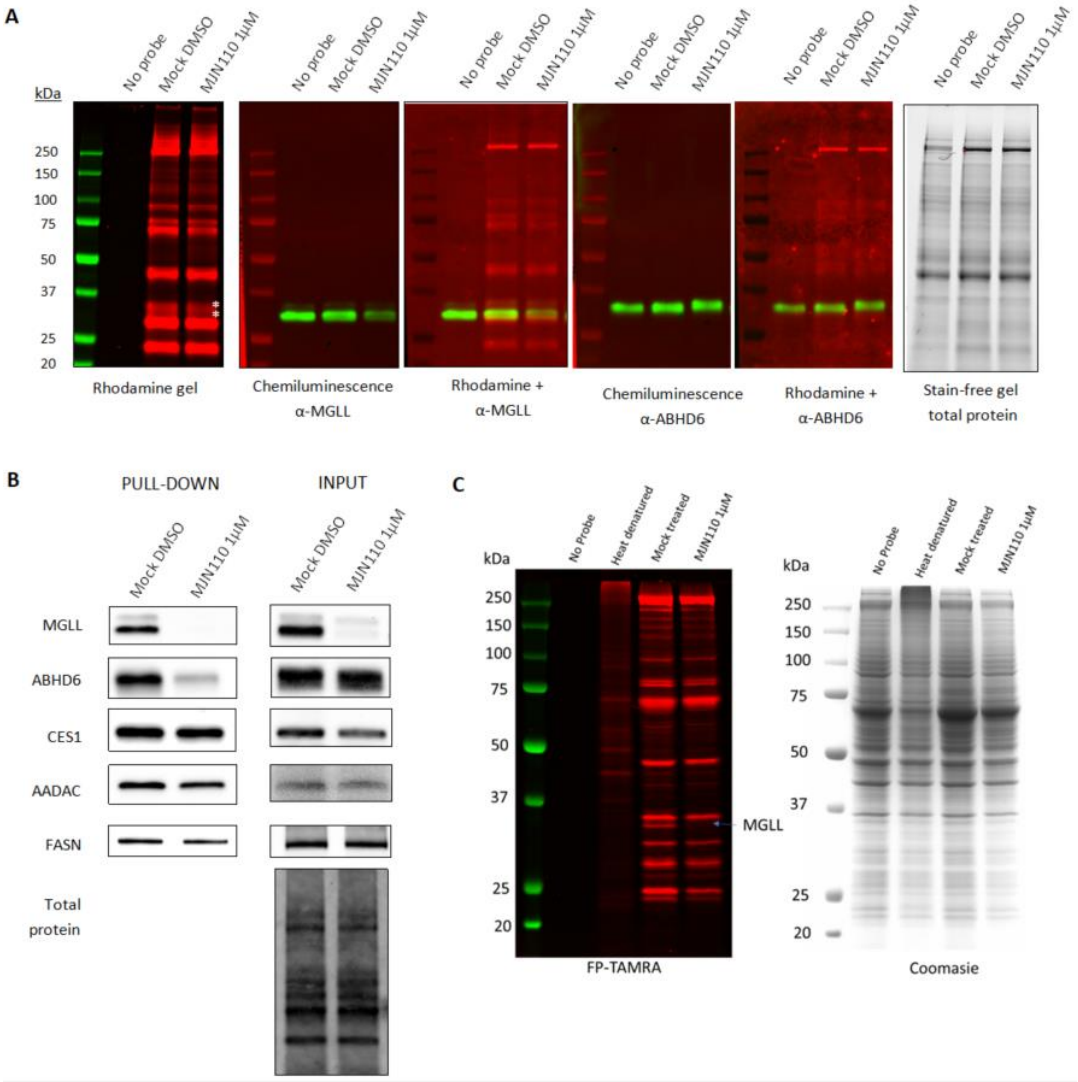

Figure 7-4. Competitive Activity-Based Protein Profiling identifies MGLL and ABHD6 as the principal targets of MJN110 in Huh7.5 cells. Related to Figure 3-5. **A.** Fluorescent gel of the active serine hydrolase proteome in cells treated with 1µM MJN110 and labelled with FP-TAMRA. The gel was transferred to a membrane and probed with antibodies against MGLL and ABHD6 to identify the location of the respective protein bands (indicated with *) **B.** Western blot pull-down of select active serine hydrolase proteome in cells treated with 1µM MJN110 and labelled with FP-Biotin. MGLL and ABHD6 are the only two tested enzymes whose activity is inhibited by the compound after 72 hours. **C.** Higher resolution fluorescent gel of MJN110-treated lysates labelled with FP-TAMRA showing a clear disappearance of the MGLL band.

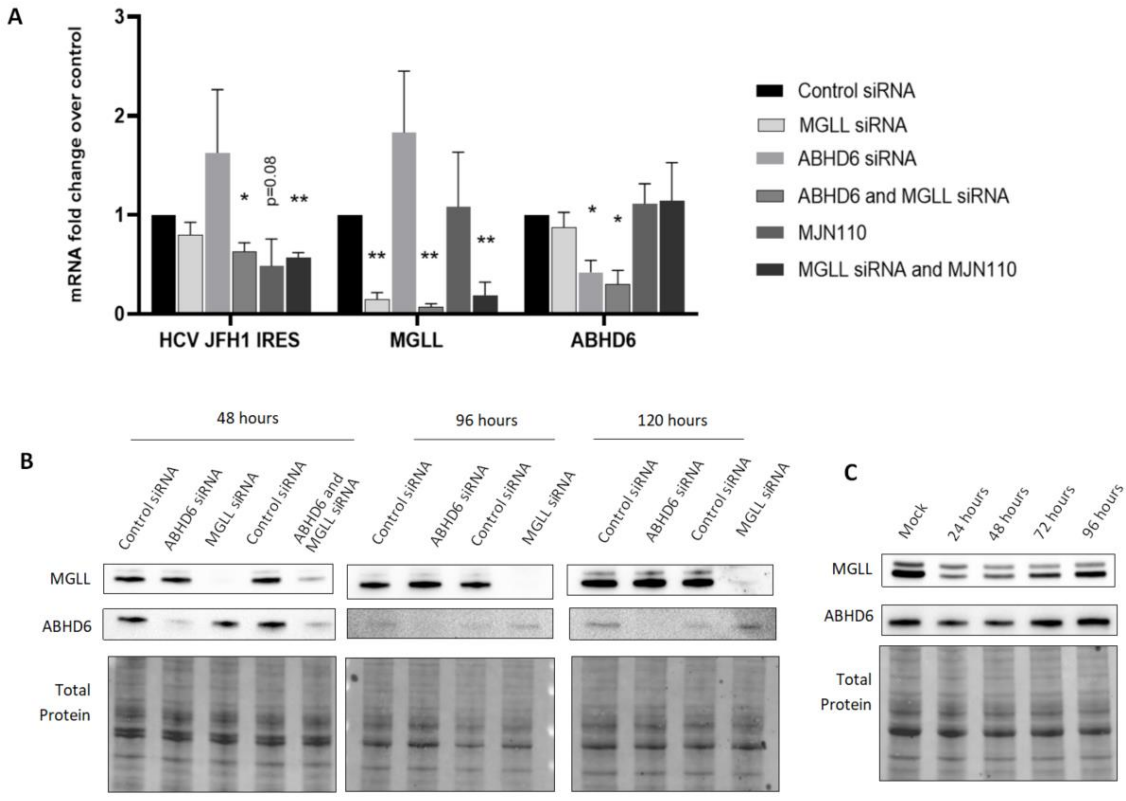

Figure 7-5. Knocking down MGLL or ABHD6 before a 48 hours HCV JHF1 infection does not have antiviral outcome. Related to Figure 3-5. **A.** siRNA-mediated knock-down of MGLL or ABHD6 alone do not result in a significant downregulation of HCV JFH1 mRNA after only 48 hours of incubation with the virus. Cells were transfected with siRNA and incubated for 48 hours before being infected with HCV and incubated for another 48 hours. HCV JFH1 mRNA was measured by RT-qPCR, n=3. Significance assessed with two-tailed, unpaired student's t-test, * = $p<0.05$, ** = $p<0.01$. **B.** siRNAs transfection successfully decreases the protein levels of MGLL and ABHD6 at 48 hours, 96 hours and 120 hours of incubation. **C.** Treatment with MJN110 at 1μM decreases the levels of MGLL in a time-dependent manner.

Table 7-1. Relative activity of serine hydrolases from miRNA-185 transfected cells compared to a non-targeting control RNA as determined with mass-spectrometry analysis. Related to Figure 3-1 and Figure 3-4. Three separate biological replicates are shown. Western blots below the table show decrease in MGLL protein levels in the whole lysates input for each trial as a result of miRNA-185 transfection (sample taken before separation of labelled proteins); PTP1D is used as a loading control.

Accession number	Gene name		Relative Activity		
			Trial 1	**Trial 2**	**Trial 3**
P22760	Arylacetamide deacetylase	AADAC	0.69	0.89	0.74
Q9NUJ1	Abhydrolase Domain Containing 10	ABHD10	0.77	0.69	0.71
Q8NFV4	Abhydrolase Domain Containing 11	ABHD11	1.01	0.36	1.06
Q8N2K0-2	Abhydrolase Domain Containing 12	ABHD12	1.17	0.72	0.62
A0A024R323	Abhydrolase Domain Containing 6	ABHD6	1.10	1.50	1.28
A1L172	Acyl-CoA Thioesterase 1	ACOT1	0.34	0.30	0.35
P23141-2	Carboxylesterase 1	CES1	0.48	0.87	0.62
A0A024RA40	Carboxypeptidase, Vitellogenic Like	CPVL	N/A	0.84	0.34
X6R8A1	Carboxypeptidase	CTSA	1.14	1.23	1.10
P27487	Dipeptidyl Peptidase 4	DPP4	0.77	0.75	0.72
A8K4U2	Dipeptidyl Peptidase 8	DPP8	0.58	1.24	0.99
Q86TI2-2	Dipeptidyl Peptidase 9	DPP9	1.34	0.88	0.83
P10768	Esterase D	ESD	1.13	0.47	0.69
P49327	Fatty Acid Synthase	FASN	0.44	0.38	0.33
P11150	Lipase C, Hepatic Type	LIPC	1.10	0.58	0.55
O95372	Acyl-protein thioesterase 2	LYPLA2	0.43	1.17	0.91
Q5VWZ2	Lysophospholipase Like 1	LYPLAL1	1.30	0.49	0.51
A0A0C4DFN3	Monoglyceride Lipase	MGLL	0.47	0.72	0.38

A0A024R0L6	Platelet Activating Factor Acetylhydrolase 1b Catalytic Subunit 3	PAFAH1B3	0.53	1.10	0.50
Q99487	Platelet-activating factor acetylhydrolase 2	PAFAH2	0.93	1.52	0.96
Q8IY17-4	Patatin Like Phospholipase Domain Containing 6	PNPLA6	0.46	0.59	0.89
Q9UMR5-3	Palmitoyl-Protein Thioesterase 2	PPT2	N/A	0.57	0.52
B2RAH7	Prolyl Endopeptidase	PREP	0.78	0.73	0.54
Q4J6C6	Prolyl Endopeptidase-Like	PREPL	0.50	0.21	0.46
O75884	Putative hydrolase RBBP9	RBBP9	1.19	0.77	0.45
Q9HB40	Retinoid-inducible serine carboxypeptidase	SCPEP1	0.88	0.86	1.07
Q9HAT2	Sialate O-acetylesterase	SIAE	N/A	0.68	0.97

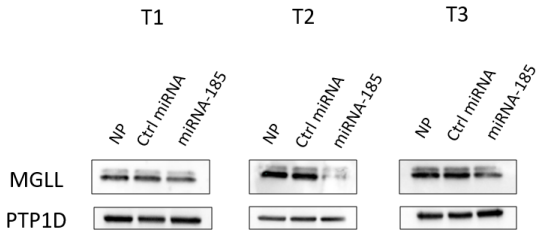

Table 7-2. Changes in transcript abundance for serine hydrolases as determined with microarray analysis. n=2. Related to Figure 3-1 and Figure 3-4. Only enzymes with downregulation below 0.8 fold or upregulation over 1.2 fold in expression are shown.

Gene name		Fold change	P-value
Endothelial lipase	LIPG	0.53	0.0524
Arylacetamide deacetylase	AADAC	0.56	0.0012
Fatty Acid Synthase	FASN	0.60	0.0054
Carboxylesterase 1	CES1	0.62	0.0035
Monoglyceride Lipase	MGLL	0.63	0.0081
Platelet Activating Factor Acetylhydrolase 1b Catalytic Subunit 3	PAFAH1B3	0.64	0.0042
Patatin-like phospholipase domain-containing protein 3	PNPLA3	0.67	0.1463
Protein phosphatase methylesterase 1	PPME1	0.75	0.0918
Valacyclovir hydrolase	BPHL	0.76	0.0874
Abhydrolase Domain Containing 6	ABHD6	1.21	0.1089
Abhydrolase domain containing 14B	ABHD14B	1.21	0.4377
Isoamyl acetate-hydrolyzing esterase 1 homolog	IAH1	1.24	0.0871
Acyl-protein thioesterase 2	LYPLA2	1.24	0.2528
Carboxypeptidase, Vitellogenic Like	CPVL	1.25	0.106
Abhydrolase Domain Containing 11	ABHD11	1.28	0.0493
Abhydrolase Domain Containing 4	ABHD4	1.31	0.0535
Lysosomal Pro-X carboxypeptidase	PRCP	1.31	0.0579
Glutamyl-tRNA(Gln) amidotransferase subunit A	QRSL1	1.32	0.0461
Acylamino-acid-releasing enzyme	APEH	1.33	0.0444
Lipoprotein lipase	LPL	1.33	0.0618
Arylacetamide deacetylase-like 2	AADACL2	1.35	0.0293
Phosphatidylcholine-sterol acyltransferase	LCAT	1.38	0.0233
Arylacetamide deacetylase-like 4	AADACL4	1.42	0.0238
Sn1-specific diacylglycerol lipase alpha	DAGLA	1.6	0.0051
Isoamyl acetate-hydrolyzing esterase 1 homolog	IAH1	1.63	0.0066
Phospholipase A1 member A	PLA1A	1.66	0.0057
Patatin-like phospholipase domain-containing protein 4	PNPLA4	1.75	0.0018
Serine hydrolase-like protein 2	SERHL2	1.85	0.0296

Table 7-3. Changes in transcript abundance for lipid metabolic enzymes as determined with microarray analysis. n=2. Related to Figure 3-1 and Figure 3-4.

Gene name			Fold change	P-value
Glycerol-3-phosphate acyltransferase	GPAT	GPAT1(GPAM)	0.64	0.0395
		GPAT2	0.85	0.144
		GPAT3	0.87	0.0072
		GPAT4	1.05	0.7077
1-acyl-sn-glycerol-3-phosphate acyltransferase		AGPAT3	0.53	0.0018
Phosphatidate Phosphatase LPIN1		PAP1 (lipin1)	0.97	0.9647
Hormone sensitive lipase		HSL (LIPE)	0.94	0.5938
Adipose Triglyceride Lipase		ATGL (PNPLA2)	1	0.9683
Diacylglycerol O-Acyltransferase 1		DGAT1	1.43	0.0112
Acetyl-CoA Acetyltransferase 1	ACAT	ACAT1	0.81	0.2388
		ACAT2	0.58	0.0152
Lecithin-Cholesterol acyltransferase		LCAT	1.38	0.0233
Lipoprotein Lipase		LPL	1.33	0.0618
Stearoyl-CoA Desaturase		SCD1	0.79	0.1426
Fatty Acid Desaturase	FADS	FADS1	0.88	0.4523
		FADS2	0.88	0.3819
ELOVL Fatty Acid Elongase	ELOVL	ELOVL2	0.65	0.0057
		ELOVL3	0.82	0.1507
		ELOVL4	0.66	0.0785
		ELOVL5	0.86	0.1625
		ELOVL6	0.66	0.0152

Table 7-4. Primers for qPCR analysis. Related to chapter 3 methods, quantitative PCR.

Gene	Forward primer	Reverse primer
18S	GCGATGCGGCGGCGTTATTC	CAATCTGTCAATCCTGTCCGTGTCC
AADAC	GAGCTCCTGGGACTTCACCAT	ATCTGGGTCATCAAGGAGCTGT
ABHD6	AGCCTGTGTCTCGTGTGTC	GGTAGACGGGATCAAGGGAAT
ACOT1	CTGTCGTCATCAACGGCTCT	GGTCAGGTCCTTCCAAAGGG
CES1	ACCCCTGAGGTTTACTCCACC	TGCACATAGGAGGGTACGAGG
FASN	GAAACTGCAGGAGCTGTC	CACGGAGTTGAGGCGCAT
LIPC	ATCAAGTGCCCTTGGACAAAG	TGACAGCCCTGATTGGTTTCT
MGLL	AATGCAGACGGACAGTACCTC	GAGCCAGCTCTTCATAGCGG
PPAR alpha	CTATCATTTGCTGTGGAGATCG	AAGATATCGTCCGGGTGGTT
JFH1 IRES	GTCTGCGGAACCGGTGAGTA	GCCCAAATGGCCGGGATA

Table 7-5. MRM transitions for the targeted LC/MS analysis of monoacylglycerols (MAG) and free fatty acids (FFA). Related to chapter 3 methods, relative analysis of MAG and FFA species.

Lipid	Precursor Ion	Product Ion	Collision Energy	Polarity
MAG 16:0	331	239	8	Positive
MAG 18:0	359	267	8	Positive
MAG 18:1	357	265	8	Positive
MAG 20:4	379	287	8	Positive
MAG 20:4-d8	384	287	8	Positive
FFA 16:0	255	255	0	Negative
FFA 18:0	283	283	0	Negative
FFA 18:1	281	281	0	Negative
FFA 20:4	303.3	303.3	0	Negative
FFA 20:4-d8	311.25	311.25	0	Negative

7.2 Supplemental material for chapter 4

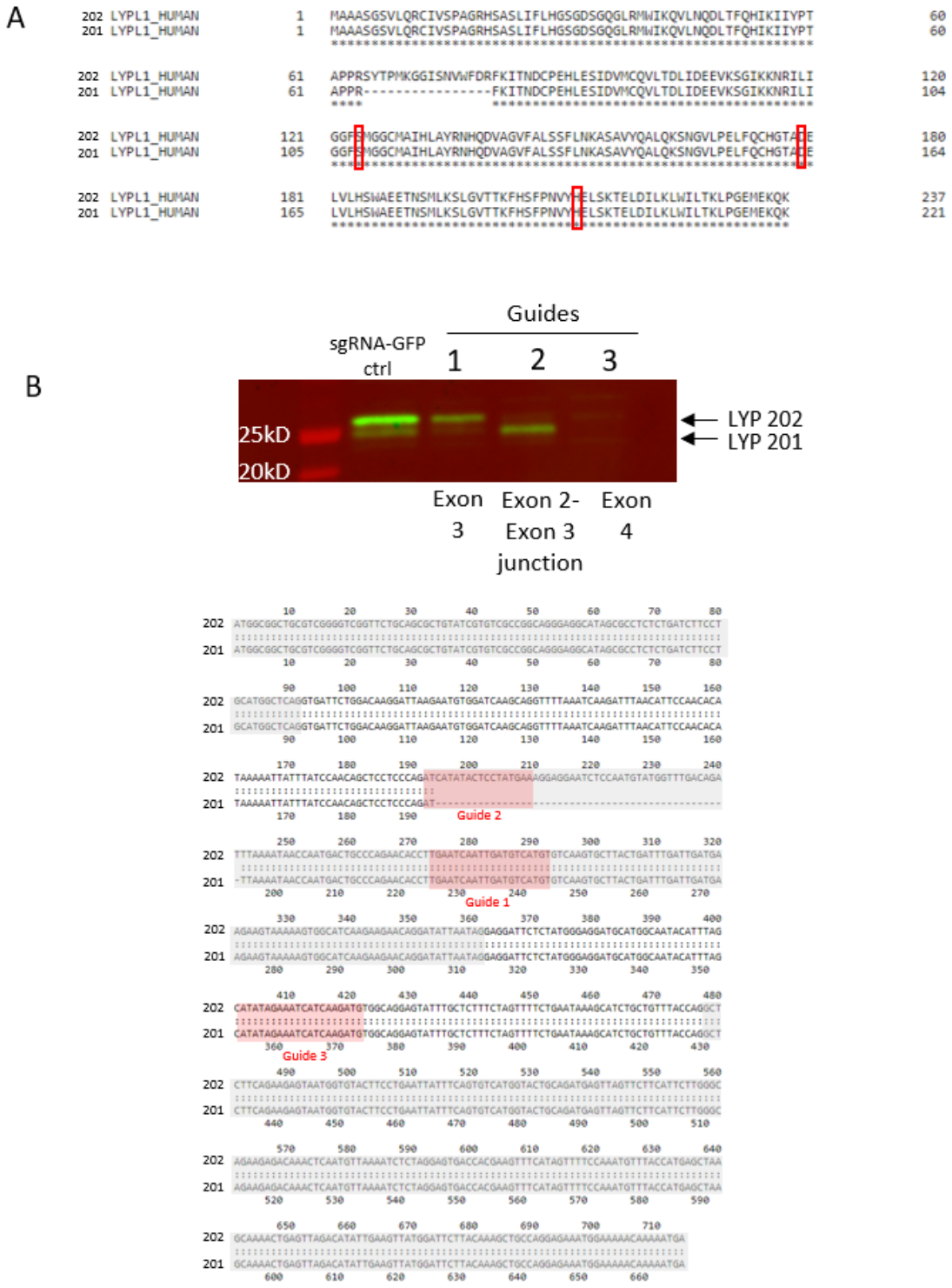

Figure 7-6. The human LYPLAL1 enzyme exists in two isoforms. A. The 202 isoform contains 16 extra amino acids. [caption continued on next page]

[Figure 7-6. Caption continued]

The serine hydrolase catalytic triad amino acids (serine, histidine, aspartic acid) are indicated in red. **B.** Western blot of Huh7.5 cells genetically engineered with CRISPR-Cas9 to knock-out LYPLAL1 using three different guide RNAs. A GFP-targeting guide was used as a non-targeting control. The two LYPLAL1 isoforms (202 and 201) are indicated. Alignment of the nucleotide sequences for both isoforms is shown with the five exons indicated in alternating grey-white shading and guide RNA locations in red. Guide 1 lead to an incomplete knock-down with the 202 isoform remaining dominant, guide 2 lead to a knock-down of only the 202 isoform and guide 3 caused a knock-out of both isoforms.

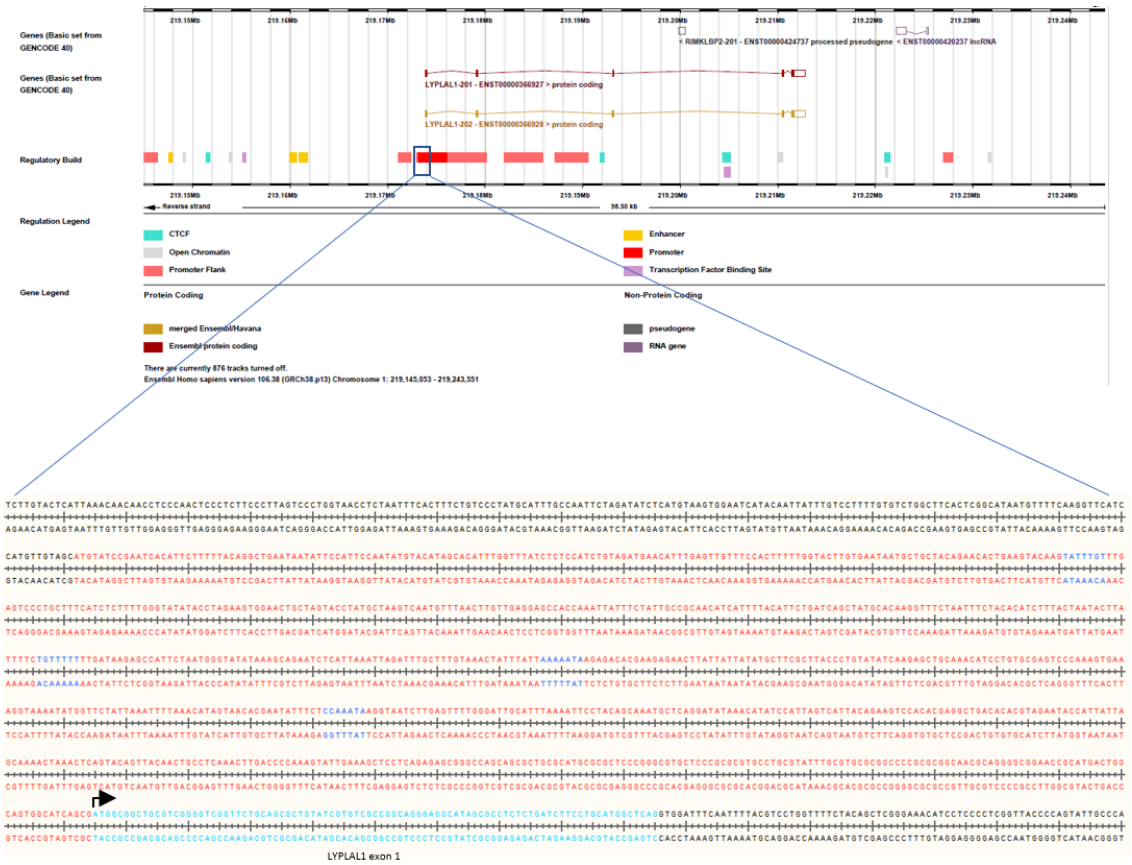

Figure 7-7. The LYPLAL1 promoter region contains potential FOXO1 binding sites of the consensus sequence 5'T(G/A)TTT(T/G)(G/T)3'. The promoter region upstream of the LYPLAL1 start codon as determined in Ensembl is denoted in red. The FOXO1 binding sequences are shown in dark blue.